Title

Developing Native Top-Down Mass Spectrometry to Reveal Information on Protein Structures

Author

Zhao, Boyu

Publication Date

2024

Peer reviewed|Thesis/dissertation

UNIVERSITY OF CALIFORNIA

Los Angeles

Developing Native Top-Down Mass Spectrometry to Reveal Information on Protein Structures

A dissertation submitted in partial satisfaction of the requirements for the degree Doctor of Philosophy in Chemistry

by

Boyu Zhao

2024

ABSTRACT OF THE DISSERTATION

Developing Native Top-Down Mass Spectrometry

to Reveal Information on Protein Structures

by

Boyu Zhao

Doctor of Philosophy in Chemistry

University of California, Los Angeles, 2024

Professor Joseph A. Loo, Chair

The interrogation of protein structure, especially identifying and localizing post-translational modifications (PTMs) and binding sites of protein and ligand/small molecule interactions, is crucial for understanding protein function. Native- and native top-down mass spectrometry (nTD-MS) have become prominent analytical tools for protein characterization. The work here has addressed several experimental issues to increase the applicability of nTD-MS for elucidating protein structures. We have selected supercharging agents based on their *pKa* values, and demonstrated that the addition of supercharging agents can help deposit more charges on the protein ions during the ESI process. Increasing

the precursor charge state enhances the efficiency of tandem mass spectrometry processes used to fragment large biomolecules. Additionally, we have investigated methods to generate sequence-specific fragments directly from protein complexes using activation/dissociation techniques alternative to traditionally used collision-based strategies, *e.g.*, electron capture dissociation (ECD). Lastly, we applied our nTD-MS methods to aid in the determination of the higher order structure of a potential human E3 ligase. My dissertation research can contribute to advancing mass spectrometry workflows to achieve more efficient structure characterization of protein complexes, and provide complementary information for conventional structure analysis (*e.g.*, electron microscopy, crystallography).

The dissertation of Boyu Zhao is approved.

Keriann M. Backus

Catherine F. Clarke

James A. Wohlschlegel

Joseph A. Loo, Committee Chair

University of California, Los Angeles

2024

In dedication

To my mother, Liu, Yizhao,

For guiding me to live a bright and courageous womanhood;

To my father, Zhao, Jianzhong,

For inspiring me to work in a diligent and determined profession;

To Deng, Wei 邓为,

For shining lights in my life;

To my friends,

For sharing my happiness.

For all their support throughout these years.

And in memory of my twenties.

TABLE OF CONTENTS

LIST OF FIGURES

Chapter1:

Chapter 2:

Chapter 4:

Appendix A:

Appendix C:

LIST OF TABLES

Chapter 2:

Chapter 4:

Appendix A:

Appendix C:

LIST OF SCHEMES

Appendix A:

ACKNOWLEDGEMENTS

I would like to express my heartfelt gratitude to my advisor, Professor Joseph Loo, for his continuous support and guidance throughout my Ph.D. Joe has been an exceptional mentor, always helping me discover my passion and encouraging me to pursue my research interests within the field of study. The completion of the work in this dissertation would not have been possible without the support, guidance, resources and instrumentation that Joe provided. I am deeply appreciative of the numerous opportunities Joe provided, including attending conferences, presenting my research, and connecting with outstanding scientists across different disciplines. Joe has always been available for guidance while encouraging me to think independently. I also want to sincerely thank Dr. Rachel Ogorzalek Loo for her invaluable support and expertise in proteomics and physical chemistry. Her insights into supercharging mechanisms have profoundly influenced my understanding of mass spectrometry and more importantly, nurtured my ability to think critically.

I would like to extend my gratitude to all the members of the Loo Lab for their invaluable help, support, and companionship throughout these years. I have thoroughly enjoyed working and hanging out with all Loo lab members. I cherish the fond memories we've shared, both professionally and personally. Special thanks to Dr. Wonhyeuk Jung and Dr. Carter Lantz for mentoring me and helping me to start my Ph.D. Journey, I learned so much from them and had so much fun working together in the past few years that I am appreciative of; Dr. Janine Fu and Dr. Benqian Wei for helping on many of my projects and being my references when I was hunting for jobs; Andrew Goring, Jessie Le, Eileen

Olivares, Merin Rixen, Megan Hong, Toy Lemmons, Luchen Wuyang, Cameron Flowers, Matthew Kensil, Scott Hale, Xuanyu Chen and Yi Qiao.

I would like to thank my committee members, Professor Keriann Backus, Professor Catherine Clarke, Professor James Wohlschlegel, and committee chair, Professor Joseph Loo. Thank you for reading and providing feedback on my proposals and this dissertation, and attending my oral exam, fourth year meeting, and my dissertation seminar.

I would also like to thank my invaluable collaborators, Dr. Steven Clarke, Dr. Jose Rodriguez, and Eric Pang for the samples I received over the years and all the conversations that furthered my research.

CURRICULUM VITAE

EDUCATION

Bachelor of Science, Chemistry

2016-2019

Indiana University, Bloomington

With Departmental Honors

With Highest Distinction

PEER REVIEWED PUBLICATIONS

Lantz, C.; Wei, B.; **Zhao, B.**; Jung, W.; Goring, A. K.; Le, J.; Miller, J.; Loo, R. R. O.; Loo, J. A., Native Top-Down Mass Spectrometry with Collisionally Activated Dissociation Yields Higher-Order Structure Information for Protein Complexes. *Journal of the American Chemical Society* **2022**, *144* (48), 21826-21830.

SELECTED CONFERENCE PRESENTATIONS

Zhao, B.; Le, J.; Mullen, C.; Huang, J.; Melani, R.; Loo, J.A., Native Top-Down MS with a Tribrid Orbitrap System Reveals Higher Order Structure Information for Protein Complexes. *72nd ASMS Conference on Mass Spectrometry and Allied Topics*. **2024**, oral presentation.

Zhao, B.; Lantz, C.; Wei, B.; Le, G.; Loo, R.R.; Loo, J.A., Native Top-Down Orbitrap Mass Spectrometry with Electron-Based Dissociation Yields Higher Order Structure Information for Soluble and Membrane Protein Complexes. *2023 Advancing Mass Spectrometry for Biophysics and Structural Biology.* **2023**, poster presentation.

Zhao, B.; Lantz, C.; Wei, B.; Loo, R.R.; Loo, J.A. Native Top-Down Orbitrap Mass Spectrometry with Electron-Based Dissociation Yields Higher Order Structure Information for Protein Complexes. *71st ASMS Conference on Mass Spectrometry and Allied Topics.* **2023**, oral presentation.

Zhao, B.; Lantz, C.; Wei, B.; Loo, R.R.; Loo, J.A. Native Top-Down Orbitrap Mass Spectrometry with Electron-Based Dissociation Yields Higher Order Structure Information for Protein Complexes with Unknown Structure. *28th Lake Arrowhead Conference on Ion*

Chemistry and Mass Spectrometry. **2023**, oral presentation.

Zhao, B.; Loo, R.R.; Loo, J.A. Native Top-Down MS Reveals Structural and Relative Stability Information of Protein Complexes. *70th ASMS Conference on Mass Spectrometry and Allied Topics.* **2022**, poster presentation.

Zhao, B.; Jung, W.; Loo, R.R.; Loo, J.A. Supercharging Proteins and Protein Complexes for MS and Top-Down MS. *69th ASMS Conference on Mass Spectrometry and Allied Topics.* **2021**, poster presentation.

SELECTED AWARDS

Upjohn Graduate Dissertation Award	**June 2024**
Department of Chemistry and Biochemistry Research Fellowship	**Spring 2024**
Department of Chemistry and Biochemistry Research Fellowship	**Spring 2022**
Andrew Loh Analytical Scholarship	**May 2019**

Chapter 1: Introduction

Mass spectrometry

Mass spectrometry (MS) has become a critical technique for revealing molecular compositions and measuring the mass of individual compounds and mixtures of small molecules[1], carbohydrates[2], oligonucleotides[3], lipids[4], and proteins[5-7], in the gas phase. Figure 1 shows the four major components for a mass spectrometer: the ionization source, mass analyzer, ion detector and data system. In an MS experiment, the sample is introduced into the mass spectrometer by direct infusion, or through gas- or liquid- chromatography, and is subsequently transformed into gas-phase ions in the ionization source. The gas-phase ions are separated and measured by the mass analyzer based on their (mass-to-charge ratio) *m/z* values, and are detected by the ion detector (and transformed to electric signals). The electric signals are then converted into digital information, and shown as a mass spectrum.

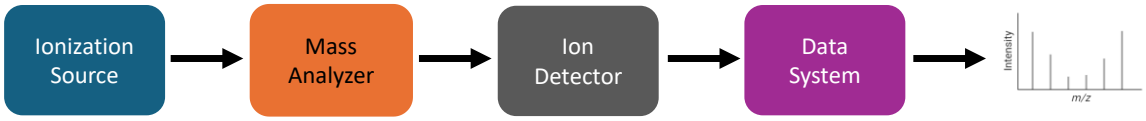

Figure 1. Four major components of a mass spectrometer.

There are several ionization techniques available, and these can be separated into *hard* ionization, for example, electron ionization (EI)[8, 9], and chemical ionization[10]; and *soft* ionization methods such as electrospray ionization (ESI)[11, 12], matrix-assisted laser desorption ionization (MALDI)[13-15], and desorption electrospray ionization (DESI)[16] that are commonly used for biomolecules, as they can preserve analytes in their intact forms during the ionization processes without significant analyte degradation (fragmentation). ESI has been widely used because of its high sensitivity and capability to couple on-line

with separation methods such as liquid chromatography (LC)[17] and capillary zone electrophoresis (CZE)[18]. During the ESI process, the analytes are transferred into the gas-phase by applying a high voltage to a glass capillary coated with Au or Pt. The high electric field creates a Taylor cone of solution that releases droplets containing analytes. These droplets become smaller and smaller as they travel towards a counterelectrode due to the charge repulsion and solvent evaporation, and are finally desolvated. The gas-phase analyte ions can be released with multiple charges for large molecules can retain multiple charge sites[12]. There are several theories explaining the ESI process including the charge residue model[19, 20], ion evaporation model[21], and the chain ejection model[22]. Each model addresses different types of analyte sizes and structures, *e.g.*, small versus large molecules, folded versus unfolded proteins, etc.

In MALDI, the ionization of analytes involves the use of a laser to ablate the analytes mixed with a matrix in excess on a metal plate.[23] The matrix molecule that has high absorptivity at the laser wavelength absorbs the photon's energy and transfers some this energy to the analyte molecules to ionize them into the gas-phase without excessive fragmentation.[24] ESI and MALDI have been used to ionize peptides[14, 25], intact proteins[26], and protein complexes[27], since the late 1980s.

After being transferred into the gas-phase, the analyte ions are transmitted from low vacuum to high vacuum to a mass analyzer through ion funnels[28, 29], quadrupoles[30], and other ion guides to prevent the scattering of ions and focus the analyte beam towards the analyte detector. This greatly increases signal-to-noise ratio, and therefore increases the sensitivity of mass spectrometers.

Mass analyzers such as quadrupole[31, 32], Time of Flight (TOF)[33-36], Fourier transform ion cyclotron resonance (FT-ICR)[37-39] and Orbitrap[40-42], are playing very important roles in separating and detecting ions based on their *m/z*. Quadrupoles are one of the most commonly used mass analyzers. They are made of four rod electrodes aligned in parallel, allowing ions to pass through. When an electric field is applied to the electrodes, the ions can be separated based on their *m/z*.[32] Quadrupoles are not only used as a mass analyzer, but also as mass selectors. As a mass selector, ions with a given range of *m/z* can be selected and transmitted for further activation[43, 44], by applying direct current (DC) and radio frequency (RF) potentials to the electrodes to filter ions.[45]

A TOF mass analyzer detects analyte ions by pushing ions from a trapping region to an electron multiplier detector[34], and measuring the time for each ion to reach the detector. The ion trajectory is depending on the kinetic energy gained from the initial ion acceleration, therefore, the time for each ion to reach the detector correlates to the *m/z* of the ion.[33, 36] TOF analyzers are among the most commonly used mass analyzers because of its fast speed and high sensitivity.[44, 46-50]

There are two mass analyzers, Orbitrap and Fourier transform ion cyclotron resonance (FT-ICR), in the Fourier Transform MS (FTMS) category.[51] In FTMS instruments, ions are excited into an orbit and the cyclotron frequency in FT-ICR MS[39] or the oscillated axial frequency in Orbitrap MS[40] is recorded. The digitized image current in the *time* domain is converted to the *frequency* domain to generate a mass spectrum by performing a Fourier transform[51, 52]. (The frequency of an ion is inversely proportional to its mass.) FTMS has been widely used to obtain very accurate masses for a wide range of molecular types because of its ultra-high resolution and the ability measure frequency accurately.[17, 53, 54]

Native Mass Spectrometry for Protein

Proteins are highly versatile biomolecules in biological systems, playing essential roles in many biochemical processes. Their functionality is intricately tied to their structures. Proteins can adopt stable structures, exhibit conformational flexibility, or even display intrinsic disorder. Factors such as mutations, post-translational modifications (PTMs), and binding with ligands (such as cofactors, drugs, proteins, oligonucleotides) have significant impacts on their structures, functions, and dynamics.[55, 56] Therefore, understanding protein structures and protein-ligand interactions is crucial for unraveling fundamental molecular mechanisms in life, as well as for advancing drug design, disease diagnosis, and therapeutic interventions. The diverse and dynamic nature of proteins and protein complexes presents significant challenges in characterizing their structures.

Native mass spectrometry (nMS) involves analysis of biomolecules, predominantly intact proteins and protein complexes, and provides high resolution information on protein, proteins and protein complexes.[27] In order to obtain a native mass spectrum, the protein is dissolved in a solution that preserves its native structure in solution, and ionized with soft ionization sources such as ESI with minimal activation to maintain its native structure. Generally, a protein is dissolved in a (50 mM-1 M, pH ~7) ammonium acetate solution that is sufficiently volatile so that the protein can be desolvated easily during the ionization process.[6] Using ammonium acetate for native ESI-MS has been considered to minimize the perturbation of the native structure of proteins and protein complexes when ionizing proteins from aqueous droplets and its transition to a gas-phase ion.[57] In addition, applying minimal activation is also critical for maintaining their native structures. This technique has become a valuable tool for examining intact proteins in their biologically active states.

Previous studies have shown that inter- and intra-molecular noncovalent interactions as well as protein-ligand interactions have been preserved during the ESI process and detected in various types of mass spectrometers.[58-61] Chapter 4 in this dissertation shows an example of using nMS to probe binding events between potential E3 ligase and its substrates.

By deconvoluting native ESI mass spectrum (to a zero-charge spectrum), an accurate mass of a protein can be obtained. The deconvolution routine involves consolidation of the protein's multiple charge states to mass values. Several algorithms have been developed for this purpose, such as UniDec[62] and PMI[63]. These algorithms have been successfully applied to various types of spectra, including spectra of large protein complexes, *e.g.*, 147 kDa alcohol dehydrogenase (ADH) homotetramer, membrane protein-lipid complexes, and intact antibodies,[63-65] demonstrating their capability to provide precise molecular weight measurements for native proteins.

Tandem MS and Fragmentation Techniques for Proteins and Peptides

Tandem MS (*i.e.*, MS/MS) is a powerful method for obtaining additional sequence, PTM and structure information for a polypeptide. Tandem MS for protein analysis can be separated into two categories: bottom-up mass spectrometry and top-down mass spectrometry (TD-MS) (Figure 2). In bottom-up mass spectrometry, before introducing proteins into the mass spectrometer, protease digestion (typically using trypsin) and reduction of disulfide bonds are required. The resulting peptide fragments are then loaded into an on-line high-performance liquid chromatograph for liquid-phase separation, and the eluants are measured by MS and tandem MS.[66] Alternatively, in TD-MS, digestion is

bypassed and the protein is directly introduced into the mass spectrometer for ionization and dissociated (via MS/MS) to generate sequence information.[67]

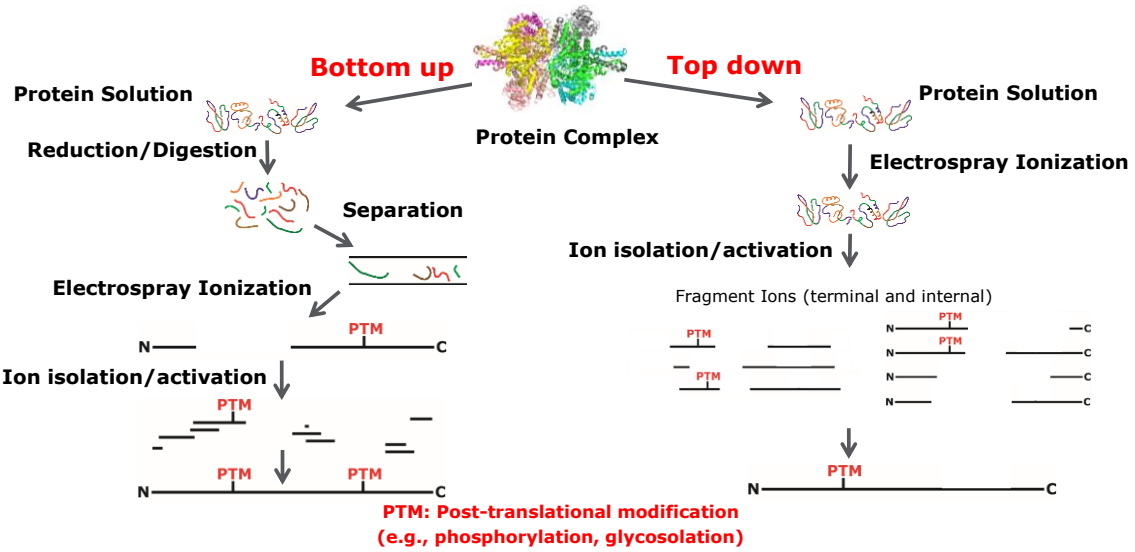

Figure 2. Workflows for bottom-up mass spectrometry (left) and top-down mass spectrometry (right).

Tandem MS has been commonly used for characterizing the primary (*i.e.*, sequence) and higher-order structure of peptides[17], proteins[60, 68], and protein complexes[61, 69, 70]. To perform MS/MS experiments, a specific *m/z* window (~10 *m/z*) or a wide *m/z* range is selected an isolated by a quadrupole filter and subjected for protein backbone cleavage to generate fragment ions that are measured by the mass analyzer and can be mapped back to the protein sequence.[71] Fragments released from N-terminus can be *a*-, *b*-, or *c*-fragment ions, and fragments released from C-terminus can be *x*-, *y*-, or *z*-fragment ions depending on the fragmentation method used.[72] Besides terminal fragments containing either terminus, internal fragments that contain neither terminus has also been observed. Internal fragments are generated by multiple protein backbone cleavages[73], and can cover sequence and PTM information located in the interior regions of the polypeptide sequence[74]. During

the past few decades, various dissociation methods have been developed including collision-, electron-, and photon-based dissociation techniques to elucidate sequence and structure information of proteins.

Collision-Based Dissociation

Collision induced dissociation (CID) is one of the most commonly used dissociation methods. CID is a relatively slow heating process, in which kinetic energy is converted into internal energy of a protein by colliding peptides or proteins with numerous non-chemically reactive gas molecules such as N_2, Ar, and Xe, which eventually causes peptide backbone cleavages.[75] This technique is robust and efficient at fragmenting peptides and proteins; it has been widely used for peptide and protein sequencing and PTM localization[76], although CID tends to cause protein unfolding during the fragmentation event due to the longer fragmentation timescale[77]. CID has also been used to reveal the composition[78, 79] and stoichiometry[80] of protein complexes. Despite its numerous applications, CID experiments (and any other dissociation method) suffers from a low mass cutoff (LMCO) in ion trap mass spectrometers, resulting in the truncation of the low *m/z* region[81], therefore limits the detection of short fragment ions. On the contrary, high energy C-trap dissociation (HCD) specific to Orbitrap analyzers, a type of CID, uses a separate collision cell for fragmentation, which overcomes the limitation of LMCO. Additionally, HCD occurs at a slightly faster timescale with high energy, and shows an ability to generate fragments that can reveal high-order structure of the protein complexes, without unfolding the proteins.[70] However, CID and HCD are considered as harsh dissociation methods due to the interruption of some noncovalent interactions. To overcome these problems, electron- and photon-based fragmentation can be used alternatively.

Electron-Based Dissociation

Electron capture dissociation (ECD)[82, 83] and electron transfer dissociation (ETD)[84] are two electron-based dissociation methods that are generally considered as soft dissociation techniques.[85] This feature enables us to easily obtain information from native protein complexes[69] and protein-ligand complexes[60], and to reveal higher-order structure information on protein complexes. In ECD, low-energy electrons (< 2 eV) are directly captured by the multiply charged protein cations to produce charge-reduced species as well as protein backbone cleavages.[86] ECD has been traditionally operated on FT-ICR MS as the magnetic field can confine the electron beam to interact with proteins. Recently, ECD has been developed to perform on TOF[87] and Orbitrap MS as well.[88] In ETD, negatively charged radical anions reacts with the multiply charged protein cations resulting in a charge reduced species and an odd-electron cation that further undergoes free-radical-driven cleavage.[89-93] However, ECD and ETD fragmentation efficiency is generally lower compared to CID and HCD, which could limit its sequence coverage. In recent years, electron induced dissociation (EID), a newer electron-based fragmentation method utilizing higher energy electrons (>20 eV),[94-96] has emerged and been applied to overcome the limitation. In EID, the reaction between protein cations and high energy electrons generates oxidized radical species resulting in protein backbone cleavages.[94] Our lab has demonstrated the application of EID for fragmentation of protein complexes and the generation of internal fragment ions.[97, 98]

Photon-Based Dissociation

Additionally, photon-based dissociation is achieved by an analyte absorbing the photons for energy deposition. A wide range of wavelengths of the photons, from low-energy infrared (IR) to high-energy ultraviolet (UV), has been commonly utilized for protein fragmentation. Infrared multiple-photon dissociation (IRMPD) is performed by slowly heating proteins with low frequency photons to cleave protein backbones, generating similar products as CID and HCD.[99] Another application of IRMPD is to break hydrogen bonds or salt bridges and release fragments generated by other dissociation methods (*e.g.*, ECD and ETD) from the protein.[69]

Ultraviolet photodissociation (UVPD) is performed by employing photons in UV range (*e.g.*, 157 nm[100], 213 nm[101], and 266 nm[102]) of the electromagnetic spectrum to cleave protein backbones. UVPD, a faster heating process, cleaves C-C_α bonds and N-C_α bonds to generate all six types of terminal fragment ions (N-terminal *a*-, *b*-, *c*-fragment ions and C-terminal *x*-, *y*-, *z*-fragment ions). UVPD has been used effectively to reveal the location of covalent and noncovalent modifications on proteins and to characterize peptides and proteins.[103, 104]

Native Top-Down Mass Spectrometry of Protein Complexes

Native mass spectrometry has been shown the capabilities in determining the molecular weight, stoichiometry, proteoforms, and binding affinity of protein complexes.[7, 105] However, certain structural details such as sequence, PTMs, subunit interfaces, and ligand binding sites cannot be directly revealed by nMS alone. Additionally, top-down mass spectrometry (TD-MS) under denaturing conditions enables sequencing of intact proteins,

localization of PTMs, and differentiating proteoforms. However, TD-MS loses information on higher order structural details, including noncovalent interactions that are essential for understanding protein functions as they fold into three-dimensional (3D) shapes, and assemble into protein complexes through noncovalent interactions. In the early years, nMS and TD-MS were performed separately. However, with the development of various dissociation approaches, the integration of nMS and TD-MS to nTD-MS has significantly enhanced higher-order structure analysis of protein complexes such as membrane proteins[106-108], and larger assemblies such as the proteasome[109] and the ribosome[110, 111].

To obtain higher-order structure information of protein complexes, native protein or protein complexes are directly subject for fragmentation. Minimal activation is applied to the protein complex (*i.e.*, native MS) prior to MS/MS fragmentation so that the TD-MS experiment probes the native state (in the gas-phase). In nTD-MS, protein complexes have traditionally been fragmentated by ExD and UVPD, as these techniques has been found to produce fragment ions that can reflect high-order structure characteristics. For example, it has been found that ExD generates predominant N-terminal fragments and few C-terminal fragments from ADH tetramer.[89, 112] The ADH fragmentation pattern is consistent with its crystal structure that shows its N-termini to be in a solvent exposed region, whereas the C-termini region is closer to buried subunit-subunit interfaces. In addition, nTD-MS can reveal regions of stability of protein complexes, for example, the glutamate dehydrogenase homohexamer.[69] UVPD has also shown the capability to preferentially generate fragments from solvent exposed regions of protein complexes, however, the vibrational excitement of the protein causes deeper sequence cleavages.[113, 114] The results from nTD-MS can also reveal locations of covalent modifications and noncovalent interactions (*e.g.*, protein-

ligand interactions) along the sequence. ECD has been used to probe the binding site of a zinc metal ion on ADH.[115] UVPD has also been utilized to localize heme on myoglobin[116] and metal ions on insulin pentamer[113] and other metalloproteins[104].

Complex-Down Mass Spectrometry of Protein Complexes

Complex-down MS (*i.e.,* pseudo-MS^3) has been used to elucidate the stoichiometry of protein complexes with noncovalent interactions, and provide sequence information at the same time. In complex-down MS, a native protein complex is ionized into the gas-phase, and dissociated into monomers by applying in-source CID (ISD) or subcomplexes by surface induced dissociation (SID). Released monomers are subsequently isolated and activated to generate fragment ions. There are several applications of complex-down MS. Complex-down MS has been used to fragment large protein complexes such as GroEL 14mer[117] and virus-like particles[118] to obtain sequence and structure information. Complex-down MS has also been used to determine different proteoforms such as mutations, modifications, and deletions on protein complexes. Complex-down fragmentation of the 20S proteosome revealed the proteoforms with acetylated N-terminus and the loss of the last two amino acids on the C-terminus.[109] Lastly, our lab has compared the difference between nTD-MS and complex-down fragmentation patterns to infer higher-order structure information of protein complexes. Complex-down fragmentation of the ADH homotetramer reveals nearly equal number of N- and C-terminal fragments, whereas native top-down MS of ADH mainly generates fragments from N-terminus, which is consistent with its higher-order structure, *e.g.*, the N-terminus of ADH is more solvent exposed, whereas the C-terminus is closer to monomer interfaces.[70] Other examples in Chapter 2, 3

and 4 in this dissertation also show that nTD-MS and complex-down MS in combination can expose higher-order structure information from intact protein MS experiments.

References

1. Kind, T.; Fiehn, O., Advances in structure elucidation of small molecules using mass spectrometry. *Bioanalytical Reviews* **2010,** *2* (1), 23-60.

2. Zaia, J., Mass spectrometry of oligosaccharides. *Mass Spectrometry Reviews* **2004,** *23* (3), 161-227.

3. Beck, J. L.; Colgrave, M. L.; Ralph, S. F.; Sheil, M. M., Electrospray ionization mass spectrometry of oligonucleotide complexes with drugs, metals, and proteins. *Mass Spectrometry Reviews* **2001,** *20* (2), 61-87.

4. Cajka, T.; Fiehn, O., Comprehensive analysis of lipids in biological systems by liquid chromatography-mass spectrometry. *TrAC Trends in Analytical Chemistry* **2014,** *61*, 192-206.

5. Domon, B.; Aebersold, R., Mass Spectrometry and Protein Analysis. *Science* **2006,** *312* (5771), 212-217.

6. Heck, A. J. R., Native mass spectrometry: a bridge between interactomics and structural biology. *Nature Methods* **2008,** *5* (11), 927-933.

7. Zhou, M.; Lantz, C.; Brown, K. A.; Ge, Y.; Paša-Tolić, L.; Loo, J. A.; Lermyte, F., Higher-order structural characterisation of native proteins and complexes by top-down mass spectrometry. *Chemical Science* **2020,** *11* (48), 12918-12936.

8. Bleakney, W., A New Method of Positive Ray Analysis and Its Application to the Measurement of Ionization Potentials in Mercury Vapor. *Physical Review* **1929,** *34* (1), 157-160.

9. Nier, A. O., A Mass Spectrometer for Isotope and Gas Analysis. *Review of Scientific Instruments* **1947,** *18* (6), 398-411.

10. Munson, M. S. B.; Field, F. H., Chemical Ionization Mass Spectrometry. I. General Introduction. *Journal of the American Chemical Society* **1966,** *88* (12), 2621-2630.

11. Yamashita, M.; Fenn, J. B., Electrospray ion source. Another variation on the free-jet theme. *The Journal of Physical Chemistry* **1984,** *88* (20), 4451-4459.

12. Fenn, J. B.; Mann, M.; Meng, C. K.; Wong, S. F.; Whitehouse, C. M., Electrospray Ionization for Mass Spectrometry of Large Biomolecules. *Science* **1989,** *246* (4926), 64-71.

13. Karas, M.; Hillenkamp, F., Laser desorption ionization of proteins with molecular masses exceeding 10,000 daltons. *Analytical Chemistry* **1988,** *60* (20), 2299-2301.

14. Karas, M.; Bachmann, D.; Bahr, U.; Hillenkamp, F., Matrix-assisted ultraviolet laser desorption of non-volatile compounds. *International Journal of Mass Spectrometry and Ion Processes* **1987,** *78*, 53-68.

15. Karas, M.; Bachmann, D.; Hillenkamp, F., Influence of the wavelength in high-irradiance ultraviolet laser desorption mass spectrometry of organic molecules. *Analytical Chemistry* **1985,** *57* (14), 2935-2939.

16. Takáts, Z.; Wiseman, J. M.; Gologan, B.; Cooks, R. G., Mass Spectrometry Sampling Under Ambient Conditions with Desorption Electrospray Ionization. *Science* **2004,** *306* (5695), 471-473.

17. Han, X.; Aslanian, A.; Yates, J. R., Mass spectrometry for proteomics. *Current Opinion in Chemical Biology* **2008,** *12* (5), 483-490.

18. Haselberg, R.; de Jong, G. J.; Somsen, G. W., Capillary electrophoresis–mass spectrometry for the analysis of intact proteins 2007–2010. *ELECTROPHORESIS* **2011,** *32* (1), 66-82.

19. Winger, B. E.; Light-Wahl, K. J.; Ogorzalek Loo, R. R.; Udseth, H. R.; Smith, R. D., Observation and implications of high mass-to-charge ratio ions from electrospray ionization mass spectrometry. *Journal of the American Society for Mass Spectrometry* **1993,** *4* (7), 536-545.

20. Fernandez de la Mora, J., Electrospray ionization of large multiply charged species proceeds via Dole's charged residue mechanism. *Analytica Chimica Acta* **2000,** *406* (1), 93-104.

21. Thomson, B. A.; Iribarne, J. V., Field induced ion evaporation from liquid surfaces at atmospheric pressure. *The Journal of Chemical Physics* **1979,** *71* (11), 4451-4463.

22. Konermann, L.; Rodriguez, A. D.; Liu, J., On the Formation of Highly Charged Gaseous Ions from Unfolded Proteins by Electrospray Ionization. *Analytical Chemistry* **2012,** *84* (15), 6798-6804.

23. Tanaka, K.; Waki, H.; Ido, Y.; Akita, S.; Yoshida, Y.; Yoshida, T.; Matsuo, T., Protein and polymer analyses up to m/z 100 000 by laser ionization time-of-flight mass spectrometry. *Rapid Communications in Mass Spectrometry* **1988,** *2* (8), 151-153.

24. Knochenmuss, R., A Quantitative Model of Ultraviolet Matrix-Assisted Laser Desorption/Ionization Including Analyte Ion Generation. *Analytical Chemistry* **2003,** *75* (10), 2199-2207.

25. Emmett, M. R.; Caprioli, R. M., Micro-electrospray mass spectrometry: Ultra-high-sensitivity analysis of peptides and proteins. *Journal of the American Society for Mass Spectrometry* **1994,** *5* (7), 605-613.

26. Smith, R. D.; Loo, J. A.; Edmonds, C. G.; Barinaga, C. J.; Udseth, H. R., New developments in biochemical mass spectrometry: electrospray ionization. *Analytical Chemistry* **1990,** *62* (9), 882-899.

27. Loo, J. A., Studying noncovalent protein complexes by electrospray ionization mass spectrometry. *Mass Spectrometry Reviews* **1997,** *16* (1), 1-23.

28. Shaffer, S. A.; Prior, D. C.; Anderson, G. A.; Udseth, H. R.; Smith, R. D., An Ion Funnel Interface for Improved Ion Focusing and Sensitivity Using Electrospray Ionization Mass Spectrometry. *Analytical Chemistry* **1998,** *70* (19), 4111-4119.

29. Kelly, R. T.; Tolmachev, A. V.; Page, J. S.; Tang, K.; Smith, R. D., The ion funnel: Theory, implementations, and applications. *Mass Spectrometry Reviews* **2010,** *29* (2), 294-312.

30. March, R. E., An Introduction to Quadrupole Ion Trap Mass Spectrometry. *Journal of Mass Spectrometry* **1997,** *32* (4), 351-369.

31. Dawson, P. H., *Quadrupole Mass Spectrometry and Its Applications*. Elsevier Scientific Publishing Company: 1976.

32. Wolfgang, P., Helmut, Steinwedel Apparatus for separating charged particles of different specific charges. 1960.

33. Guilhaus, M., Special feature: Tutorial. Principles and instrumentation in time-of-flight mass spectrometry. Physical and instrumental concepts. *Journal of Mass Spectrometry* **1995,** *30* (11), 1519-1532.

34. Wolff, M. M.; Stephens, W. E., A Pulsed Mass Spectrometer with Time Dispersion. *Review of Scientific Instruments* **1953,** *24* (8), 616-617.

35. Mamyrin, B. A., Time-of-flight mass spectrometry (concepts, achievements, and prospects). *International Journal of Mass Spectrometry* **2001,** *206* (3), 251-266.

36. Boesl, U., Time-of-flight mass spectrometry: Introduction to the basics. *Mass Spectrometry Reviews* **2017,** *36* (1), 86-109.

37. Comisarow, M. B.; Marshall, A. G., Fourier transform ion cyclotron resonance spectroscopy. *Chemical Physics Letters* **1974,** *25* (2), 282-283.

38. Comisarow, M. B.; Marshall, A. G., Resolution-enhanced Fourier transform ion cyclotron resonance spectroscopy. *The Journal of Chemical Physics* **1975,** *62* (1), 293-295.

39. Marshall, A. G.; Hendrickson, C. L.; Jackson, G. S., Fourier transform ion cyclotron resonance mass spectrometry: A primer. *Mass Spectrometry Reviews* **1998,** *17* (1), 1-35.

40. Hu, Q.; Noll, R. J.; Li, H.; Makarov, A.; Hardman, M.; Graham Cooks, R., The Orbitrap: a new mass spectrometer. *Journal of Mass Spectrometry* **2005,** *40* (4), 430-443.

41. Zubarev, R. A.; Makarov, A., Orbitrap Mass Spectrometry. *Analytical Chemistry* **2013,** *85* (11), 5288-5296.

42. Scigelova, M.; Makarov, A., Orbitrap Mass Analyzer – Overview and Applications in Proteomics. *PROTEOMICS* **2006,** *6* (S2), 16-21.

43. Yost, R. A.; Boyd, R. K., [7] Tandem mass spectrometry: Quadrupole and hybrid instruments. In *Methods in Enzymology*, Academic Press: 1990; Vol. 193, pp 154-200.

44. Chernushevich, I. V.; Loboda, A. V.; Thomson, B. A., An introduction to quadrupole–time-of-flight mass spectrometry. *Journal of Mass Spectrometry* **2001,** *36* (8), 849-865.

45. Miller, P. E.; Denton, M. B., The quadrupole mass filter: Basic operating concepts. *Journal of Chemical Education* **1986,** *63*, 617-622.

46. Wang, L.; Amphlett, G.; Lambert, J. M.; Blättler, W.; Zhang, W., Structural Characterization of a Recombinant Monoclonal Antibody by Electrospray Time-of-Flight Mass Spectrometry. *Pharmaceutical Research* **2005,** *22* (8), 1338-1349.

47. Cotter, R. J., Time-of-Flight Mass Spectrometry for the Structural Analysis of Biological Molecules. *Analytical Chemistry* **1992,** *64* (21), 1027A-1039A.

48. Nielen, M. W. F., MALDI TIME-OF-FLIGHT MASS SPECTROMETRY OF SYNTHETIC POLYMERS. *Mass Spectrometry Reviews* **1999,** *18*, 309-344.

49. Weickhardt, C.; Moritz, F.; Grotemeyer, J., Time-of-flight mass spectrometry: State-of the-art in chemical analysis and molecular science. *Mass Spectrometry Reviews* **1996,** *15* (3), 139-162.

50. Williams, J. P.; Morrison, L. J.; Brown, J. M.; Beckman, J. S.; Voinov, V. G.; Lermyte, F., Top-Down Characterization of Denatured Proteins and Native Protein Complexes Using Electron Capture Dissociation Implemented within a Modified Ion Mobility-Mass Spectrometer. *Analytical Chemistry* **2020,** *92* (5), 3674-3681.

51. Scigelova, M.; Hornshaw, M.; Giannakopulos, A.; Makarov, A., Fourier Transform Mass Spectrometry. *Molecular & Cellular Proteomics* **2011,** *10* (7), M111.009431.

52. Cochran, W. T.; Cooley, J. W.; Favin, D. L.; Helms, H. D.; Kaenel, R. A.; Lang, W. W.; Maling, G. C.; Nelson, D. E.; Rader, C. M.; Welch, P. D., What is the fast Fourier transform? *Proceedings of the IEEE* **1967,** *55* (10), 1664-1674.

53. Tucholski, T.; Ge, Y., Fourier-transform ion cyclotron resonance mass spectrometry for characterizing proteoforms. *Mass Spectrometry Reviews* **2022,** *41* (2), 158-177.

54. Lange, O.; Damoc, E.; Wieghaus, A.; Makarov, A. A., Enhanced Fourier transform for Orbitrap mass spectrometry. *International Journal of Mass Spectrometry* **2014,** *369*, 16-22.

55. Britt, H. M.; Cragnolini, T.; Thalassinos, K., Integration of Mass Spectrometry Data for Structural Biology. *Chemical Reviews* **2022,** *122* (8), 7952-7986.

56. Stollar, E. J.; Smith, D. P., Uncovering protein structure. *Essays in Biochemistry* **2020,** *64* (4), 649-680.

57. Leney, A. C.; Heck, A. J. R., Native Mass Spectrometry: What is in the Name? *Journal of the American Society for Mass Spectrometry* **2017,** *28* (1), 5-13.

58. Katta, V.; Chait, B. T., Observation of the heme-globin complex in native myoglobin by electrospray-ionization mass spectrometry. *Journal of the American Chemical Society* **1991,** *113* (22), 8534-8535.

59. Ganem, B.; Li, Y. T.; Henion, J. D., Detection of noncovalent receptor-ligand complexes by mass spectrometry. *Journal of the American Chemical Society* **1991,** *113* (16), 6294-6296.

60. Yin, S.; Loo, J. A., Elucidating the Site of Protein-ATP Binding by Top-Down Mass Spectrometry. *Journal of the American Society for Mass Spectrometry* **2010,** *21* (6), 899-907.

61. Li, H.; Wolff, J. J.; Van Orden, S. L.; Loo, J. A., Native Top-Down Electrospray Ionization-Mass Spectrometry of 158 kDa Protein Complex by High-Resolution Fourier Transform Ion Cyclotron Resonance Mass Spectrometry. *Analytical Chemistry* **2014,** *86* (1), 317-320.

62. Marty, M. T.; Baldwin, A. J.; Marklund, E. G.; Hochberg, G. K. A.; Benesch, J. L. P.; Robinson, C. V., Bayesian Deconvolution of Mass and Ion Mobility Spectra: From Binary Interactions to Polydisperse Ensembles. *Analytical Chemistry* **2015,** *87* (8), 4370-4376.

63. Bern, M.; Caval, T.; Kil, Y. J.; Tang, W.; Becker, C.; Carlson, E.; Kletter, D.; Sen, K. I.; Galy, N.; Hagemans, D.; Franc, V.; Heck, A. J. R., Parsimonious Charge Deconvolution for Native Mass Spectrometry. *Journal of Proteome Research* **2018,** *17* (3), 1216-1226.

64. Kostelic, M. M.; Marty, M. T., Deconvolving Native and Intact Protein Mass Spectra with UniDec. In *Proteoform Identification: Methods and Protocols*, Sun, L.; Liu, X., Eds. Springer US: New York, NY, 2022; pp 159-180.

65. Marty, M. T.; Hoi, K. K.; Gault, J.; Robinson, C. V., Probing the Lipid Annular Belt by Gas-Phase Dissociation of Membrane Proteins in Nanodiscs. *Angewandte Chemie International Edition* **2016,** *55* (2), 550-554.

66. Aebersold, R.; Mann, M., Mass spectrometry-based proteomics. *Nature* **2003,** *422* (6928), 198-207.

67. Cui, W.; Rohrs, H. W.; Gross, M. L., Top-down mass spectrometry: Recent developments, applications and perspectives. *Analyst* **2011,** *136* (19), 3854-3864.

68. Zhang, J.; Loo, R. R. O.; Loo, J. A., Increasing fragmentation of disulfide-bonded proteins for top–down mass spectrometry by supercharging. *International Journal of Mass Spectrometry* **2015,** *377*, 546-556.

69. Li, H.; Nguyen, H. H.; Ogorzalek Loo, R. R.; Campuzano, I. D. G.; Loo, J. A., An integrated native mass spectrometry and top-down proteomics method that connects

sequence to structure and function of macromolecular complexes. *Nature Chemistry* **2018,** *10* (2), 139-148.

70. Lantz, C.; Wei, B.; Zhao, B.; Jung, W.; Goring, A. K.; Le, J.; Miller, J.; Loo, R. R. O.; Loo, J. A., Native Top-Down Mass Spectrometry with Collisionally Activated Dissociation Yields Higher-Order Structure Information for Protein Complexes. *Journal of the American Chemical Society* **2022,** *144* (48), 21826-21830.

71. Wysocki, V. H.; Resing, K. A.; Zhang, Q.; Cheng, G., Mass spectrometry of peptides and proteins. *Methods* **2005,** *35* (3), 211-222.

72. Roepstorff, P.; Fohlman, J., Proposal for a common nomenclature for sequence ions in mass spectra of peptides. *Biomed Mass Spectrom* **1984,** *11* (11), 601.

73. Durbin, K. R.; Skinner, O. S.; Fellers, R. T.; Kelleher, N. L., Analyzing Internal Fragmentation of Electrosprayed Ubiquitin Ions During Beam-Type Collisional Dissociation. *Journal of the American Society for Mass Spectrometry* **2015,** *26* (5), 782-787.

74. Wei, B.; Lantz, C.; Liu, W.; Viner, R.; Ogorzalek Loo, R. R.; Campuzano, I. D. G.; Loo, J. A., Added Value of Internal Fragments for Top-Down Mass Spectrometry of Intact Monoclonal Antibodies and Antibody–Drug Conjugates. *Analytical Chemistry* **2023,** *95* (24), 9347-9356.

75. Macias, L. A.; Santos, I. C.; Brodbelt, J. S., Ion Activation Methods for Peptides and Proteins. *Analytical Chemistry* **2020,** *92* (1), 227-251.

76. Smith, R. D.; Loa, J. A.; Barinaga, C. J.; Edmonds, C. G.; Udseth, H. R., Collisional activation and collision-activated dissociation of large multiply charged

polypeptides and proteins produced by electrospray ionization. *Journal of the American Society for Mass Spectrometry* **1990,** *1* (1), 53-65.

77. Mitchell Wells, J.; McLuckey, S. A., Collision-Induced Dissociation (CID) of Peptides and Proteins. In *Methods in Enzymology*, Academic Press: 2005; Vol. 402, pp 148-185.

78. Aquilina, J. A.; Benesch, J. L. P.; Bateman, O. A.; Slingsby, C.; Robinson, C. V., Polydispersity of a mammalian chaperone: Mass spectrometry reveals the population of oligomers in αB-crystallin. *Proceedings of the National Academy of Sciences* **2003,** *100* (19), 10611-10616.

79. Schwartz, B. L.; Bruce, J. E.; Anderson, G. A.; Hofstadler, S. A.; Rockwood, A. L.; Smith, R. D.; Chilkoti, A.; Stayton, P. S., Dissociation of tetrameric ions of noncovalent streptavidin complexes formed by electrospray ionization. *Journal of the American Society for Mass Spectrometry* **1995,** *6* (6), 459-465.

80. Light-Wahl, K. J.; Schwartz, B. L.; Smith, R. D., Observation of the Noncovalent Quaternary Associations of Proteins by Electrospray Ionization Mass Spectrometry. *Journal of the American Chemical Society* **1994,** *116* (12), 5271-5278.

81. Yang, Y.-H.; Lee, K.; Jang, K.-S.; Kim, Y.-G.; Park, S.-H.; Lee, C.-S.; Kim, B.-G., Low mass cutoff evasion with qz value optimization in ion trap. *Analytical Biochemistry* **2009,** *387* (1), 133-135.

82. Zubarev, R. A.; Kelleher, N. L.; McLafferty, F. W., Electron Capture Dissociation of Multiply Charged Protein Cations. A Nonergodic Process. *Journal of the American Chemical Society* **1998,** *120* (13), 3265-3266.

83. Zubarev, R. A.; Horn, D. M.; Fridriksson, E. K.; Kelleher, N. L.; Kruger, N. A.; Lewis, M. A.; Carpenter, B. K.; McLafferty, F. W., Electron Capture Dissociation for Structural Characterization of Multiply Charged Protein Cations. *Analytical Chemistry* **2000,** *72* (3), 563-573.

84. Syka, J. E. P.; Coon, J. J.; Schroeder, M. J.; Shabanowitz, J.; Hunt, D. F., Peptide and protein sequence analysis by electron transfer dissociation mass spectrometry. *Proceedings of the National Academy of Sciences* **2004,** *101* (26), 9528-9533.

85. McLuckey, S. A.; Goeringer, D. E., SPECIAL FEATURE: TUTORIAL Slow Heating Methods in Tandem Mass Spectrometry. *Journal of Mass Spectrometry* **1997,** *32* (5), 461-474.

86. Zhang, H.; Cui, W.; Gross, M. L., Native electrospray ionization and electron-capture dissociation for comparison of protein structure in solution and the gas phase. *International Journal of Mass Spectrometry* **2013,** *354-355*, 288-291.

87. Beckman, J. S.; Voinov, V. G.; Hare, M.; Sturgeon, D.; Vasil'ev, Y.; Oppenheimer, D.; Shaw, J. B.; Wu, S.; Glaskin, R.; Klein, C.; Schwarzer, C.; Stafford, G., Improved Protein and PTM Characterization with a Practical Electron-Based Fragmentation on Q-TOF Instruments. *Journal of the American Society for Mass Spectrometry* **2021,** *32* (8), 2081-2091.

88. Shaw, J. B.; Malhan, N.; Vasil'ev, Y. V.; Lopez, N. I.; Makarov, A.; Beckman, J. S.; Voinov, V. G., Sequencing Grade Tandem Mass Spectrometry for Top–Down Proteomics Using Hybrid Electron Capture Dissociation Methods in a Benchtop Orbitrap Mass Spectrometer. *Analytical Chemistry* **2018,** *90* (18), 10819-10827.

89. Lermyte, F.; Valkenborg, D.; Loo, J. A.; Sobott, F., Radical solutions: Principles and application of electron-based dissociation in mass spectrometry-based analysis of protein structure. *Mass Spectrometry Reviews* **2018,** *37* (6), 750-771.

90. Qi, Y.; Volmer, D. A., Electron-based fragmentation methods in mass spectrometry: An overview. *Mass Spectrometry Reviews* **2017,** *36* (1), 4-15.

91. Qi, Y.; Volmer, D. A., Structural analysis of small to medium-sized molecules by mass spectrometry after electron-ion fragmentation (ExD) reactions. *Analyst* **2016,** *141* (3), 794-806.

92. Riley, N. M.; Coon, J. J., The Role of Electron Transfer Dissociation in Modern Proteomics. *Analytical Chemistry* **2018,** *90* (1), 40-64.

93. Zhurov, K. O.; Fornelli, L.; Wodrich, M. D.; Laskay, Ü. A.; Tsybin, Y. O., Principles of electron capture and transfer dissociation mass spectrometry applied to peptide and protein structure analysis. *Chemical Society Reviews* **2013,** *42* (12), 5014-5030.

94. Fung, Y. M. E.; Adams, C. M.; Zubarev, R. A., Electron Ionization Dissociation of Singly and Multiply Charged Peptides. *Journal of the American Chemical Society* **2009,** *131* (29), 9977-9985.

95. Zubarev, R. A.; Yang, H., Multiple Soft Ionization of Gas-Phase Proteins and Swift Backbone Dissociation in Collisions with ⩽99 eV Electrons. *Angewandte Chemie International Edition* **2010,** *49* (8), 1439-1441.

96. Kaczorowska, M. A.; Cooper, H. J., Electron induced dissociation (EID) tandem mass spectrometry of octaethylporphyrin and its iron(iii) complex. *Chemical Communications* **2011,** *47* (1), 418-420.

97. Li, H.; Sheng, Y.; McGee, W.; Cammarata, M.; Holden, D.; Loo, J. A., Structural Characterization of Native Proteins and Protein Complexes by Electron Ionization Dissociation-Mass Spectrometry. *Analytical Chemistry* **2017,** *89* (5), 2731-2738.

98. Zenaidee, M. A.; Lantz, C.; Perkins, T.; Jung, W.; Loo, R. R. O.; Loo, J. A., Internal Fragments Generated by Electron Ionization Dissociation Enhance Protein Top-Down Mass Spectrometry. *Journal of the American Society for Mass Spectrometry* **2020,** *31* (9), 1896-1902.

99. Little, D. P.; Speir, J. P.; Senko, M. W.; O'Connor, P. B.; McLafferty, F. W., Infrared Multiphoton Dissociation of Large Multiply Charged Ions for Biomolecule Sequencing. *Analytical Chemistry* **1994,** *66* (18), 2809-2815.

100. Fung, Y. M. E.; Kjeldsen, F.; Silivra, O. A.; Chan, T. W. D.; Zubarev, R. A., Facile Disulfide Bond Cleavage in Gaseous Peptide and Protein Cations by Ultraviolet Photodissociation at 157 nm. *Angewandte Chemie International Edition* **2005,** *44* (39), 6399-6403.

101. Theisen, A.; Black, R.; Corinti, D.; Brown, J. M.; Bellina, B.; Barran, P. E., Initial Protein Unfolding Events in Ubiquitin, Cytochrome c and Myoglobin Are Revealed with the Use of 213 nm UVPD Coupled to IM-MS. *Journal of the American Society for Mass Spectrometry* **2019,** *30* (1), 24-33.

102. Ly, T.; Julian, R. R., Elucidating the Tertiary Structure of Protein Ions in Vacuo with Site Specific Photoinitiated Radical Reactions. *Journal of the American Chemical Society* **2010,** *132* (25), 8602-8609.

103. Mayfield, J. E.; Robinson, M. R.; Cotham, V. C.; Irani, S.; Matthews, W. L.; Ram, A.; Gilmour, D. S.; Cannon, J. R.; Zhang, Y. J.; Brodbelt, J. S., Mapping the

Phosphorylation Pattern of Drosophila melanogaster RNA Polymerase II Carboxyl-Terminal Domain Using Ultraviolet Photodissociation Mass Spectrometry. *ACS Chemical Biology* **2017,** *12* (1), 153-162.

104. Crittenden, C. M.; Novelli, E. T.; Mehaffey, M. R.; Xu, G. N.; Giles, D. H.; Fies, W. A.; Dalby, K. N.; Webb, L. J.; Brodbelt, J. S., Structural Evaluation of Protein/Metal Complexes via Native Electrospray Ultraviolet Photodissociation Mass Spectrometry. *Journal of the American Society for Mass Spectrometry* **2020,** *31* (5), 1140-1150.

105. Tamara, S.; den Boer, M. A.; Heck, A. J. R., High-Resolution Native Mass Spectrometry. *Chemical Reviews* **2022,** *122* (8), 7269-7326.

106. Gault, J.; Liko, I.; Landreh, M.; Shutin, D.; Bolla, J. R.; Jefferies, D.; Agasid, M.; Yen, H.-Y.; Ladds, M. J. G. W.; Lane, D. P.; Khalid, S.; Mullen, C.; Remes, P. M.; Huguet, R.; McAlister, G.; Goodwin, M.; Viner, R.; Syka, J. E. P.; Robinson, C. V., Combining native and 'omics' mass spectrometry to identify endogenous ligands bound to membrane proteins. *Nature Methods* **2020,** *17* (5), 505-508.

107. Ro, S. Y.; Schachner, L. F.; Koo, C. W.; Purohit, R.; Remis, J. P.; Kenney, G. E.; Liauw, B. W.; Thomas, P. M.; Patrie, S. M.; Kelleher, N. L.; Rosenzweig, A. C., Native top-down mass spectrometry provides insights into the copper centers of membrane-bound methane monooxygenase. *Nature Communications* **2019,** *10* (1), 2675.

108. Sipe, S. N.; Patrick, J. W.; Laganowsky, A.; Brodbelt, J. S., Enhanced Characterization of Membrane Protein Complexes by Ultraviolet Photodissociation Mass Spectrometry. *Analytical Chemistry* **2020,** *92* (1), 899-907.

109. Vimer, S.; Ben-Nissan, G.; Morgenstern, D.; Kumar-Deshmukh, F.; Polkinghorn, C.; Quintyn, R. S.; Vasil'ev, Y. V.; Beckman, J. S.; Elad, N.; Wysocki, V. H.; Sharon,

M., Comparative Structural Analysis of 20S Proteasome Ortholog Protein Complexes by Native Mass Spectrometry. *ACS Central Science* **2020,** *6* (4), 573-588.

110. Belov, A. M.; Viner, R.; Santos, M. R.; Horn, D. M.; Bern, M.; Karger, B. L.; Ivanov, A. R., Analysis of Proteins, Protein Complexes, and Organellar Proteomes Using Sheathless Capillary Zone Electrophoresis - Native Mass Spectrometry. *Journal of the American Society for Mass Spectrometry* **2017,** *28* (12), 2614-2634.

111. van de Waterbeemd, M.; Tamara, S.; Fort, K. L.; Damoc, E.; Franc, V.; Bieri, P.; Itten, M.; Makarov, A.; Ban, N.; Heck, A. J. R., Dissecting ribosomal particles throughout the kingdoms of life using advanced hybrid mass spectrometry methods. *Nature Communications* **2018,** *9* (1), 2493.

112. Zhang, H.; Cui, W.; Wen, J.; Blankenship, R. E.; Gross, M. L., Native electrospray and electron-capture dissociation in FTICR mass spectrometry provide top-down sequencing of a protein component in an intact protein assembly. *Journal of the American Society for Mass Spectrometry* **2010,** *21* (12), 1966-1968.

113. O'Brien, J. P.; Li, W.; Zhang, Y.; Brodbelt, J. S., Characterization of Native Protein Complexes Using Ultraviolet Photodissociation Mass Spectrometry. *Journal of the American Chemical Society* **2014,** *136* (37), 12920-12928.

114. Zhou, M.; Liu, W.; Shaw, J. B., Charge Movement and Structural Changes in the Gas-Phase Unfolding of Multimeric Protein Complexes Captured by Native Top-Down Mass Spectrometry. *Analytical Chemistry* **2020,** *92* (2), 1788-1795.

115. Li, H.; Wongkongkathep, P.; Van Orden, S. L.; Ogorzalek Loo, R. R.; Loo, J. A., Revealing Ligand Binding Sites and Quantifying Subunit Variants of Noncovalent Protein

Complexes in a Single Native Top-Down FTICR MS Experiment. *Journal of the American Society for Mass Spectrometry* **2014,** *25* (12), 2060-2068.

116. Cammarata, M. B.; Brodbelt, J. S., Structural characterization of holo- and apo-myoglobin in the gas phase by ultraviolet photodissociation mass spectrometry. *Chemical Science* **2015,** *6* (2), 1324-1333.

117. Belov, M. E.; Damoc, E.; Denisov, E.; Compton, P. D.; Horning, S.; Makarov, A. A.; Kelleher, N. L., From Protein Complexes to Subunit Backbone Fragments: A Multi-stage Approach to Native Mass Spectrometry. *Analytical Chemistry* **2013,** *85* (23), 11163-11173.

118. Greisch, J.-F.; Tamara, S.; Scheltema, R. A.; Maxwell, H. W. R.; Fagerlund, R. D.; Fineran, P. C.; Tetter, S.; Hilvert, D.; Heck, A. J. R., Expanding the mass range for UVPD-based native top-down mass spectrometry. *Chemical Science* **2019,** *10* (30), 7163-7171.

Chapter 2: Native Top-Down Mass Spectrometry with Orbitrap-Based Electron Capture Dissociation Reveals Higher Order Structure Information for Protein Complexes

Boyu Zhao[1], Carter Lantz[1], Benqian Wei[1], Rachel R. Ogorzalek Loo[1,2,3], Joseph A. Loo[1,2,3,4]*

[1]Department of Chemistry and Biochemistry, University of California-Los Angeles, Los Angeles, CA, USA

[2]UCLA-DOE Institute, University of California-Los Angeles, Los Angeles, CA, USA

[3]Molecular Biology Institute, University of California-Los Angeles, Los Angeles, CA, USA

[4]Department of Biological Chemistry, University of California-Los Angeles, Los Angeles, CA, USA

***Corresponding Author**

Joseph A. Loo

University of California-Los Angeles, Los Angeles, CA, United States

Email: jloo@chem.ucla.edu

Abstract

Electron capture dissociation (ECD) is an activation/dissociation technique that utilizes electrons to dissociate the backbone bonds of large biomolecules, including proteins and protein complexes. It is particularly effective for top-down mass spectrometry (TD-MS) to determine the presence of posttranslational modifications and for extending the sequence coverage of TD-MS measurements. When combined with native MS, ECD offers information on the binding site(s) of ligands and the surface topology of proteins and complexes. Conventionally, ECD has been performed on Fourier transform ion cyclotron resonance (FT-ICR) mass spectrometers because the magnetic field used to trap ions can also be used to focus the electron beam for effective ion dissociation. Recently, ECD devices have been adapted to other types of mass spectrometers, including quadrupole time-of-flight (QTOF) and Orbitrap systems. As a result, ECD has become available to a greater number of labs. The present work demonstrates that native TD-MS with ECD on an Orbitrap mass spectrometer provides extensive sequence information for numerous protein complexes. For proteins that do not release fragment ions when subjected to collision induced dissociation (CID), sequence-bearing product ions are measured when subjected to ECD and subsequent CID. In addition, the sites of ECD cleavage appear to correlate well with the protein's solvent accessibility and its native structure.

Introduction

Many proteins assemble into complexes to function in the cell and that structure often relates to function, making precise structure characterization (*e.g.*, stoichiometry and subunit interactions) important. Conventional methods for high-resolution, three-dimensional structure analysis, such as X-ray crystallography[1], electron microscopy (EM)[2] and nuclear magnetic resonance (NMR)[3], can fail due to sample heterogeneity or the limited size range of the technique. Native mass spectrometry (nMS) and native top-down mass spectrometry (nTD-MS) complement high resolution techniques in a selective and sensitive manner[4, 5], delivering information on sequence[6], sites of post-translational modifications (PTMs)[7], stoichiometry and spatial layout[8]. Although nMS and nTD-MS provide only low-resolution structural information, their compatibility with sample heterogeneity[4], wide mass range[9], and high throughput[5] often enable mass spectrometry's utility to surpass that of other techniques. Merging information from nMS experiments with that from other analyses can deliver a comprehensive characterization for an analyte[10].

The range of experimental approaches and applications of tandem MS (MS/MS) to protein complexes continues to expand[11, 12]. As defined[12], nTD-MS entails activating one or more charge states of a noncovalent assembly and analyzing the products, *e.g.*, subunits, multimers, and/or covalently cleaved polypeptides. In complex-down MS[12], a noncovalently bound assembly (one or more charge states) is first activated (usually through in-source dissociation) to release subunits, some of which are charge-state isolated for subsequent activation and dissociation. With either method, isotopically-resolved product ions[13] are assigned to cleavage sites, confirming primary structure, *i.e.*, sequence. Differences between the product ion distributions obtained by nTD-MS and complex-down

MS (pseudo-MS^3)[12] may reveal vestiges of quaternary structure. Popular dissociation methods for TD-MS include collisional induced dissociation (CID)[14], electron-based dissociation (ExD)[15-18], and photon-based dissociation[19, 20]. The product ions formed by top-down MS can be terminal, including either the N-terminus (*a, b,* or *c* products) or the C-terminus (*x, y,* or *z* products). Less commonly considered are internal fragments (*ax, ay, az, bx, by, bz, cx, cy,* or *cz* products) that result from multi-site cleavages of the polypeptide backbone[6, 21, 22]. We have found that higher energy collisional dissociation (HCD), a type of CID that is found on orbitrap analyzers, cleaves some polypeptide bonds directly from noncovalent assemblies[23], in contrast to the sequential process typically envisioned, *i.e.*, unfolded monomer ejection followed by activation and covalent bond cleavage. The timescale for the former pathway appears faster than that of conventional CID[23]. Nevertheless, HCD's utility can be constrained by the extent of backbone cleavage obtained, limiting sequence coverage and PTM localization[24], especially for large complexes.

Electron-based dissociation, such as electron capture dissociation (ECD), electron transfer dissociation (ETD), and electron ionization dissociation (EID), are alternatives that overcome some of those disadvantages. Traditionally performed on Fourier transform-ion cyclotron resonance (FT-ICR)[6, 25] and quadrupole time-of-flight (Q-TOF) MS instruments[26], ECD is now enabled on quadrupole TOF and Orbitrap-based instruments by a commercially available ExD cell[27, 28]. With extended *m/z* isolation and detection, the Orbitrap can perform ECD on a single charge state of a large protein complex. When the precursor transits the confined electron-beam, charge reduction occurs, followed by N-Cα backbone cleavage[18, 26], generating *c*/*z*- terminal and, potentially, internal fragments. One

of ECD's important advantages is that it preserves labile, noncovalent bonds, while cleaving covalent backbone N-Cα bonds, to yield product ions from solvent-exposed regions[29-31]. Thus, ECD is a powerful tool for localizing noncovalent interactions, *e.g.*, ligand binding sites[32].

Here, we report on the coupling of ECD with nTD-MS on an ultra-high mass range Orbitrap analyzer. For native protein complexes up to 464 kDa, nTD-MS with ECD returns structural information from protein complexes, and the data are comparable to previous FT-ICR measurements.

Experimental

Sample preparation. Malate dehydrogenase (MDH) from pig (66 kDa), rabbit aldolase (158 kDa), β-galactosidase (β-GTD) from *E. coli* (464 kDa), glutamate dehydrogenase (GDH) from bovine liver (334 kDa), yeast alcohol dehydrogenase (yADH) (147 kDa), and 50 kDa and 100 kDa Millipore Amicon Ultra filters were purchased from Sigma-Aldrich (St. Louis, MO, USA). Samples were buffer exchanged with 50 kDa or 100 kDa filters into 150 mM ammonium acetate (pH ca. 6.8) to a final concentration of 5-15 µM.

Native Top-Down and Complex-Down ECD MS. All experiments were performed on a Thermo Fisher Scientific Q Exactive Ultra-High Mass Range (UHMR) Orbitrap mass spectrometer with an ExD cell developed by e-MSion (Corvallis, OR, USA). The ExD cell is mounted between the split lens/ion selection quadrupole and the C-trap of the UHMR Orbitrap. The ExD cell itself is a cylinder containing two high-temperature magnets and a set of electrostatic lenses arranged symmetrically around the central hot electron-emitting filament. Thermal electrons are produced by a hot circular rhenium wire filament located

in the middle of the ExD cell, encircling the ion beam. The high temperature magnets provide a magnetic field that confine the high densities of low energy electrons to the ion flight path in the ExD cell.

Protein solutions were loaded into Pt-coated borosilicate capillaries on a nanospray ionization source and electrosprayed at 0.7 – 1.7 kV, 200 ℃. The S-lens RF was set at 100 eV. In-source CID was set over a range of 40-120 eV for complex-down experiments. A single charge state or a few charge states were isolated by the quadrupole for top-down or complex-down MS for each protein complex. The ions were transferred into the ECD cell, where they were subject to electron capture, then into the HCD cell for post-ECD collisional activation, i.e., activated ion ECD or EChcD. The filament current was set at 2.23 A. The HCD collision energy was optimized to minimize the generation of b/y ions. Additional details of ExD cell (Figure S1) tuning parameters are provided in the Supporting Information (Table S2). All spectra were acquired at 100,000 resolution (*m/z* 400) with a noise threshold set to 3. Each spectrum is a result of an averaging 500 scans.

Data Analysis. All spectra were deconvolved using BioPharma Finder 5.0 (ThermoFisher Scientific, Waltham, USA). Deconvolved peaks were assigned by ClipsMS 2.0.0[33] with an error tolerance of 3 ppm. Sequence assignments accommodated the major ECD (*c, c+H, c-H, z, z+H, z-H, cz, cz+H, cz-H*) and HCD (*b, y*) ion types without considering neutral losses ions, except when explicitly mentioned. N-terminal acetylation and a V58T mutation were included in the fragmentation assignments for yADH. Terminal and internal fragments were manually validated by confirming that measured isotope distributions matched closely with the theoretical distributions for each fragment ion. An example of spectra for a validated internal fragment are shown in Figure S2.

Solvent Accessible Surface Area (SASA) Calculation. SASA was calculated by uploading the deposited Protein Data Bank (PDB) file for each protein complex to the website http://cib.cf.ocha.ac.jp/bitool/ASA/. This site calculated accessible surface area by Shrake and Rupley's method[34]. Relative accessible surface area was determined by dividing the sum of accessible surface areas by the maximum accessible surface area. The latter value was obtained by modeling each side chain in its extended form[35].

Results and Discussion

Previous reports of nTD-MS using ECD suggests that information can be returned for protein complexes that is relevant to its three-dimensional structure.[12, 24, 31, 36] For example, ECD-MS of homotetrameric aldolase reveals primarily z-ions, consistent with a more solvent-exposed C-terminus.[36] To determine if ECD using an orbitrap instrument can also provide not only sequence information but also reveal conformation-sensitive product ions, nTD-ECD/MS experiments were performed on a series of protein complexes. This data was compared to complex-down MS experiments[12], in which a subunit of from the protein complex is ejected by in-source CID, and this ejected subunit is subsequently subjected to ECD fragmentation. In principle, released protein subunits via complex-down MS should be unfolded and/or have more surface area exposed compared to the intact native complex.

Native Top-Down ECD of Aldolase

Aldolase is an enzyme that reversibly catalyzes cleavage of fructose-1,6-biphosphate to dihydroxyacetone phosphate (DHAP) and glyceraldehydes-3-phosphate in glycolysis[37]. Each subunit has 363 amino acids with an average mass of 39,212 Da, and the measured mass of its corresponding tetrameric complex is 156,939 Da. Figure S3 shows the mass

spectrum of the aldolase tetramer under native solution conditions. The 26+ charge state ion was isolated and subjected to ECD aided by post-ECD collisional activation of 70 V to disrupt any intramolecular interactions preventing ECD fragments from being released and observed.

Figure 1 shows the nTD ECD spectrum of the aldolase tetramer. Product ions resulting from the cleavage of N-Cα bonds were found in the *m/z* 500-3200 region and assigned. nTD-MS yielded 57 z-ions (bearing the C-terminus) from residues 215-350, but only 2 c-ions and 10 cz-internal fragments, resulting in a sequence coverage of 21%. (Sequence coverage in TD-MS experiments is defined as the number of inter-residue cleavages relative to the total number of inter-residue cleavages defined by the protein's amino acid sequence.) The relatively high proportion of z-ions in the aldolase native ECD spectrum is similar to previous results obtained by HCD on the same instrument[23]. The three-dimensional structure of aldolase tetramer (PDB 1ADO)[38] is shown in Figure 1D. Mapping fragments onto the crystal structure shows that the C-terminal region is more solvent exposed than the interface-forming N-terminal region.

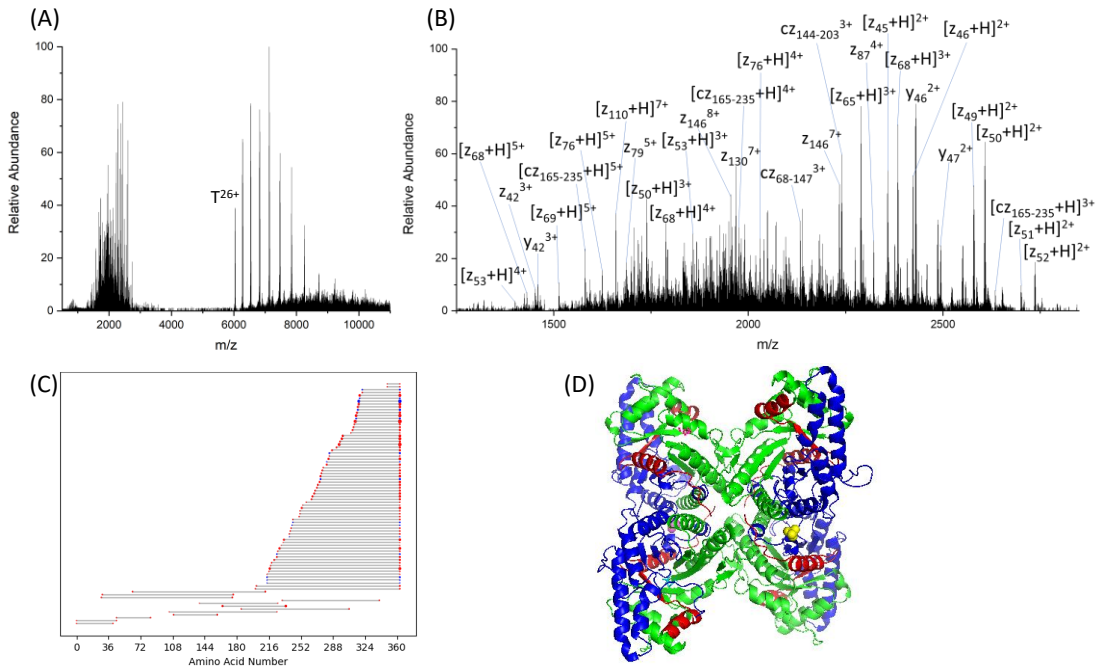

Figure 1. (A) nTD ECD mass spectrum of aldolase tetramer 26+ charge state. (B) Expanded region from m/z 1000 to 3000. (C) Fragment location map of aldolase tetramer with ECD. ECD c/z-fragments are indicated by red dots, HCD b/y fragments are shown by blue dots; the size of the dots represents the relative intensity of each fragment. (D) ECD fragments mapped onto the aldolase tetramer crystal structure. N-terminal fragments are colored in red, C-terminal fragments in blue, and protected region in green.

To demonstrate that nTD-MS probes the native structures of protein/complexes, complex-down MS of the aldolase tetramer was performed by using in-source CID to release a monomer subunit. The resulting 15+-charged released monomer subunit was subjected to ECD; both N- and C-terminal fragments of aldolase were generated: 9 c- ions, 16 z-ions and 11 cz internal fragment ions, covering 11% of the sequence (Figure 2). The lower sequence coverage for complex-down MS compared to native top-down MS could reflect the lower intensity of the monomer precursors in the former (6.57E3) compared to tetramer precursors in the latter workflow (1.12E4), but it more likely reflects the quaternary structure of aldolase. Previous activation of this same protein by HCD also delivered higher

sequence coverage by nTD relative to complex-down MS on the same instrument[23].

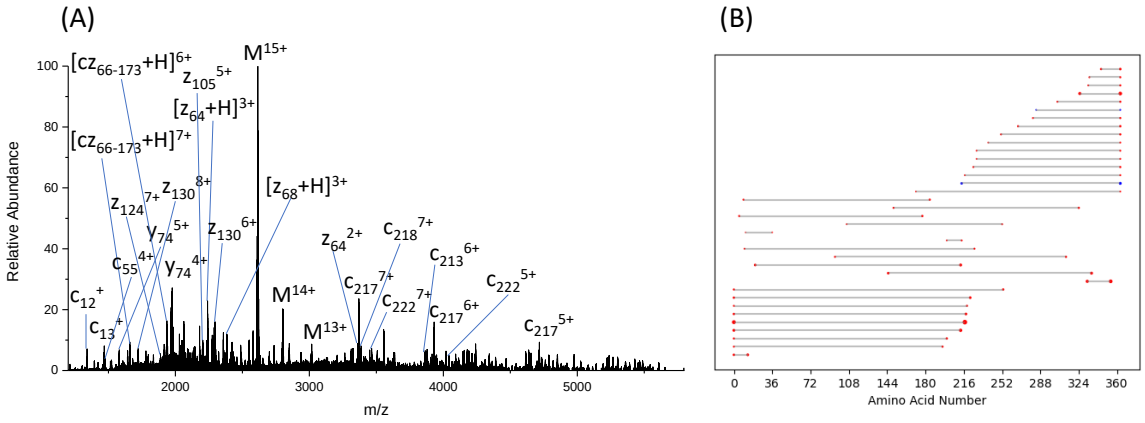

Figure 2. (A) Complex-down MS of aldolase 15+ charged monomer with ECD. (B) Fragment location map of aldolase monomer with ECD. ECD fragments showed in red dots, HCD fragments showed in blue dots.

Surprisingly, even though the complex-down precursor is a charge-enriched 15+ subunit, its product ions in common with nTD of 26+ tetramers (*i.e.*, z_{68} and z_{130}) carry charge amounts similar to those in nTD. The z_{68} product was observed with 3-5 charges by nTD and 3 charges by complex-down. Likewise, z_{130} was observed bearing 6-8 charges by complex-down and 7 charges by nTD. These similar charge densities are not consistent with the typical rationalizations for monomer ejection based on the dominating effects of charge repulsion and proton migration[39]. Likewise, the higher sequence coverage delivered by nTD compared to complex-down might be unexpected, given that the dominant paradigm assumes that ejected monomers are unfolded. These results should encourage the native mass spectrometry field to revisit long-held assumptions about gas phase structures and forces.

To compare the complex's surface accessibility to the nTD ECD data, we mapped c-ions

onto the crystal structure in red, z-ions in blue and protected regions in green (Figure 1D). The nTD ECD product ions are mainly located on the exterior of the tetramer. To further understand these results, we calculated relative solvent accessible surface area (SASA) and B-factors of each residue. In X-ray crystallography, the B-factor indicates the flexibility and dynamics of a polypeptide chain[40, 41]; a higher B-factor indicates greater side chain flexibility. The SASA of proteins is a decisive factor in protein folding and stability, and is defined as the surface around a protein created by rolling a solvent sphere over the van der Waals surface of the molecule[42]. Relative SASA of each residue was calculated as described[35]. A higher relative SASA indicates more solvent accessibility. We averaged B-factor and relative SASA separately for all four chains, plotting the average B-factor (Figure S4A) and averaged relative SASA (Figure S4B) as a function of the residue location, and found that their correlation to fragmentation was similar, but incomplete. Clearly, other factors contribute to ECD fragmentation and its efficiency, *e.g.*, electron density distribution on the protein complex surface, N-terminal proline effects[43, 44], and strength of noncovalent interactions. The calculations confirm that regions of the sequence with low solvent accessibility correspond to regions where limited or no cleavage is observed. These results also support the idea that nTD ECD cleaves without altering the native conformation of protein complexes. Direct ECD fragmentation of some protein complexes can reveal regions of solvent accessibility.

For the aldolase complex, in comparing these Orbitrap-based ECD fragmentation patterns to our previously published data that applied ECD on a Bruker 15T FT-ICR mass spectrometer[25, 36], we note that the FT-ICR products mainly covered the solvent-exposed C-terminus, providing 20% sequence coverage[25]. The largest ECD fragment generated by

FT-ICR was z_{168}, while the largest fragment generated by Orbitrap-based ECD is z_{162}. In sequence coverage and product ion locations, Orbitrap-based ECD fragmentation efficiency is similar to FT-ICR ECD. However, the entire charge state distribution was subjected to ECD with the FT-ICR, due to its quadrupole upper isolation limit (*m/z* ~6000)[25], whereas we were able to isolate a single precursor charge state (26+) on the Orbitrap, significantly reducing chemical noise and the impact of potential impurities, potentially increasing signal-to-noise ratio.

Native Top-Down ECD of Glutamate Dehydrogenase (GDH)

To further examine the potential of Orbitrap-based ECD fragmentation for revealing structural information from larger protein complexes, intact (bovine) GDH homohexamer (334 kDa) was subjected to ECD. GDH reversibly converts L-glutamate into β-ketoglutarate using NADP(H) or NAD(H). GDH is a dimer of trimers, and each subunit has 501 amino acids with an average mass of 56 kDa, and the measured mass of its corresponding complex is 335,143 +/- 707 Da (Figure S5). Perhaps due to its large mass and strong inter- and intra-subunit gas-phase interactions, we were unable to decompose hexameric GDH by in-source dissociation (ISD) or to generate fragments by HCD, colliding with either N_2 or Ar. ECD and ISD-ECD were similarly unable to generate product ions. Ultimately, c/z-products were obtained by applying 50 V in-source activation, isolating and subjecting the hexamer 34+-36+ charge states to ECD succeeded by 270 V collisional activation (HCD). nTD-MS of GDH hexamer with this ISD-ECD-HCD strategy (Figure 3) yielded only 17 z-fragments from residues 399-483, and 28 cz-internal fragments, resulting in 12% sequence coverage. We also found y-fragment ions from the post-ECD activation. These results suggest that strong noncovalent interactions around the

N-termini region prevent the release of N-terminal products. The fact that only z-ions presented in the native ECD spectrum of GDH is similar to results derived from infrared multiphoton dissociation (IRMPD) experiments performed on the 15T FT-ICR previously[25]. This result is also consistent with the crystal structure of GDH (PDB 1HWZ); Asp6 and Asn8 form hydrogen bonds and salt bridges to Lys329[45], which therefore prevent fragments from departing from the N-terminal region. We also compared the sequence coverage of GDH hexamer between FT-ICR ECD and Orbitrap-based ECD. FT-ICR ECD did not yield fragments from the GDH hexamer, whereas IRMPD generated fragments mainly from the C-terminus, to give 24% sequence coverage[25].

The GDH hexamer appears to be an example of a gas-phase complex that is highly stable to activation/dissociation methods because strong intra-molecular forces that prevent the release of product ions. Despite using in-source activation combined with post-ECD ion heating, *e.g.*, EChcD, a sequence coverage of only 12% could be achieved. A slightly higher sequence coverage was measured previously using infrared heating with FT-ICR mass spectrometry. Future work using IRMPD interfaced to the Orbitrap could result in higher sequence coverage. Nonetheless, the resulting products remain consistent with nTD-MS probing the outer surface of protein complexes.

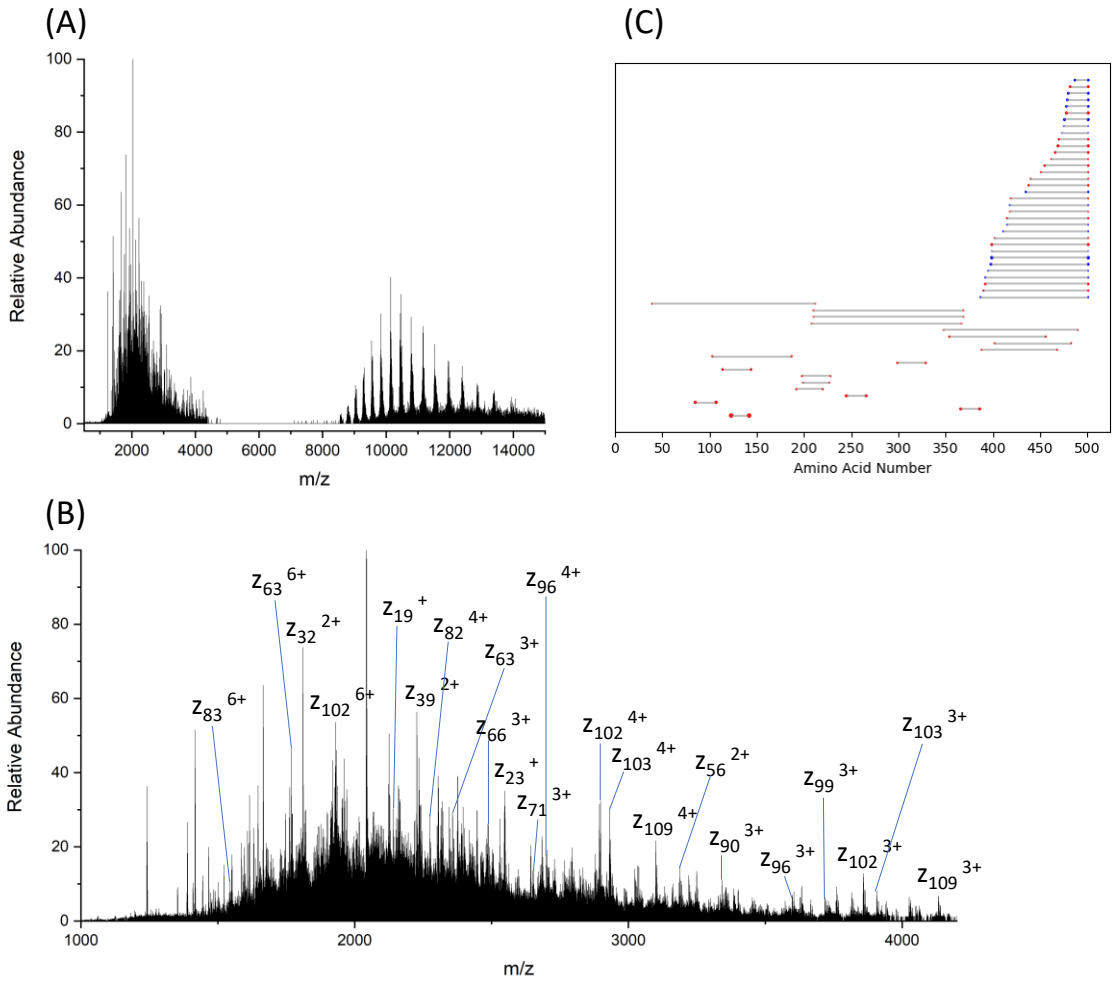

Figure 3. (A) nTD-MS with EChcD of GDH hexamer 34+ to 36+ charge state. (B) Expanded fragmentation region from m/z 1000 to 4200. (C) Fragment location map of GDH hexamer. ECD fragments showed in red dots, HCD fragments showed in blue dots.

Orbitrap-Based ECD Fragmentation on Several Other Protein Complexes.

A range of other homomeric protein complexes were examined (Table S1). Complex-down ECD fragmentation of yeast alcohol dehydrogenase (yADH) 147 kDa tetramer (Figure S6A) revealed 42 N-terminal c-fragment ions, 7 C-terminal z-fragment ions and 10 cz internal fragment ions, resulting in 19% sequence coverage. In contrast, the nTD ECD spectrum (Figure S7A) of yADH revealed 50 N-terminal c-fragments from residues 15-

123, and 30 cz-internal fragments, resulted in 29% sequence coverage, consistent with the yADH crystal structure (PDB 4W6Z)[46] showing that the N-terminus is more solvent exposed than the C-terminus (Figure S7D). Our B-factor and relative SASA calculations also showed similar trends in extent of fragmentation (Figure S8). Moreover, the fragmentation patterns also revealed N-terminal acetylation, and a V58T proteoform. The higher sequence coverage in nTD-MS compared to complex-down could be attributed to the higher precursor ion intensity. Comparing to our previous HCD study on yADH[23], the observation that complex-down by ECD generated fewer C-terminal fragments than complex-down by HCD could suggest that the monomers ejected in-source from collisionally activated complexes are *not* fully unfolded, as they need additional rearranging to eject C-terminal products.

For the malate dehydrogenase (MDH) 66 kDa homodimer, 50 c-ion products, 27 z-ion products and 20 cz internal fragment ions were generated by complex-down MS (Figure S9A), resulting in 35% sequence coverage. nTD-MS revealed 41 z-ions from residues 234-314, and 8 cz-internal fragments (Figure S10A), resulting in 19% sequence coverage. The crystal structure of MDH (PDB 1MLD[47], Figure S10D) indicates that the C-terminus is solvent exposed and not involved in monomer interactions, consistent with our B-factor and relative SASA calculation (Figure S11), and the nTD-MS measurement revealing only C-terminal fragments.

The largest complex examined in this study was β-galactosidase (β-GTD) from *E. coli* (464 kDa). The β-GTD homotetramer did not release monomer ions from in-source dissociation for complex-down fragmentation; however, ECD of the native complex still returned a few product ions for structural information. Native ECD of β-GTD revealed 7 z-ions, and 1 c-

ion (Figure S12). The few fragments generated from N- and C-termini suggest both termini are not solvent-exposed; this suggestion aligns with the crystal structure (PDB 1F4A), indicating that both N- and C-termini are involved in interaction interfaces.[48, 49] This result is also consistent with our previous study on a 15T FT-ICR instrument, finding that ECD generated no fragments, whereas CID released N-terminal fragments and IRMPD released C-terminal fragments.[25]

Conclusions

Here we demonstrated that Orbitrap-based ECD fragmentation can reveal sequence, modification, and structure information on large proteins and protein complexes, including particularly refractive ones. Native TD-MS of the complexes with ECD reveals fragments that correspond to the solvent exposed regions, which contrasts with fragmentation of the ejected monomer (complex-down) by ECD. Orbitrap-based ECD fragmentation increased the sequence coverages for many of the protein complexes examined, perhaps due to enhanced fragmentation efficiency compared to the one with FT-ICR. It is challenging to sort out all of the factors that contribute to ECD effectiveness for a given analyte and for specific instrumentation systems. The ExD cell coupled to the Orbitrap is a unique design that allows nearly all of the ions to intersect with the electron beam. This geometry is very different compared to the one used in the FT-ICR instrument; a beam of negatively charge electrons is directed towards the positively charge analyte stream in the focusing quadrupole; ECD product ions are subsequently injected into the ion cyclotron resonance cell for detection.

However, our results strongly suggest that nTD-MS using an Orbitrap/ECD system is

highly effective for generating information that can be used to confirm protein structural features. This method can be broadly integrated with other biomolecule structural analysis techniques, for example, cryo-electron microscopy. This potential integration will provide an experimental platform for helping to solve important structural and functional details of protein complexes, such as ligand and substrate binding, functional dynamics, and protein interfacial binding regions.

Acknowledgment

We acknowledge support from the US National Institutes of Health (R35GM145286) and the US Department of Energy (DE-FC02-02ER63421). C.L. acknowledges support from the Ruth L. Kirschstein National Research Service Award program (GM007185).

Chapter 2: Supporting Information

Supplementary Figures

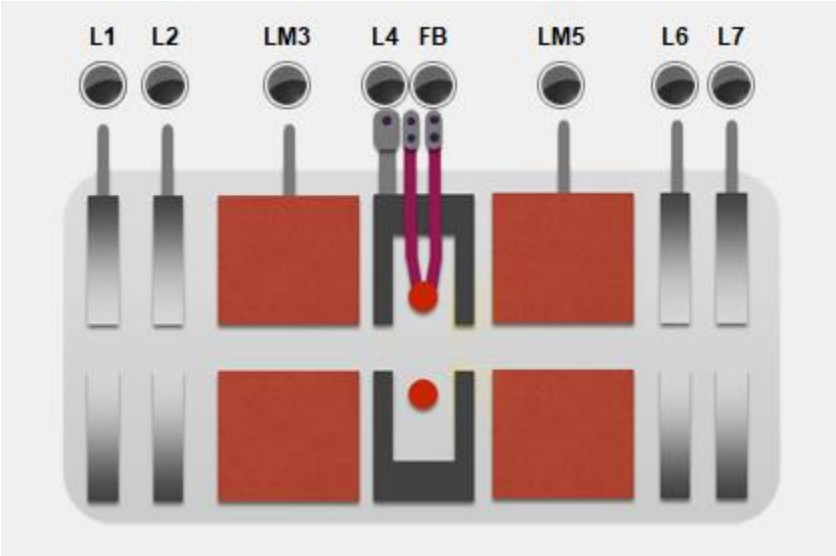

Figure S1. Schematic of the electromagnetostatic ExD cell.[1]

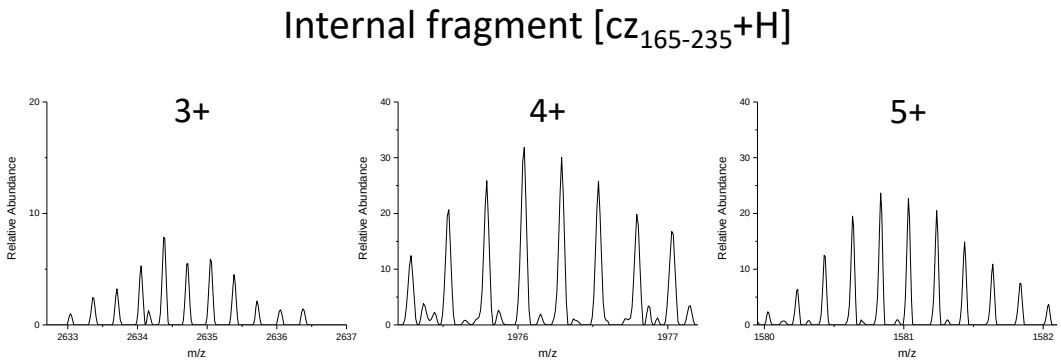

Figure S2. Example of the internal fragment, three charge states were observed.

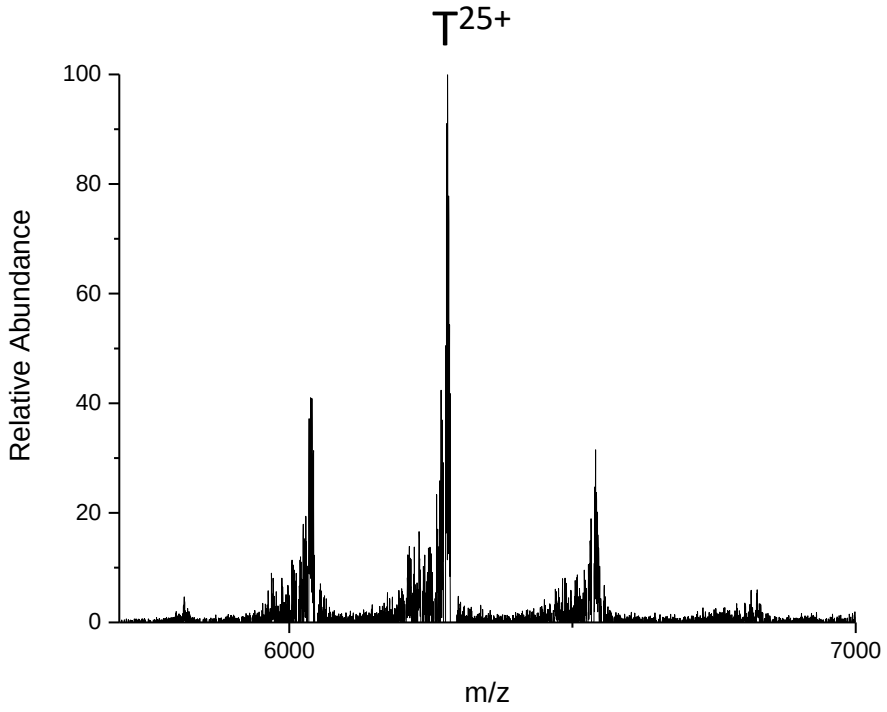

Figure S3. Native mass spectrum of the aldolase homotetramer.

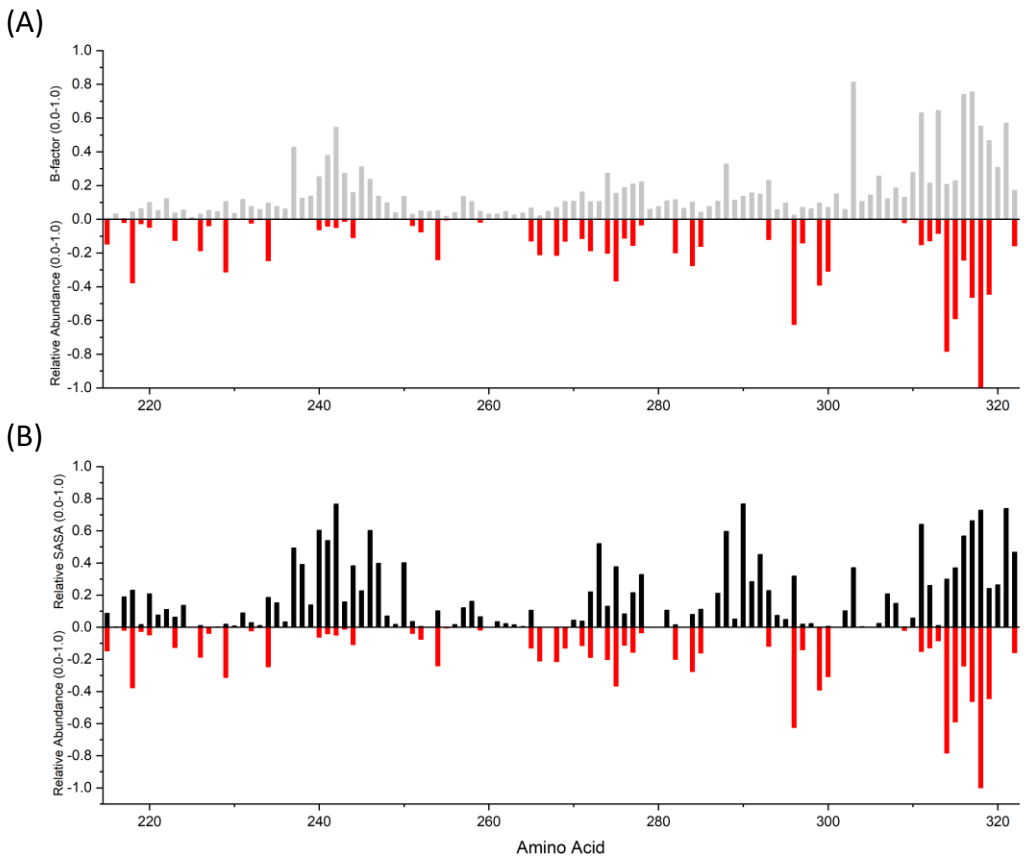

Figure S4. (A) Averaged B-factor in gray and (B) averaged relative SASA in black of aldolase compared to fragmentation intensity in red of each residue from residue 215 to 322.

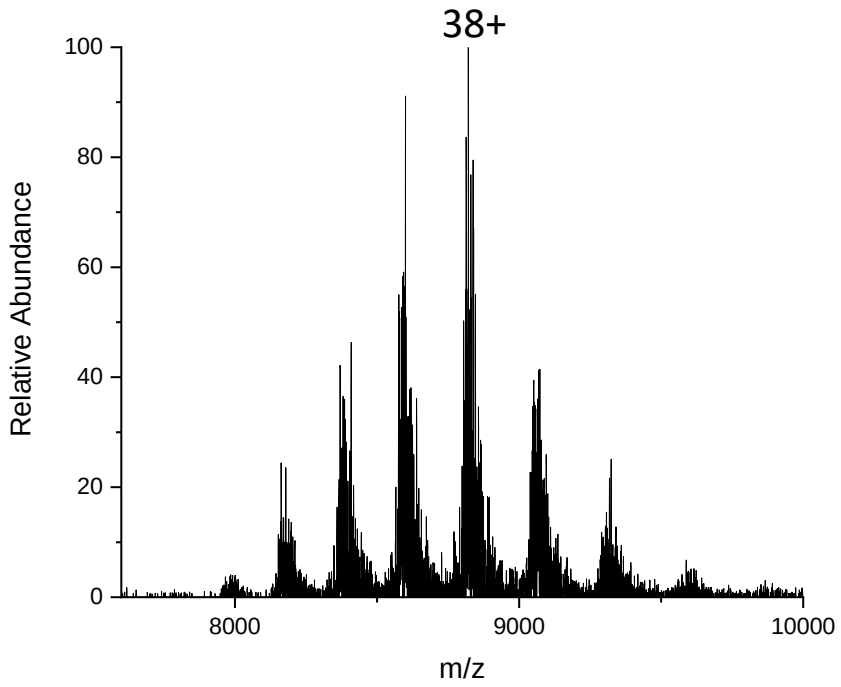

Figure S5. Native mass spectrum of GDH homohexamer.

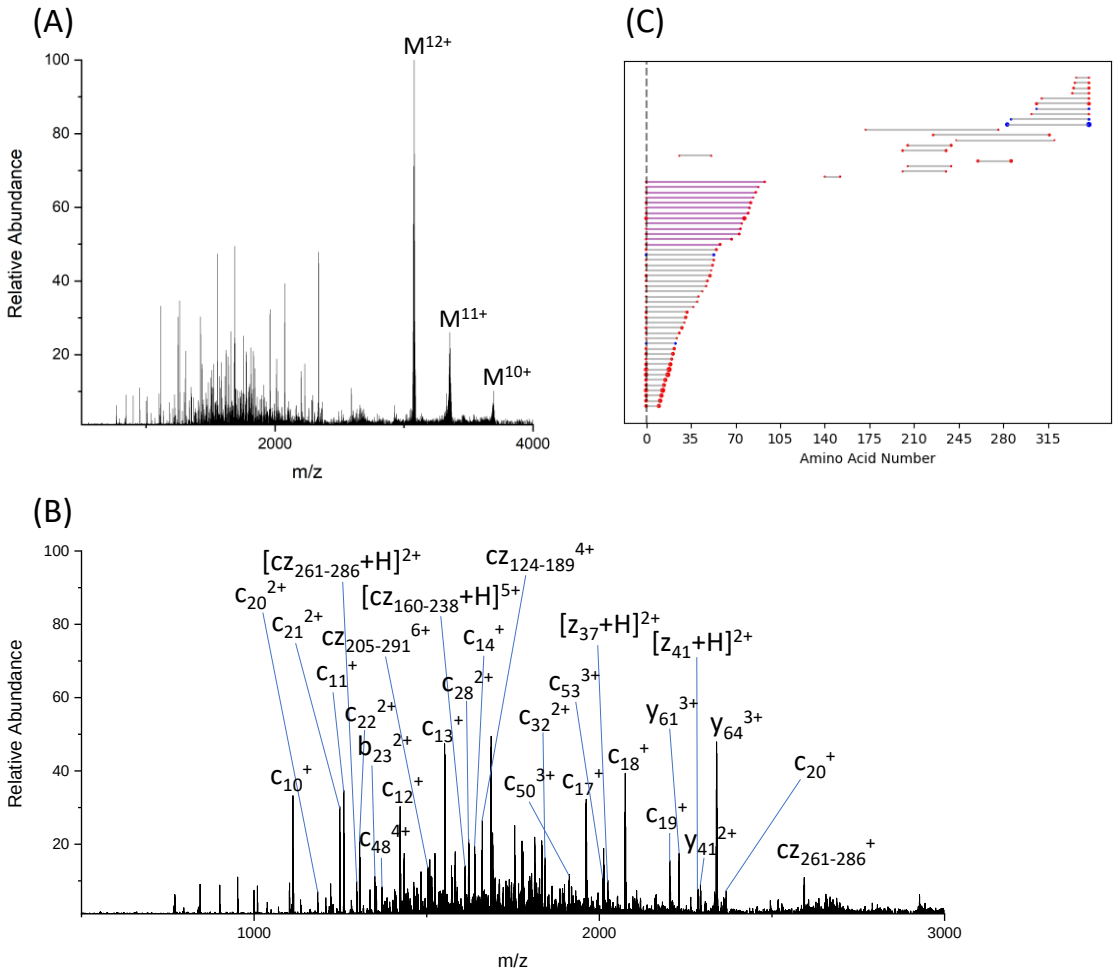

Figure S6. (A) Complex-down mass spectrum of ADH 12+ charged monomer with ECD; (B) zoomed-in fragmentation region from *m/z* 500 to 3000; (C) fragment location map of ADH monomer with ECD. ECD fragments labeled with red dots, HCD fragments labeled with blue dots, purple lines indicate V58T mutation, the vertical dotted line represents N-terminal acetylation.

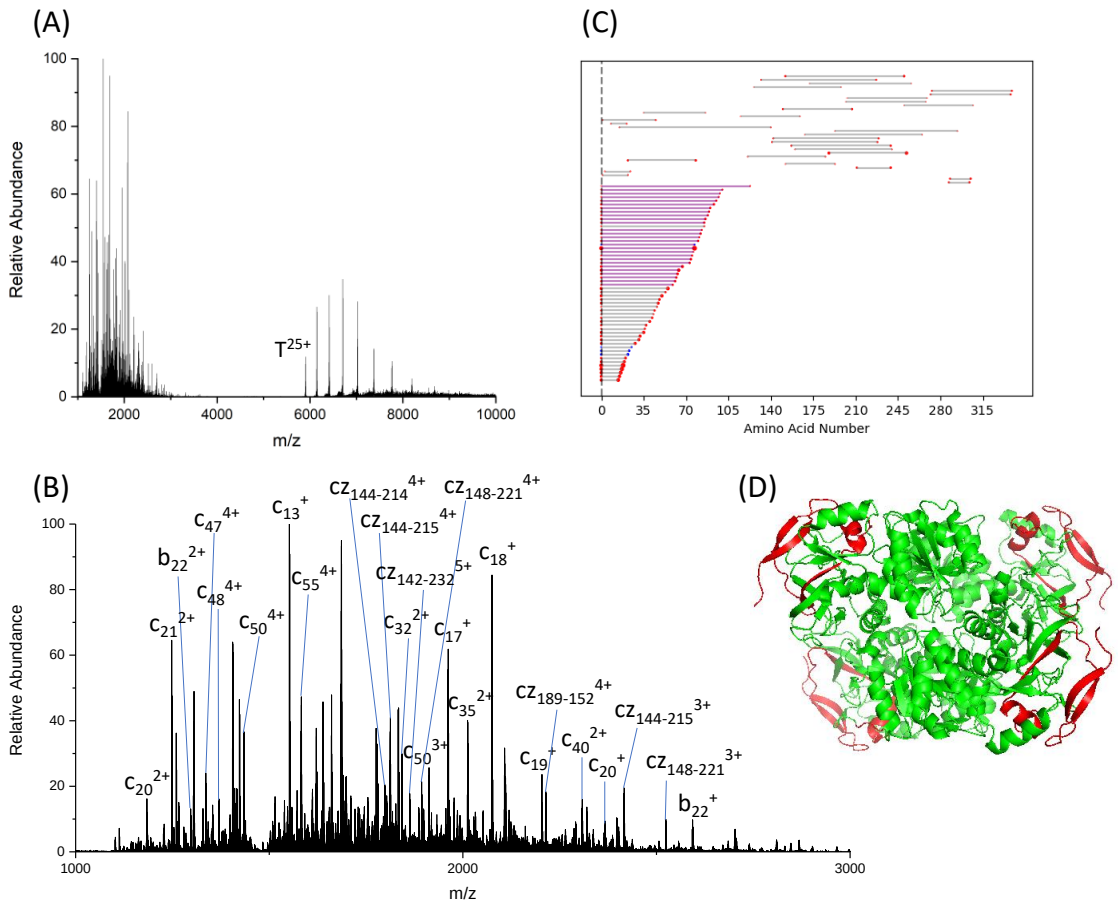

Figure S7. (A) nTD-MS with ECD of ADH tetramer 25+ charge state; (B) zoomed-in fragmentation region from m/z 1000 to 3000; (C) fragment location map of ADH tetramer with ECD. ECD fragments labeled with red dots, HCD fragments labeled with blue dots, purple lines indicate V58T mutation, the vertical dotted line represents N-terminal acetylation. (D) ECD fragments mapped onto ADH tetramer crystal structure. N-terminal fragments colored in red, and protected region colored in green.

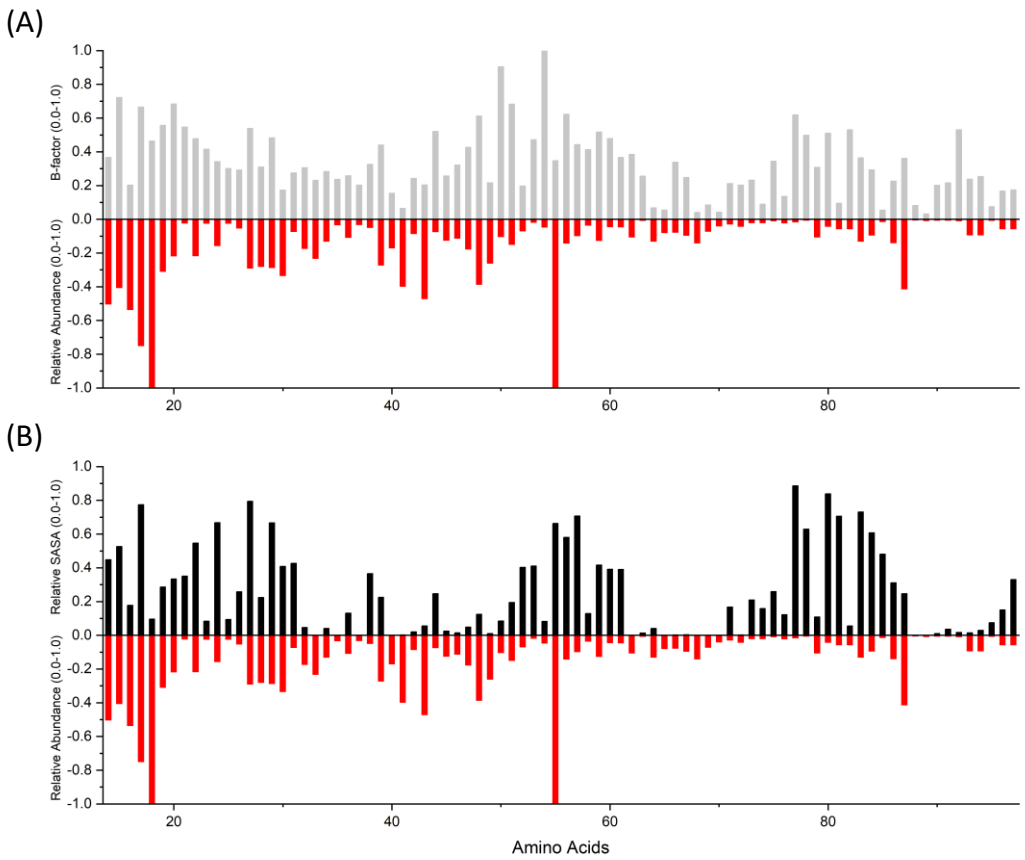

Figure S8. (A) Averaged B-factor in gray and (B) averaged relative SASA in black of yADH compared to fragmentation intensity in red of each residue from residue 14 to 97.

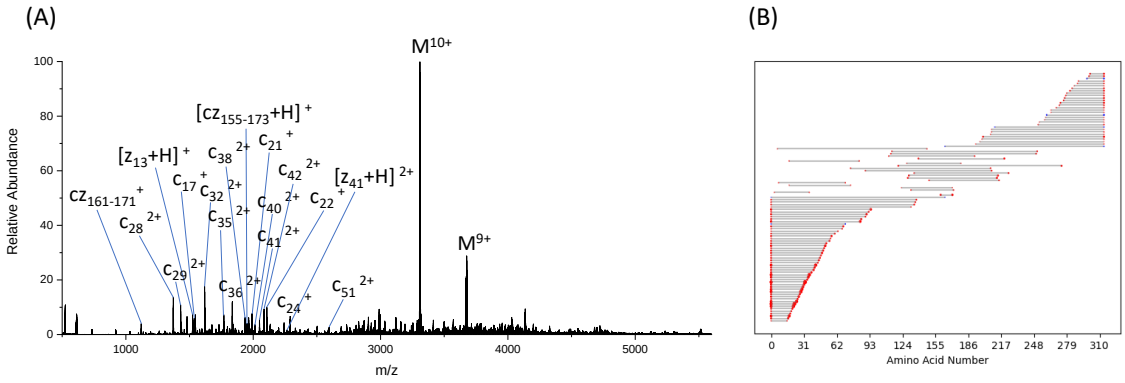

Figure S9. (A) Complex-down mass spectrum of MDH 10+ charged monomer with ECD; (B) fragment location map of MDH monomer with ECD. ECD fragments labeled with red dots, HCD fragments labeled with blue dots.

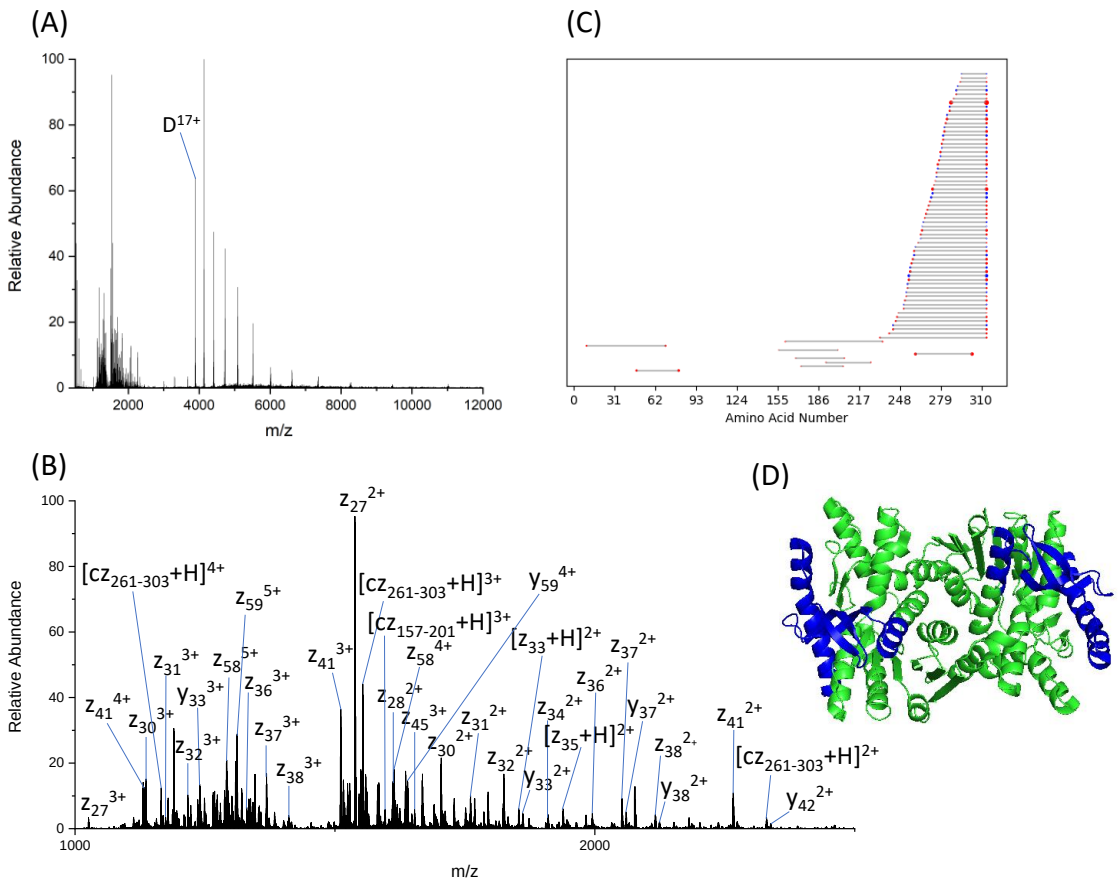

Figure S10. (A) nTD ECD MS of MDH dimer 17+ charge state; (B) zoomed-in fragmentation region from *m/z* 1000 to 2500; (C) fragment location map of MDH dimer with ECD. ECD fragments are labeled with red dots, HCD fragments are labeled with blue dots. (D) ECD fragments mapped on MDH dimer crystal structure. C terminal fragments in blue, and protected region in green.

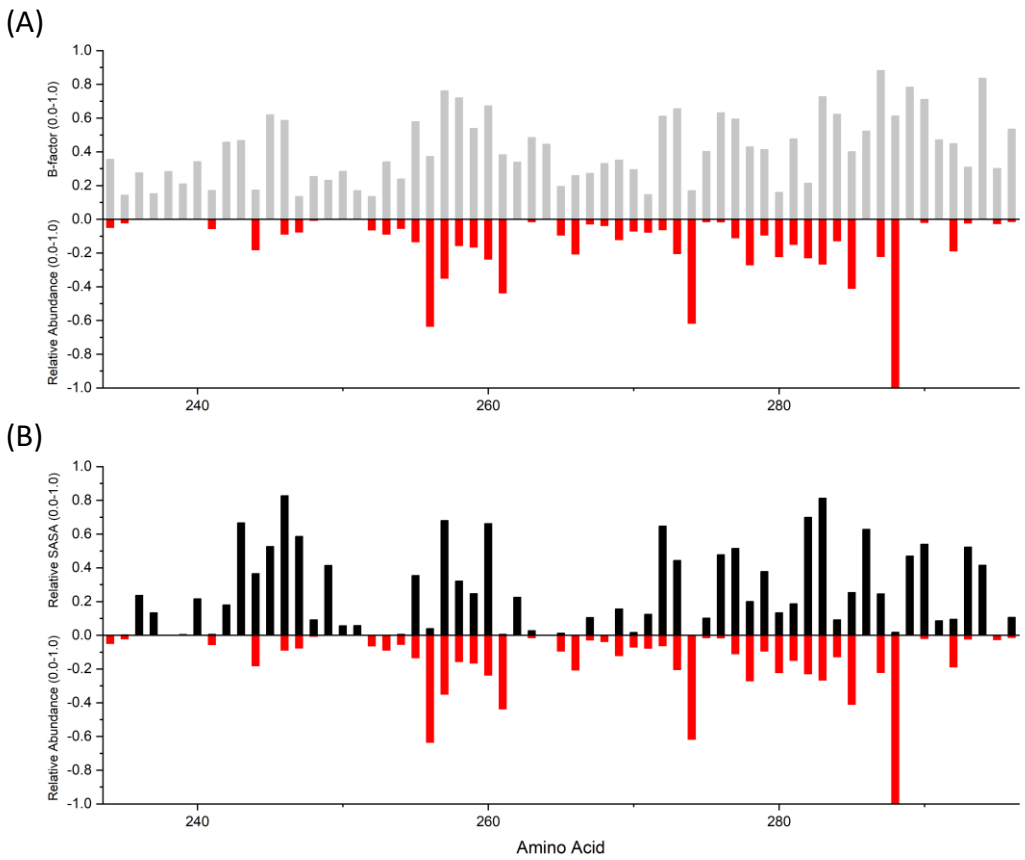

Figure S11. (A) Averaged B-factor in gray and (B) averaged relative SASA in black of MDH compared to fragmentation intensity in red of each residue from residue 234 to 296.

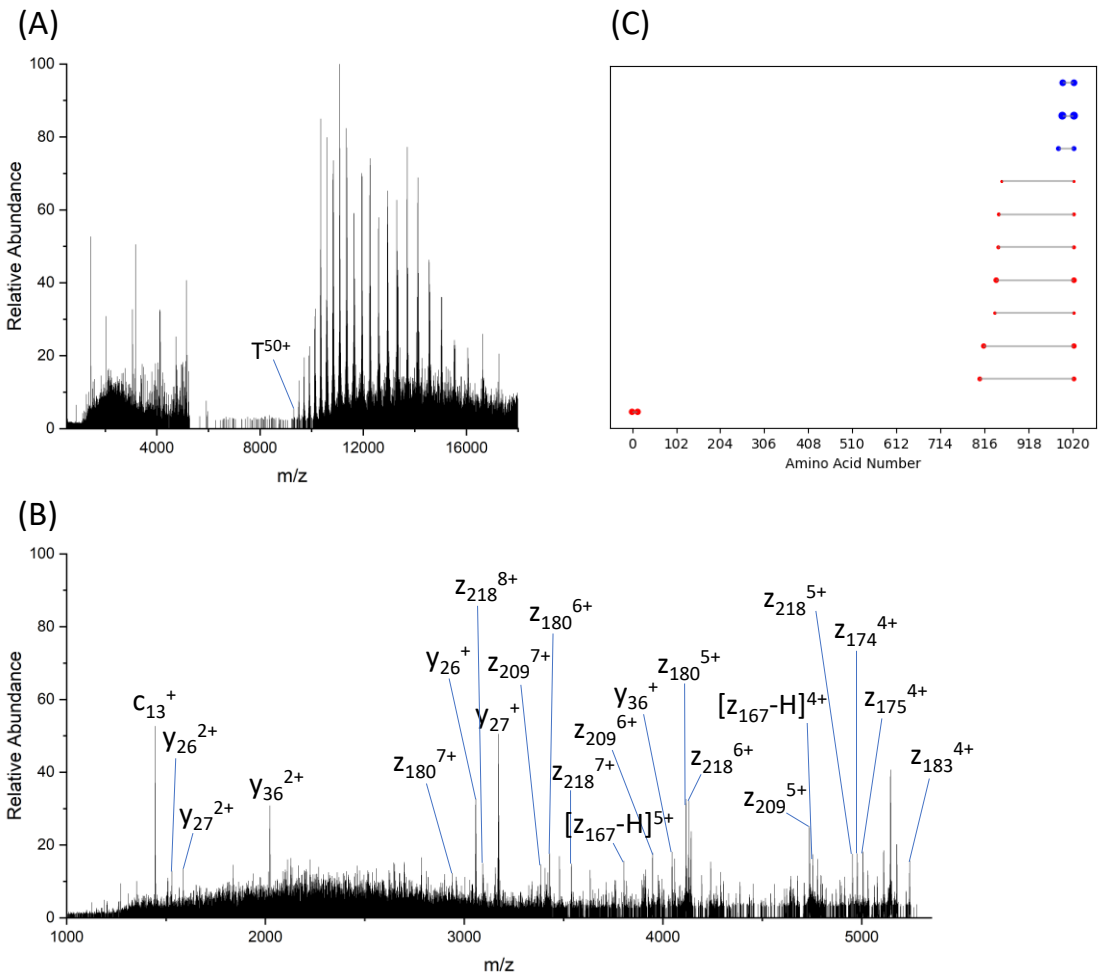

Figure S12. (A) nTD ECD MS of β-GTD tetramer 50+ to 52+ charge states; (B) zoomed-in fragmentation region from m/z 1000 to 5350; (C) fragment location map of β-GTD tetramer with ECD. ECD fragments are labeled with red dots, HCD fragments are labeled with blue dots.

Supplementary Tables

Table S1. Information on the protein complexes analyzed in this study.

General Information				Native TD-MS Fragmentation			Complex-Down Fragmentation			
Complex	Complex Type	Complex Mass (Da)	Monomer Mass (Da)	# c-frags	# z-frags	Sequence Coverage	Monomer Released w/ ISD	# c-frags	# z-frags	Sequence Coverage
Aldolase	Homotetramer	156,939	39,212	2	57	21%	Yes	9	16	11%
GDH	Homohexamer	335,143	55,726	0	17	12%	No	N/A	N/A	N/A
ADH	Homotetramer	147,472	36,738	50	0	29%	Yes	42	7	19%
MDH	Homodimer	66,165	33,081	0	41	19%	Yes	50	27	35%
β-GTD	Homotetramer	467,232	116,351	1	7	1%	No	N/A	N/A	N/A

Table S2. ExD cell parameters for the protein complexes analyzed in the study.

Protein Complex	L1	L2	LM3	L4	FB	LM5	L6
Aldolase	-0.82	-40.0	1.0	4.11	-8.0	1.0	-40.0
GDH	-1.27	-52.0	4.7	12.2	0.8	4.7	-52.0
ADH	-0.82	-40.0	1.0	4.11	-8.0	1.0	-40.0
MDH	-2.0	-50.0	10.5	11.0	2.5	10.5	-50.0
β-GTD	-1.0	-55.0	4.1	22.0	0.5	4.1	-55.0

Reference

1. Shaw, J. B.; Malhan, N.; Vasil'ev, Y. V.; Lopez, N. I.; Makarov, A.; Beckman, J. S.; Voinov, V. G., Sequencing Grade Tandem Mass Spectrometry for Top–Down Proteomics Using Hybrid Electron Capture Dissociation Methods in a Benchtop Orbitrap Mass Spectrometer. *Analytical Chemistry* **2018,** *90* (18), 10819-10827.

References

1. Garman, E. F., Developments in X-ray Crystallographic Structure Determination of Biological Macromolecules. *Science* **2014,** *343* (6175), 1102-1108.

2. Bai, X.-C.; McMullan, G.; Scheres, S. H., How cryo-EM is revolutionizing structural biology. *Trends in biochemical sciences* **2015,** *40* (1), 49-57.

3. Clore, G. M.; Gronenborn, A. M., Structures of Larger Proteins in Solution: Three- and Four-Dimensional Heteronuclear NMR Spectroscopy. *Science* **1991,** *252* (5011), 1390-1399.

4. Heck, A. J. R., Native mass spectrometry: a bridge between interactomics and structural biology. *Nature Methods* **2008,** *5* (11), 927-933.

5. van Duijn, E., Current limitations in native mass spectrometry based structural biology. *Journal of the American Society for Mass Spectrometry* **2010,** *21* (6), 971-978.

6. Zenaidee, M. A.; Lantz, C.; Perkins, T.; Jung, W.; Loo, R. R. O.; Loo, J. A., Internal Fragments Generated by Electron Ionization Dissociation Enhance Protein Top-Down Mass Spectrometry. *J Am Soc Mass Spectrom* **2020,** *31* (9), 1896-1902.

7. Shi, S. D. H.; Hemling, M. E.; Carr, S. A.; Horn, D. M.; Lindh, I.; McLafferty, F. W., Phosphopeptide/Phosphoprotein Mapping by Electron Capture Dissociation Mass Spectrometry. *Analytical Chemistry* **2001,** *73* (1), 19-22.

8. van den Heuvel, R. H.; Heck, A. J., Native protein mass spectrometry: from intact oligomers to functional machineries. *Curr Opin Chem Biol* **2004,** *8* (5), 519-26.

9. Karabacak, N. M.; Li, L.; Tiwari, A.; Hayward, L. J.; Hong, P.; Easterling, M. L.; Agar, J. N., Sensitive and specific identification of wild type and variant proteins from 8 to 669 kDa using top-down mass spectrometry. *Mol Cell Proteomics* **2009,** *8* (4), 846-

56.

10. Lössl, P.; van de Waterbeemd, M.; Heck, A. J., The diverse and expanding role of mass spectrometry in structural and molecular biology. *The EMBO Journal* **2016,** *35* (24), 2634-2657.

11. Kelleher, N. L.; Lin, H. Y.; Valaskovic, G. A.; Aaserud, D. J.; Fridriksson, E. K.; McLafferty, F. W., Top Down versus Bottom Up Protein Characterization by Tandem High-Resolution Mass Spectrometry. *Journal of the American Chemical Society* **1999,** *121* (4), 806-812.

12. Lermyte, F.; Tsybin, Y. O.; O'Connor, P. B.; Loo, J. A., Top or Middle? Up or Down? Toward a Standard Lexicon for Protein Top-Down and Allied Mass Spectrometry Approaches. *Journal of the American Society for Mass Spectrometry* **2019,** *30* (7), 1149-1157.

13. Haverland, N. A.; Skinner, O. S.; Fellers, R. T.; Tariq, A. A.; Early, B. P.; LeDuc, R. D.; Fornelli, L.; Compton, P. D.; Kelleher, N. L., Defining Gas-Phase Fragmentation Propensities of Intact Proteins During Native Top-Down Mass Spectrometry. *J Am Soc Mass Spectrom* **2017,** *28* (6), 1203-1215.

14. McLuckey, S. A., Principles of collisional activation in analytical mass spectrometry. *Journal of the American Society for Mass Spectrometry* **1992,** *3* (6), 599-614.

15. Zubarev, R. A.; Horn, D. M.; Fridriksson, E. K.; Kelleher, N. L.; Kruger, N. A.; Lewis, M. A.; Carpenter, B. K.; McLafferty, F. W., Electron capture dissociation for structural characterization of multiply charged protein cations. *Analytical chemistry* **2000,** *72* (3), 563-573.

16. Zubarev, R. A.; Kelleher, N. L.; McLafferty, F. W., Electron capture dissociation of multiply charged protein cations. A nonergodic process. *Journal of the American Chemical Society* **1998,** *120* (13), 3265-3266.

17. Good, D. M.; Wirtala, M.; McAlister, G. C.; Coon, J. J., Performance Characteristics of Electron Transfer Dissociation Mass Spectrometry *. *Molecular & Cellular Proteomics* **2007,** *6* (11), 1942-1951.

18. Cooper, H. J.; Hakansson, K.; Marshall, A. G., The role of electron capture dissociation in biomolecular analysis. *Mass Spectrom Rev* **2005,** *24* (2), 201-22.

19. Brodbelt, J. S., Photodissociation mass spectrometry: new tools for characterization of biological molecules. *Chemical Society Reviews* **2014,** *43* (8), 2757-2783.

20. Woodin, R.; Bomse, D.; Beauchamp, J., Multiphoton dissociation of molecules with low power continuous wave infrared laser radiation. *Journal of the American Chemical Society* **1978,** *100* (10), 3248-3250.

21. Wei, B.; Zenaidee, M. A.; Lantz, C.; Williams, B. J.; Totten, S.; Ogorzalek Loo, R. R.; Loo, J. A., Top-down mass spectrometry and assigning internal fragments for determining disulfide bond positions in proteins. *Analyst* **2022,** *148* (1), 26-37.

22. Zenaidee, M. A.; Wei, B.; Lantz, C.; Wu, H. T.; Lambeth, T. R.; Diedrich, J. K.; Ogorzalek Loo, R. R.; Julian, R. R.; Loo, J. A., Internal Fragments Generated from Different Top-Down Mass Spectrometry Fragmentation Methods Extend Protein Sequence Coverage. *J Am Soc Mass Spectrom* **2021,** *32* (7), 1752-1758.

23. Lantz, C.; Wei, B.; Zhao, B.; Jung, W.; Goring, A. K.; Le, J.; Miller, J.; Loo, R. R. O.; Loo, J. A., Native Top-Down Mass Spectrometry with Collisionally Activated Dissociation Yields Higher-Order Structure Information for Protein Complexes. *Journal*

of the American Chemical Society **2022,** *144* (48), 21826-21830.

24. Lermyte, F.; Valkenborg, D.; Loo, J. A.; Sobott, F., Radical solutions: Principles and application of electron-based dissociation in mass spectrometry-based analysis of protein structure. *Mass Spectrom Rev* **2018,** *37* (6), 750-771.

25. Li, H.; Nguyen, H. H.; Ogorzalek Loo, R. R.; Campuzano, I. D. G.; Loo, J. A., An integrated native mass spectrometry and top-down proteomics method that connects sequence to structure and function of macromolecular complexes. *Nature Chemistry* **2018,** *10* (2), 139-148.

26. Beckman, J. S.; Voinov, V. G.; Hare, M.; Sturgeon, D.; Vasil'ev, Y.; Oppenheimer, D.; Shaw, J. B.; Wu, S.; Glaskin, R.; Klein, C.; Schwarzer, C.; Stafford, G., Improved Protein and PTM Characterization with a Practical Electron-Based Fragmentation on Q-TOF Instruments. *J Am Soc Mass Spectrom* **2021,** *32* (8), 2081-2091.

27. Fort, K. L.; Cramer, C. N.; Voinov, V. G.; Vasil'ev, Y. V.; Lopez, N. I.; Beckman, J. S.; Heck, A. J. R., Exploring ECD on a Benchtop Q Exactive Orbitrap Mass Spectrometer. *J Proteome Res* **2018,** *17* (2), 926-933.

28. Shaw, J. B.; Malhan, N.; Vasil'ev, Y. V.; Lopez, N. I.; Makarov, A.; Beckman, J. S.; Voinov, V. G., Sequencing Grade Tandem Mass Spectrometry for Top–Down Proteomics Using Hybrid Electron Capture Dissociation Methods in a Benchtop Orbitrap Mass Spectrometer. *Analytical Chemistry* **2018,** *90* (18), 10819-10827.

29. Zhurov, K. O.; Fornelli, L.; Wodrich, M. D.; Laskay, U. A.; Tsybin, Y. O., Principles of electron capture and transfer dissociation mass spectrometry applied to peptide and protein structure analysis. *Chem Soc Rev* **2013,** *42* (12), 5014-30.

30. Yin, S.; Loo, J. A., Elucidating the site of protein-ATP binding by top-down mass

spectrometry. *Journal of the American Society for Mass Spectrometry* **2010,** *21* (6), 899-907.

31. Zhang, H.; Cui, W.; Wen, J.; Blankenship, R. E.; Gross, M. L., Native Electrospray and Electron-Capture Dissociation FTICR Mass Spectrometry for Top-Down Studies of Protein Assemblies. *Analytical Chemistry* **2011,** *83* (14), 5598-5606.

32. Xie, Y.; Zhang, J.; Yin, S.; Loo, J. A., Top-Down ESI-ECD-FT-ICR Mass Spectrometry Localizes Noncovalent Protein-Ligand Binding Sites. *Journal of the American Chemical Society* **2006,** *128* (45), 14432-14433.

33. Lantz, C.; Zenaidee, M. A.; Wei, B.; Hemminger, Z.; Ogorzalek Loo, R. R.; Loo, J. A., ClipsMS: An Algorithm for Analyzing Internal Fragments Resulting from Top-Down Mass Spectrometry. *J Proteome Res* **2021,** *20* (4), 1928-1935.

34. Shrake, A.; Rupley, J. A., Environment and exposure to solvent of protein atoms. Lysozyme and insulin. *Journal of Molecular Biology* **1973,** *79* (2), 351-371.

35. GO, M.; MIYAZAWA, S., RELATIONSHIP BETWEEN MUTABILITY, POLARITY AND EXTERIORITY OF AMINO ACID RESIDUES IN PROTEIN EVOLUTION. *International Journal of Peptide and Protein Research* **1980,** *15* (3), 211-224.

36. Li, H.; Wolff, J. J.; Van Orden, S. L.; Loo, J. A., Native Top-Down Electrospray Ionization-Mass Spectrometry of 158 kDa Protein Complex by High-Resolution Fourier Transform Ion Cyclotron Resonance Mass Spectrometry. *Analytical Chemistry* **2014,** *86* (1), 317-320.

37. Lebherz, H. G.; Rutter, W. J., Distribution of fructose diphosphate aldolase variants in biological systems. *Biochemistry* **1969,** *8* (1), 109-21.

38. Blom, N.; Sygusch, J., Product binding and role of the C-terminal region in Class I D-fructose 1, 6-bisphosphate aldolase. *Nature Structural Biology* **1997,** *4* (1), 36-39.

39. Wanasundara, S. N.; Thachuk, M., Theoretical investigations of the dissociation of charged protein complexes in the gas phase. *Journal of the American Society for Mass Spectrometry* **2007,** *18* (12), 2242-2253.

40. Daggett, V.; Levitt, M., A model of the molten globule state from molecular dynamics simulations. *Proceedings of the National Academy of Sciences* **1992,** *89* (11), 5142-5146.

41. Parthasarathy, S.; Murthy, M., Protein thermal stability: insights from atomic displacement parameters (B values). *Protein engineering* **2000,** *13* (1), 9-13.

42. Ali, S. A.; Hassan, M. I.; Islam, A.; Ahmad, F., A review of methods available to estimate solvent-accessible surface areas of soluble proteins in the folded and unfolded states. *Curr Protein Pept Sci* **2014,** *15* (5), 456-476.

43. Breci, L. A.; Tabb, D. L.; Yates, J. R.; Wysocki, V. H., Cleavage N-Terminal to Proline: Analysis of a Database of Peptide Tandem Mass Spectra. *Analytical Chemistry* **2003,** *75* (9), 1963-1971.

44. Loo, J. A.; Edmonds, C. G.; Smith, R. D., Tandem mass spectrometry of very large molecules. 2. Dissociation of multiply charged proline-containing proteins from electrospray ionization. *Analytical Chemistry* **1993,** *65* (4), 425-438.

45. Carrigan, J. B.; Engel, P. C., The structural basis of proteolytic activation of bovine glutamate dehydrogenase. *Protein Science* **2008,** *17* (8), 1346-1353.

46. Raj, S. B.; Ramaswamy, S.; Plapp, B. V., Yeast Alcohol Dehydrogenase Structure and Catalysis. *Biochemistry* **2014,** *53* (36), 5791-5803.

47. Gleason, W. B.; Fu, Z.; Birktoft, J.; Banaszak, L., Refined Crystal Structure of Mitochondrial Malate Dehydrogenase from Porcine Heart and the Consensus Structure for Dicarboxylic Acid Oxidoreductases. *Biochemistry* **1994,** *33* (8), 2078-2088.

48. Jacobson, R. H.; Zhang, X. J.; DuBose, R. F.; Matthews, B. W., Three-dimensional structure of β-galactosidase from E. coli. *Nature* **1994,** *369* (6483), 761-766.

49. Matthews, B. W., The structure of E. coli β-galactosidase. *Comptes Rendus Biologies* **2005,** *328* (6), 549-556.

Chapter 3: Native Top-Down Orbitrap Mass Spectrometry with Electron Transfer Dissociation Preserves and Yields Higher-Order Structure Information for Protein Complexes

Boyu Zhao[1], Rachel R. Ogorzalek Loo[2], Joseph Loo[1,2]

[1]Department of Chemistry and Biochemistry, [2]Department of Biological Chemistry, University of California Los Angeles, Los Angeles, CA

Abstract

Native top-down mass spectrometry (nTD-MS), *i.e.*, dissociation of gas phase proteins and protein complexes that yields sequence-bearing product ions, has been conventionally used to obtain mass, binding stoichiometry, sites of post-translational modifications (PTMs), primary and higher-order structure information. nTD-MS has also been utilized to locate ligand binding sites. However, the dissociation method used can greatly affect the resultant information related to protein higher-order structure. Fragmentation methods used on Orbitrap-based mass spectrometers, for example, electron-based dissociation (ExD), including electron capture dissociation (ECD), and higher energy C-trap dissociation (HCD), have been demonstrated to produce product ions that can inform on the higher-order structure of protein complexes. However, revealing higher-order structure characteristics of a protein complex with weak noncovalent interactions among its subunits in the gas phase, such as the streptavidin homotetramer, is challenging because release of the subunits can preclude generation of product ions from the intact complex. Here we show that sequence information and also higher-order structure information can be

obtained for streptavidin complex by electron transfer dissociation (ETD) and coupled with proton transfer charge reduction (PTCR) on an Orbitrap tribrid mass spectrometer.

Introduction

In biological systems, most proteins assemble into complexes for proper function. Therefore, characterizing their structures is critical for understanding how they function in the biological systems. Conventional structure analysis methods, such as cryo-electron microscopy (cryo-EM), NMR or X-ray crystallography are used for probing the structures and dynamics of proteins, protein complexes and other biomolecules.[1-4] Native mass spectrometry (nMS) and native top-down mass spectrometry (nTD-MS) have emerged and has been widely used to provide complementary information on stoichiometry[5], conformation[6] and structure[6-9]. To confidently obtain the structure characteristics of protein complexes, electrospray ionization (ESI)-MS has been used prominently because of its isotopic resolving power[6], high mass accuracy[6] and capabilities for maintaining native-like structures of protein complexes during the transfer from solution to the gas phase[1, 2]. Compared to other more traditionally used structure analysis methods, although nMS and nTD-MS provide only indirect and low-resolution structure information, the compatibility with sample heterogeneity[10], wide mass range[11], and high throughput[12] make mass spectrometry one of the most widely used structure analysis techniques today.

Structural information for protein complexes can be obtained by comparing the fragmentation patterns of nTD-MS (native folded structure) with complex-down MS (pseudo-MS[3] that generates data more consistent with unfolded protein structures)[13]. Several dissociation methods has been used for top-down mass spectrometry, including collisional induced dissociation (CID)[14], electron-based dissociation (ExD)[15-18], and photon-based dissociation[19, 20]. The product ions formed by top-down MS can be either terminal fragments, which are generated from the N-terminus (a, b, or c fragments) or C-

terminus (x, y, or z fragments), or internal fragments (ax, ay, az, bx, by, bz, cx, cy, or cz fragments) resulting from multi-cleavage events of the peptide backbone.[21-23] The Loo group has previously found that high energy C-trap dissociation (HCD), a type of CID, fragments most protein complexes directly, potentially revealing higher order structural information of those assemblies in a faster timescale than conventional CID[7]. However, HCD fragmentation becomes limited in the extent of revealing higher-order structure information for protein complexes with weak gas-phase inter-molecular interactions between subunits, such as the streptavidin homotetrameric complex. Electron-based dissociation, for example electron capture dissociation (ECD) and electron transfer dissociation (ETD), are alternative methods to overcome this HCD fragmentation disadvantage. One of the advantages of ECD/ETD is the preservation of labile bonds, including noncovalent interactions, while cleaving peptide backbone N-Cα bonds at the solvent exposed regions.[9, 24, 25]

For an isotopically resolved MS/MS spectrum, generating deconvoluted mass lists and assigning fragments can be challenging due to the increased complexity of fragmentation spectra caused by the increase of a combination of charge states and isotopes[26], especially for the proteins larger than 30 kDa. To reduce the complexity of fragmentation spectra, proton transfer charge reduction (PTCR) has been developed and utilized.[27] PTCR reduces spectra complexity by charge reducing the fragment ions and distributing them to a higher *m/z* range, where peak overlap is limited.[28-31]

Here, we demonstrated that nMS and nTD-MS with HCD and activated ion ECD (ECD coupled with HCD, or EChcD) analysis confirm the sequence, and stoichiometry of the

streptavidin tetramer. In addition, native top-down ETD and ETD-PTCR MS analysis of the tetramer reveals the dimer of dimer composition and higher-order structure information.

Experimental

Sample preparation. Streptavidin from *Streptomyces avidinii* (52 kDa), and 30 kDa Millipore Amicon Ultra filters were purchased from Sigma-Aldrich (St. Louis, MO, USA). Samples were buffer exchanged with 30 kDa filters into 150 mM ammonium acetate without or with (a) 10 mM L-proline, (b) 60 μM biotin, and (c) both 10 mM L-proline and 60 μM biotin to a final concentration of 10 μM.

Native Top-Down and Complex-Down HCD and EChcD MS. Both HCD and electron capture dissociation with supplement HCD (EChcD) experiments were performed on a ThermoFisher Scientific Q Exactive Ultra-High Mass Range (UHMR) Orbitrap mass spectrometer with an ExD cell developed by e-MSion (Corvallis, OR, USA). Protein solutions were loaded into Pt-coated borosilicate capillaries on a nanospray ionization source and sprayed at 0.8-1.2 kV, 200 ℃. The S-lens RF was set at 100 V. In-source CID was set over a range of 55-92 eV for complex-down experiments. A single charge state was isolated by the quadrupole for the protein complex. In EChcD experiments, the precursor ions were transferred into the ECD cell, where they were subject to electron capture, then into the HCD cell for post-ECD collisional activation. The ExD filament current was set at 2.23 A. The HCD collision energy was optimized to minimize the generation of b/y ions. Additional details of ExD cell tuning parameters are provided in the Supporting Information. In HCD experiments, the precursor ions were subjected into the HCD cell for

fragmentation. All top-down mass spectra were acquired at 100,000 resolution (*m/z* 400) with a noise threshold set to 3. Each spectrum was the result of 300 averaged scans.

Denatured MS. Protein was denatured in denaturing solution (0.1% formic acid, 99.9% ammonium acetate solution). The denatured protein solution was analyzed on the UHMR Orbitrap mass spectrometer with a nanospray ionization source and sprayed at 1.1 kV, 200 ℃. The S-lens RF was set at 100 V.

Native Top-Down ETD MS. All ETD and ETD-PTCR experiments were performed on a ThermoFisher Scientific Orbitrap Ascend Structural Biology Tribrid MS (Figure S1). Protein solutions were loaded into Pt-coated borosilicate capillaries on a nanospray ionization source and sprayed at 1.4-1.6 kV, 200 ℃. The S-lens RF was set at 100 V. A single charge state was isolated by the front ion-routing multipole for the protein complex. For ETD experiments, the precursor ions were transferred into the linear ion trap, where they reacted with fluoranthene anions generated at the EASY-ETD ion source to produce fragment ions. The ETD module contains a chemical ionization (CI) source, a fluoranthene vial, and a carrier gas (nitrogen). The nitrogen collides with 70 eV electrons from the CI filament, resulting in secondary electrons knocked off from the nitrogen molecules. The fluoranthene molecules captures these secondary electrons to form the ETD reagent radical anions. For ETD-PTCR experiments, fragment ions generated by ETD were isolated by the linear ion trap. The isolated fragment ions subsequently reacted with the PTCR reagent, perfluoroperhydrophenanthrene (PFPP) ions generated at the PTCR ion source by capturing the secondary electrons released from nitrogen molecules. This gas-phase ion-ion reaction produced charge reduced fragment ions. ETD reaction time was set to 7 ms, and PTCR reaction time was set to 20 ms. The product ions from ETD and ETD-PTCR

were transferred to Orbitrap for mass analysis. All ETD and ETD-PTCR mass spectra were acquired at 100,000 resolution (*m/z* 400) with a noise threshold set to 3. Each spectrum was the result of 300 averaged scans.

Data Analysis. All spectra were deconvoluted with BioPharma Finder 5.0 (ThermoFisher Scientific, Waltham, USA). Deconvoluted peaks were assigned by ClipsMS 2.0.035 with an error tolerance of 3 ppm. Sequence assignments accommodated the major ECD/ETD (c, c+H, c-H, z, z+H, z-H) and HCD (b, y) ion types without annotating neutral losses ions, except when explicitly mentioned. Terminal fragments were manually validated by confirming the isotopic distributions.

Results and Dissociation

Accurate Mass Measurement of Streptavidin Tetramer

Streptavidin is composed of a dimer of dimers, with four identical monomers. The streptavidin complex subunit from *Streptomyces avidinii* is composed of 123 amino acids and an average mass of 12,971 Da, and its corresponding homotetramer complex has a calculated mass of 51,884 Da.

Figure 1A shows the MS spectrum of streptavidin under native nanoESI conditions using a Thermo Q-Exactive UHMR with the ExD cell installed. A relative narrow charge state distribution from 15+ to 13+ was observed between *m/z* 3400 and 4100. Figure 1B shows the expanded mass spectrum for the 14+ charge state ions. We identified 3 proteoforms for the monomers, including wild type (WT), monomers with one serine (Ser123) removed from the C-terminus, and monomers with one alanine (Ala124) addition on the C-terminus; the presence of all 3 proteoforms were verified from denatured MS experiments (Figure

S2). These 3 proteoforms assemble into the tetramer complex such that 5 total proteoforms of the assembled tetramers were observed. Complex-down HCD experiment (Figure S3A and B) was further performed to confirm the sequence of the WT monomer (UniProtKB: P22629). The observation of a series of fragment ions from both termini, particularly the complementary ion pairs, b_9/y_{114}, b_{31}/y_{92}, and b_{67}/y_{56} confirms the sequence and no presence of any PTMs. Native top-down HCD MS experiments were performed for the streptavidin tetramer. At low HCD energy (CE 5 V), only monomers and trimers were observed (Figure 2A). At a resolution 100,000 (at *m/z* 400), the 6+ charged WT streptavidin monomer peak was isotopically resolved (Figure 2B). The calculated isotopic mass for streptavidin monomer is 12,963.2956 Da with a 1.2 ppm mass accuracy. As the molecular mass increases, the isotopic distribution becomes wider and obtaining isotopically resolved peaks becomes challenging[32]. Therefore, for the ~52 kDa streptavidin tetramer, and ~39 kDa streptavidin trimer, the monoisotopic peaks are no longer observable. As a result, the average mass of the streptavidin tetramer is reported by calculating with the highest intensity peak for each WT tetramer charge state, which is 51,887.03 +/- 0.72 Da.

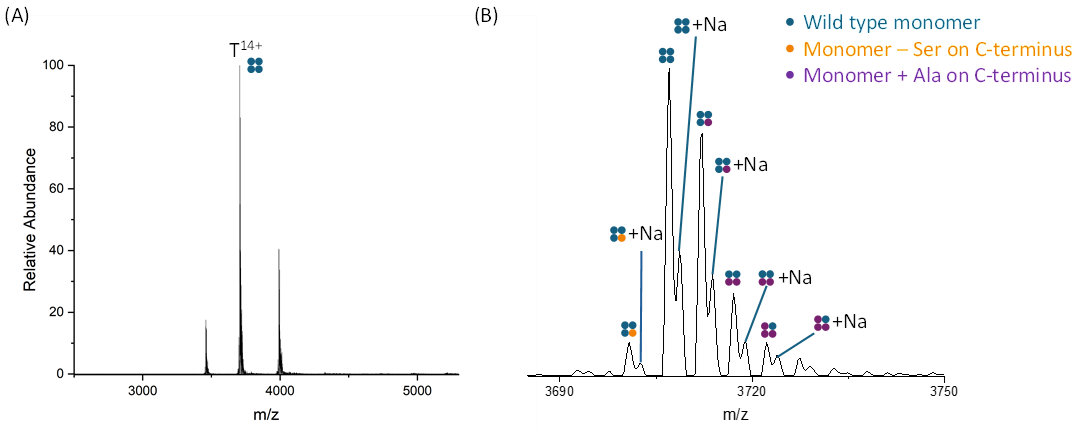

Figure 1. Native ESI-mass spectrum of streptavidin tetramer with (A) the Q-Exactive UHMR MS. (B) An expanded MS spectrum of the 14+ charge state of streptavidin tetramer

is shown, with the wild type monomer labels in blue, the monomer without S123 labeled in yellow, and the monomer with A124 labeled in purple.

Native Top-Down HCD of Streptavidin Complex

Our previous research suggested that native top-down HCD can reveal higher-order structure information for protein complexes to generate product ions originating near the complex surface, or solvent exposed regions[7]. Therefore, the WT streptavidin 14+ charge state was isolated and subjected to HCD. However, native top-down HCD of the streptavidin tetramer yields monomers at low HCD (CE 50 V) and no sequence information was obtained (Figure 2A and 2B). Further increasing HCD energy to 160 V yields product ions (Figure 2C). By increasing HCD energy, although more fragments are generated, most of the fragments originate from C-terminus, which is at the monomer binding interface (Figure 2D) and *not* in the solvent exposed region. Our result suggests that monomer subunits are ejected before generating sequence-bearing fragments, and the fragments are all generated from the monomer, not directly from the tetramer. To confirm this claim, complex-down HCD was performed, and compared to native top-down HCD fragmentation pattern. Complex-down MS was performed by using in-source CID (ISD) to eject a monomer from the tetramer and to subsequently subject the released 6+ WT streptavidin monomer for fragmentation[7]. The resultant complex-down HCD spectrum also revealed both N-terminal b-ions and C-terminal y-ions of WT streptavidin (Figure S3A and B). The presence of near equal numbers of both b- and y-fragments from the complex-down HCD spectrum suggests that both N- and C-termini of the WT streptavidin monomer are accessible by HCD fragmentation. Complex-down MS typically reveals no 3D structure information of the native intact complex. For the streptavidin case, the similarity

between both complex-down and nTD fragmentation patterns supports the notion that the monomers were ejected from the tetramers prior to the backbone cleavages in the HCD cell, *i.e.*, the measured nTD fragments originate from the ejected monomers. Therefore, native top-down HCD did not reveal higher-order structure information for streptavidin complex.

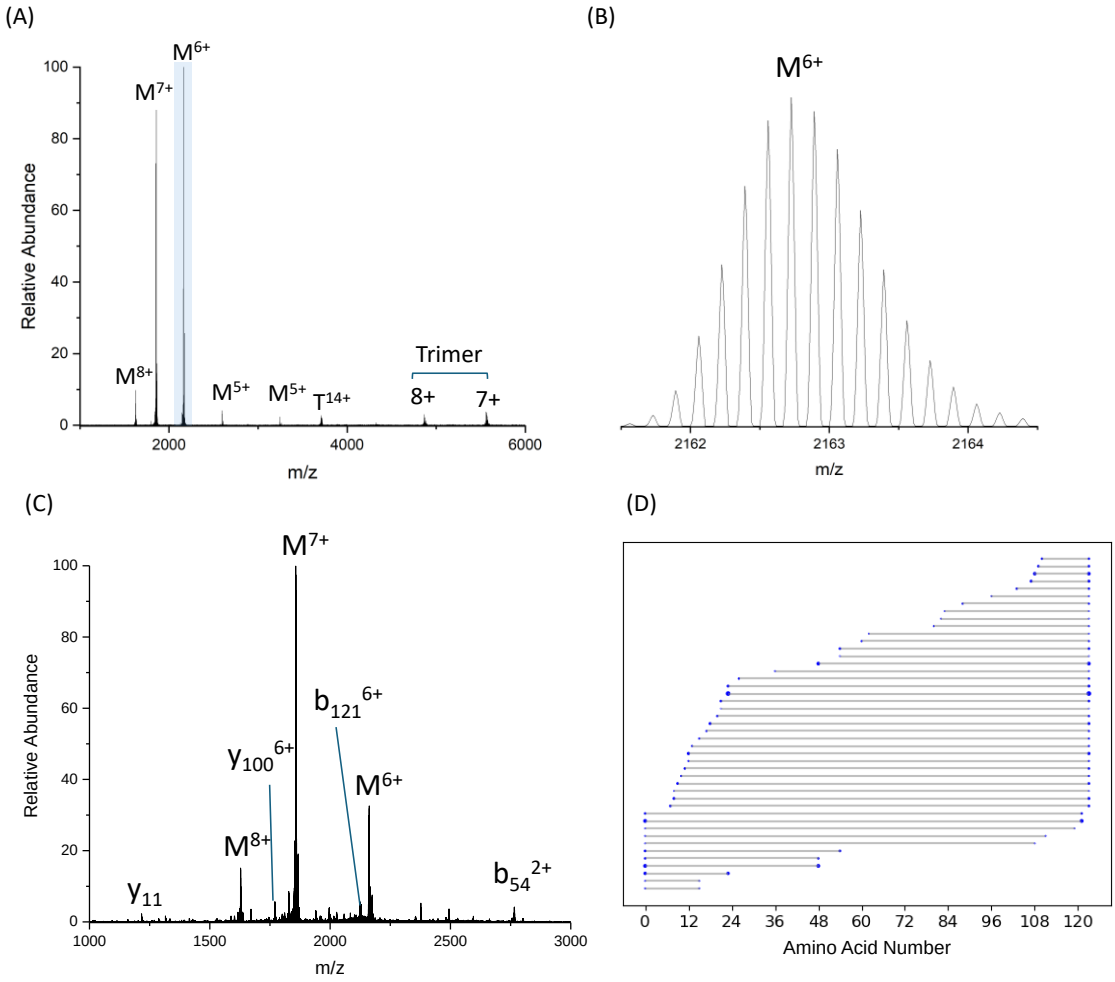

Figure 2. (A) Native top-down spectrum of the streptavidin tetramer at low HCD energy (CE 50 V); (B) the expanded MS spectrum of the 6+ charge state of streptavidin monomer; (C) native top-down HCD spectrum of the streptavidin tetramer at high HCD energy (CE 160 V); (D) fragmentation location map of top-down MS/MS by HCD of the 14+ charge state of native streptavidin tetramer. The b/y ions from the native top-down HCD of the 14+ charge state of native streptavidin tetramer are indicated by each horizontal line and the blue dots. The size of dots indicates the intensity of each fragmentation.

Native Top-Down EChcD of Streptavidin Complex

One of the features of electron-based dissociation (ECD or ETD) is preserving labile bonds, including noncovalent interactions, while cleaving peptide backbone N-Cα bonds on the solvent exposed regions.[9, 24, 25] Thus, ECD is a powerful tool for locating noncovalent interactions, for example, protein-protein/ligand binding sites.[25, 33-35] Previously, Gross group have examined that the fragment region of a protein complex from native top-down ECD correlates with the B-factor of that protein.[9] In X-ray crystallography, the B-factor is used to describe the relative vibrational motion of atoms in a structure.[36, 37] An amino acid with a larger B-factor value indicates that the amino acid is in a more flexible region (more solvent exposed).[38] In another word, ECD fragments at the solvent accessible region of a native protein.

To examine whether EChcD can reveal structure information from WT streptavidin tetramer, the 14+ charge state was subjected to EChcD for fragmentation. The supplemental HCD energy was optimized to minimize generating b/y ions. Figure 3A shows the top-down EChcD mass spectrum of the streptavidin tetramer with HCD energy 50 V. However, with the optimized ECD and HCD energy, released monomer charge states are still dominating, and the fragments are generated from both termini (Figure 3B). Although it might be possible that generating fragments from both termini may be due to the excess ECD or HCD energy during the EChcD experiment, EChcD experiments with reduced HCD and ECD energy were performed and resulted in reducing the number of fragments from both termini, while still observing monomer ejection as the major process. Although EChcD fragmentation of native streptavidin does not reveal higher-order

structure information, it does suggest that the interaction between monomer subunits in the gas phase is relative weak.

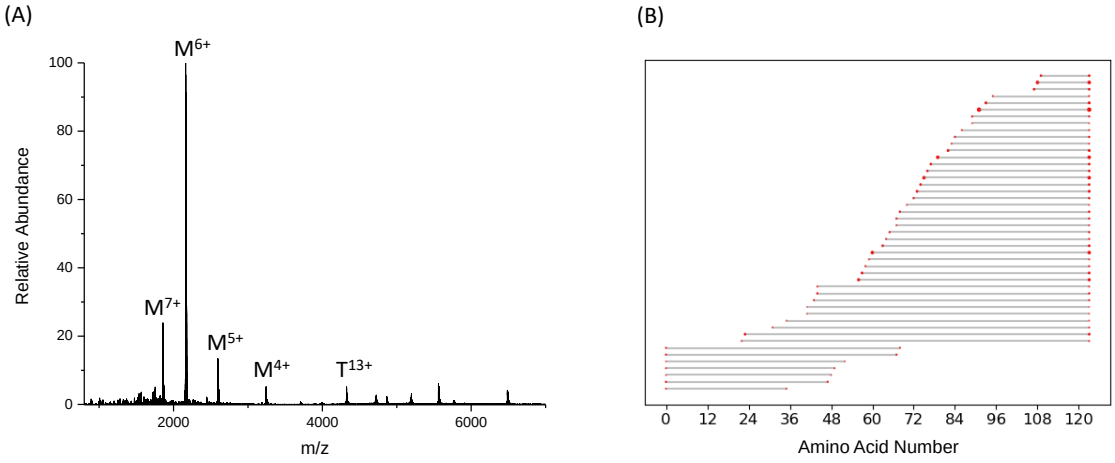

Figure 3. (A) Native top-down EChcD spectrum of the streptavidin tetramer, and (B) fragmentation location map from the top-down MS/MS experiment. The c/z ions from the native top-down EChcD of the 14+ charge state of native streptavidin tetramer are indicated by each horizontal line and the red dots.

The Venter group has previously proposed that the addition of L-proline can (somehow) reduce the extent of protein unfolding during the transition from the protein in the solution phase to the gas phase, and therefore preserves the noncovalent interactions within the monomeric protein.[39] Inspired by that, we performed top-down EChcD of streptavidin complex with L-proline and biotin, respectively. The interaction between streptavidin and biotin is one of the strongest noncovalent interactions in the solution phase in nature.[40, 41] Each streptavidin tetramer can bind up to 4 biotin molecules. Taking advantage of this feature, this strong noncovalent interaction has been widely used in biochemical sensing applications.[42] Therefore, we would like to investigate whether the addition of biotin shows a stabilization effect on streptavidin tetramers in the gas phase. With the presence of L-proline, we observed all 5 proteoforms for streptavidin tetramer with no L-proline bound

(Figure S4A), similar to streptavidin tetramer 19+ charge state without the addition of L-proline. With the addition of excess biotin in molar ratio, we observed tetramer with 4 to 6 biotins bounded (Figure S4B), although an additional step of buffer exchange with 150 mM ammonium acetate was performed to remove the excess nonspecifically bounded biotins, *i.e.*, 5 and 6 biotins bounded form. To investigate whether the addition of L-proline or biotin can stabilize the WT streptavidin gas-phase tetramer during EChcD, the streptavidin tetramer 14+ charge state with L-proline or biotin was subjected to EChcD for fragmentation. With the addition of L-proline, we observed high intensity peaks assigned to monomer 6+ and 7+ charge states (Figure 4A) and fragments from both N- and C-termini (Figure 4B). The resultant spectrum and fragmentation pattern suggest that with the presence of L-proline, the streptavidin *was not* stabilized, therefore; the EChcD product ions did not reveal higher-order structure information. With the addition of biotin, we observed high intensity peaks assigned to the apo streptavidin monomer 5+ to 6+ charge states, apo charge reduced tetramers 11+ to 13+ charge states, apo trimer 7+ charge state (Figure 4C), and fragments from both N- and C-termini (Figure 4D). This result indicates that biotin molecules might be released during the electron capture process, as no biotin bounded tetramer, trimer and monomers were observed in the spectrum. Thus, the streptavidin gas-phase tetramer was not stabilized with the addition of biotins, and the EChcD product ions did not reveal higher-order structure information. Our result is consistent with a previous report that the streptavidin/biotin complex showed a relatively low affinity in the gas phase[43] due to the absence of the surrounded water molecules. In addition, the streptavidin tetramer 14+ charge state with the addition of both L-proline and biotin was subjected to EChcD for fragmentation. However, the monomers were released

prior to fragmentation (Figure 4E). Additionally, the corresponding fragmentation pattern did not reveal higher-order structure information for the streptavidin tetramer.

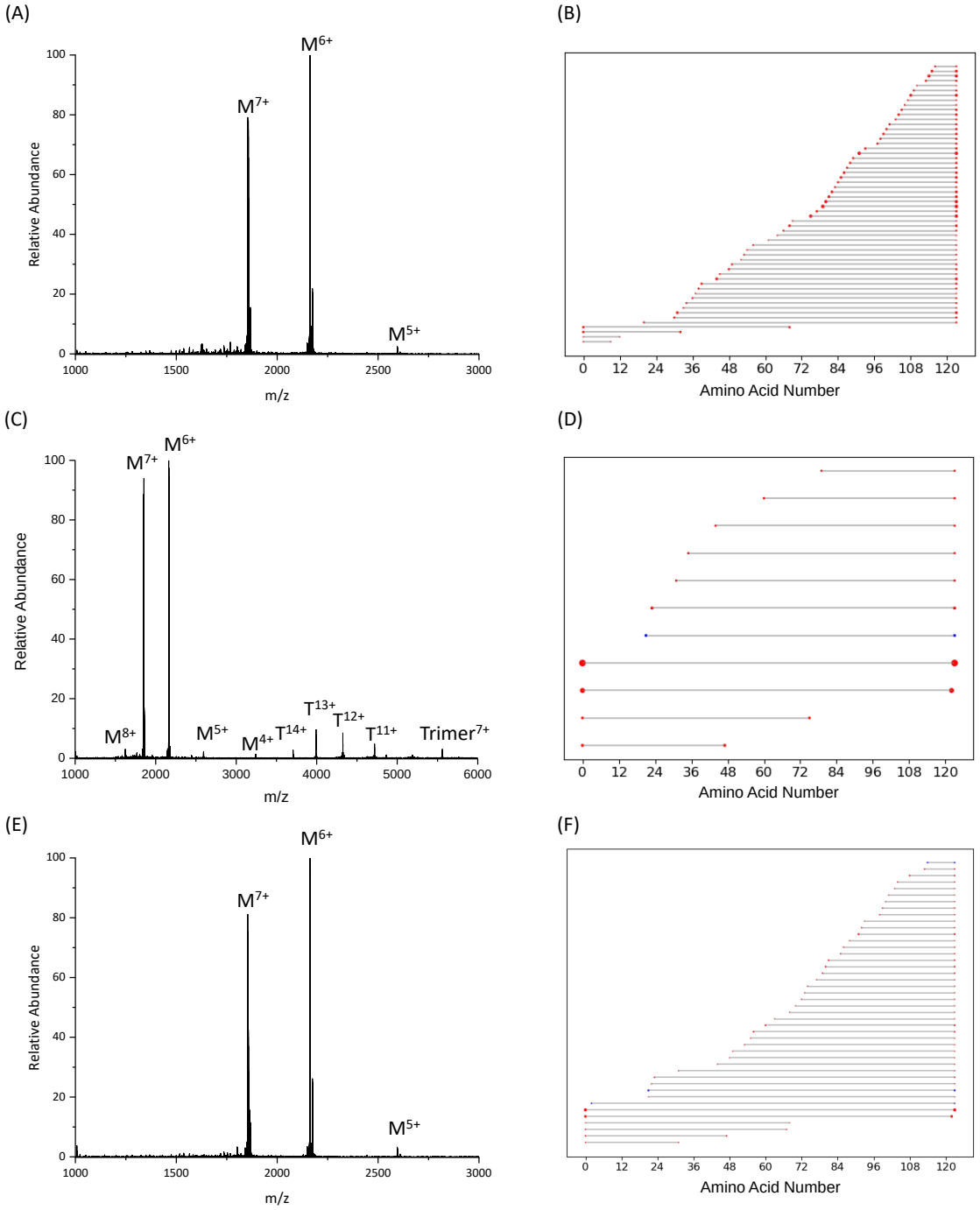

Figure 4. (A) Native top-down EChcD spectrum of streptavidin tetramer with 10 mM L-proline, and (B) fragmentation location map of streptavidin by top-down MS/MS (c/z ions

from the native top-down EChcD of the 14+ charge state of native streptavidin tetramer with L-proline); (C) native top-down EChcD spectrum of the streptavidin tetramer with biotin, and (D) fragmentation location map of streptavidin by top-down MS/MS (c/z ions from the native top-down EChcD of the 14+ charge state of native streptavidin tetramer with biotin); (E) native top-down EChcD spectrum of the streptavidin tetramer with L-proline and biotin, and (F) fragmentation location map of streptavidin by top-down MS/MS (c/z ions from the native top-down EChD of the 14+ charge state of native streptavidin tetramer with L-proline and biotin).

Native Top-Down ETD of Streptavidin Complex

Native top-down ETD and ETD-PTCR experiments were also performed for the streptavidin tetramer using the Orbitrap Tribrid Ascend instrument; dissociation of the tetramer to yield dimers and low abundant monomers (0.5% for monomers) were observed in both approaches and remarkably only *N-terminal fragments* were observed (Figure 5). This result differs from the complex-down HCD mass spectrum of streptavidin, which shows a nearly equal proportion of N-terminal b-fragments and C-terminal y-fragments (Figure S3C and D). Due to the ejection of dimers, obtaining the higher-order structure information for the streptavidin tetramer directly is still challenging; however, the ETD fragmentation patterns suggests that the tetramer is a dimer of dimers. ETD and ETD-PTCR fragmentation patterns (Figure 5D) are consistent with the published crystal structure (PDB: 1SWA, Figure 5B)[44] that the N-termini are at the solvent exposed regions. Even though the C-terminal regions are not directly involved in the interfaces between subunits, they are located in the regions that are partially buried, which can limit ETD backbone cleavages.

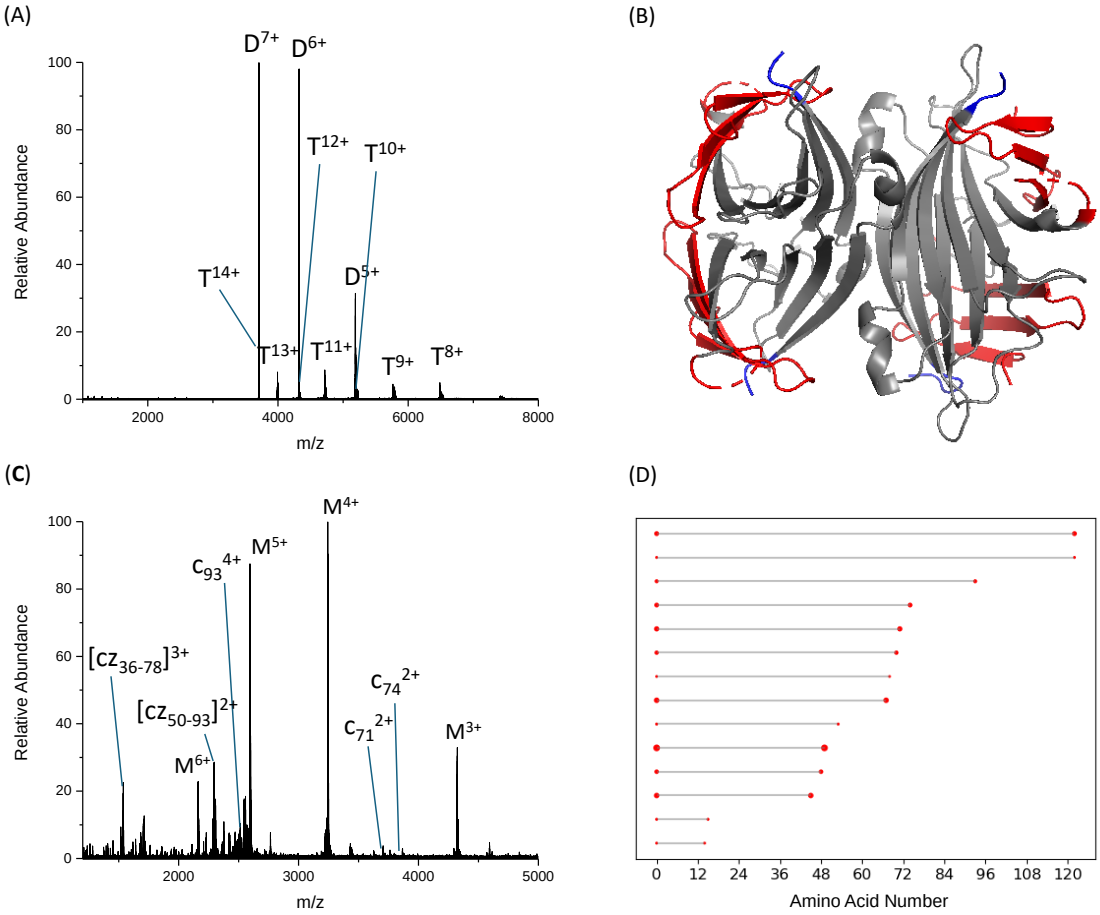

Figure 5. (A) Native top-down ETD spectrum of the streptavidin tetramer; (B) structure of tetrameric streptavidin (PDB: 1SWA), with the native ETD fragments labeled in red, and the last 10 amino acids (AA 114-123) on each C-terminus in blue. (C) Native top-down ETD-PTCR spectrum of the streptavidin tetramer; (D) fragmentation location map of streptavidin by top-down MS/MS (c/z ions from the native top-down EChcD of the 14+ charge state of native streptavidin tetramer.)

Conclusion

In summary, unit mass resolution analysis for a 52 kDa protein complex as well as its proteoforms under native MS with high mass accuracy are demonstrated. The results demonstrate that higher-order structure information of a protein complex with weak noncovalent interactions among monomers can be revealed by ETD and ETD-PTCR on an Ascend Orbitrap mass spectrometer.

It is not clear why performing ECD on a quadrupole-Orbitrap instrument should yield different results on an Orbitrap tribrid (quadrupole-linear ion trap-Orbitrap) system with ETD. In general, ECD and ETD are thought to generate similar fragmentation patterns for peptides and proteins because of their similar dissociation mechanisms and energetics. However, a definitive and thorough study comparing ECD and ETD on the same instrument has yet to be performed. There might be differences in how the analyte ions are activated prior to ECD/ETD on the UHMR and Ascend Orbitrap platforms. Future work will address this question. But it remains clear that the ETD/Ascend Orbitrap generates fragmentation patterns for a fragile protein complex (streptavidin) that are consistent with its higher order structure.

Acknowledgment

We acknowledge Rafael Melani, Chris Mullen and Jingjing Huang from ThermoFisher Scientific for granting us access to the Orbitrap Ascend Structural Biology Tribrid MS.

Chapter 3: Supporting Information

Supplementary Figures

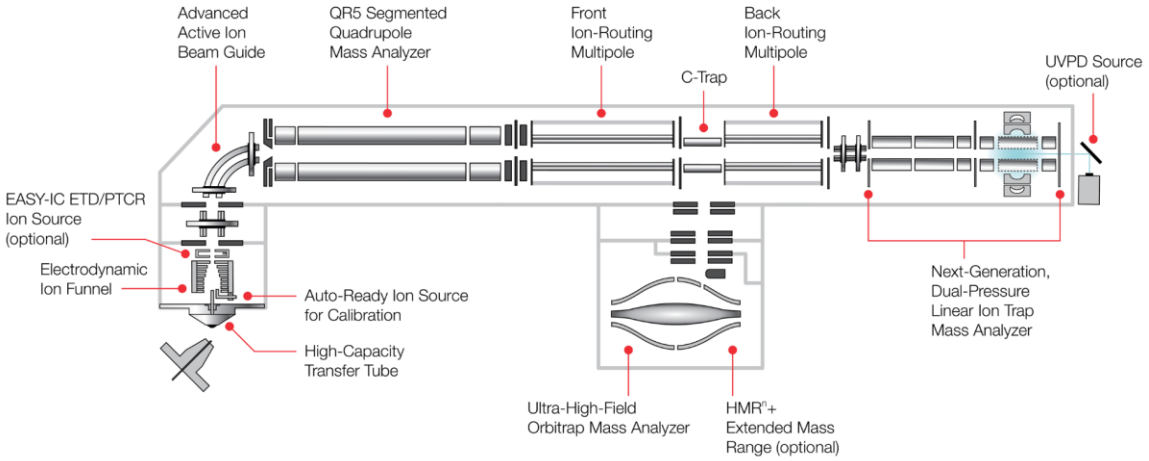

Figure S1. The schematic of an Orbitrap Ascend Structural Biology Tribrid mass spectrometer.

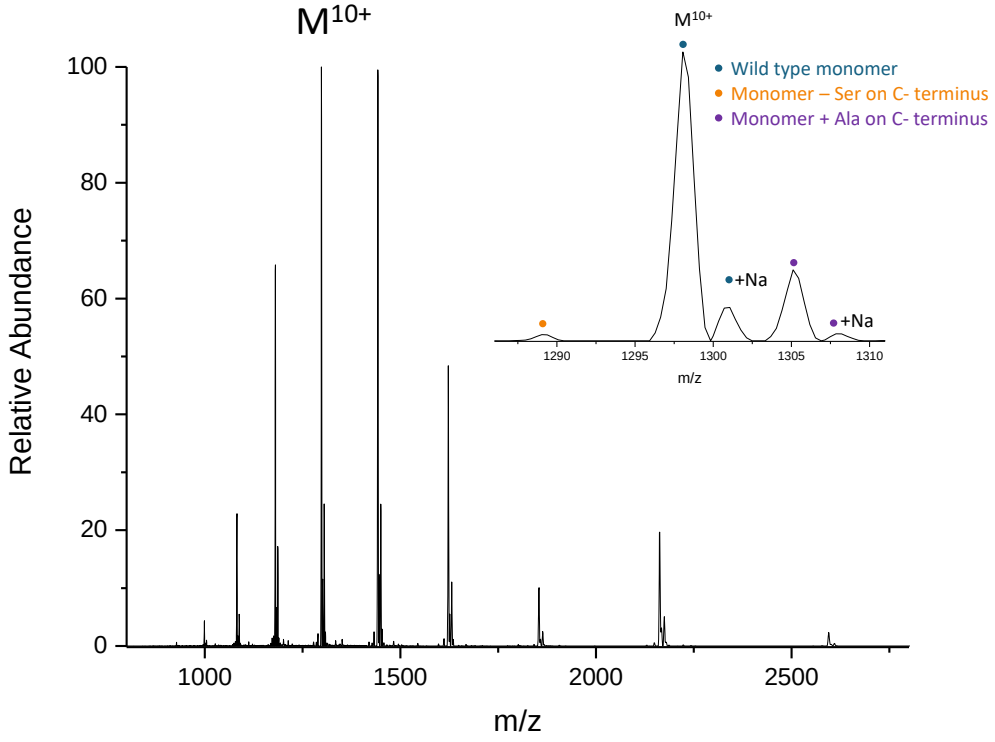

Figure S2. Denatured mass spectrum of streptavidin monomer obtained on UHMR Orbitrap MS. All three proteoforms were observed for each charge state. An expanded MS spectrum of the 10+ charge state of streptavidin monomer is shown, with the wild type monomer labels in blue, the monomer without S123 labels in yellow, and the monomer with A124 labels in purple.

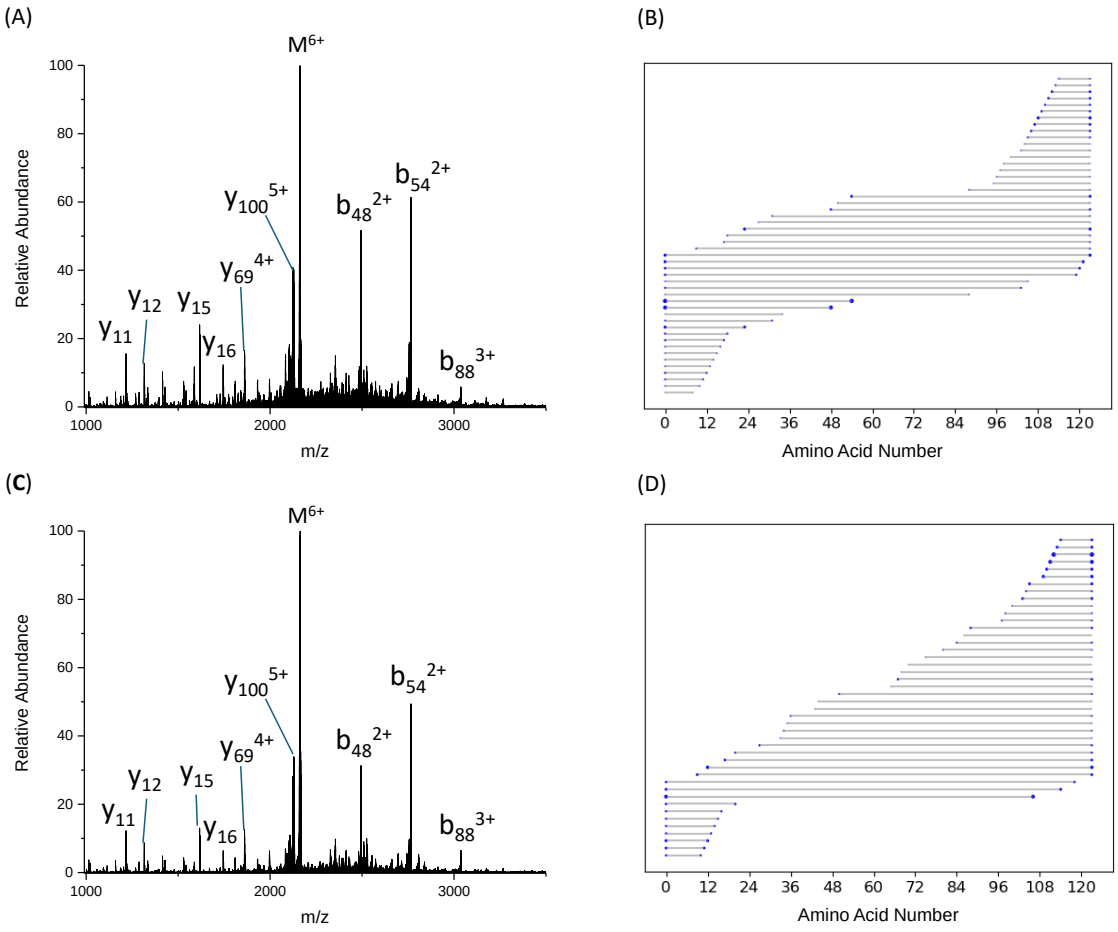

Figure S3. (A) Complex-down HCD spectrum of the streptavidin (monomer, 6+ charge state), and (B) the corresponding fragmentation location map. (C) Complex-down HCD spectrum of the streptavidin (monomer, 6+ charge state) collected on Ascend MS; and (D) the corresponding fragmentation location map.

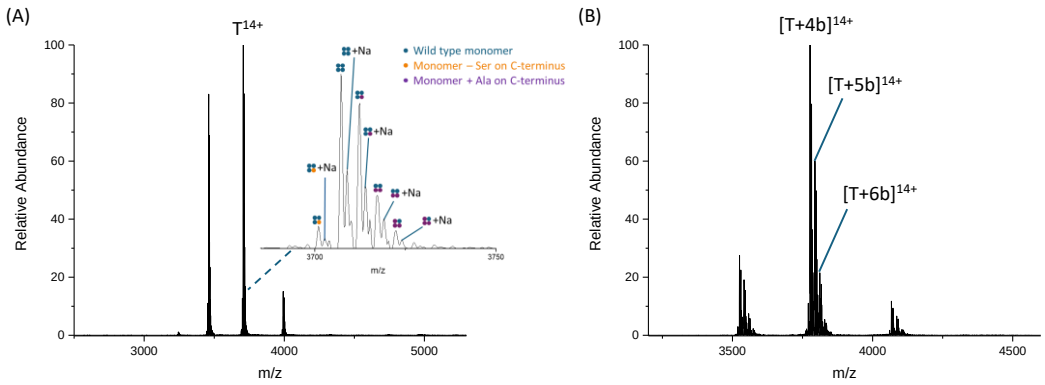

Figure S4. (A) Native mass spectrum of streptavidin tetramer with 10 mM L-proline, no L-proline bonded form was observed, and (B) native mass spectrum of streptavidin tetramer with biotin (1:6).

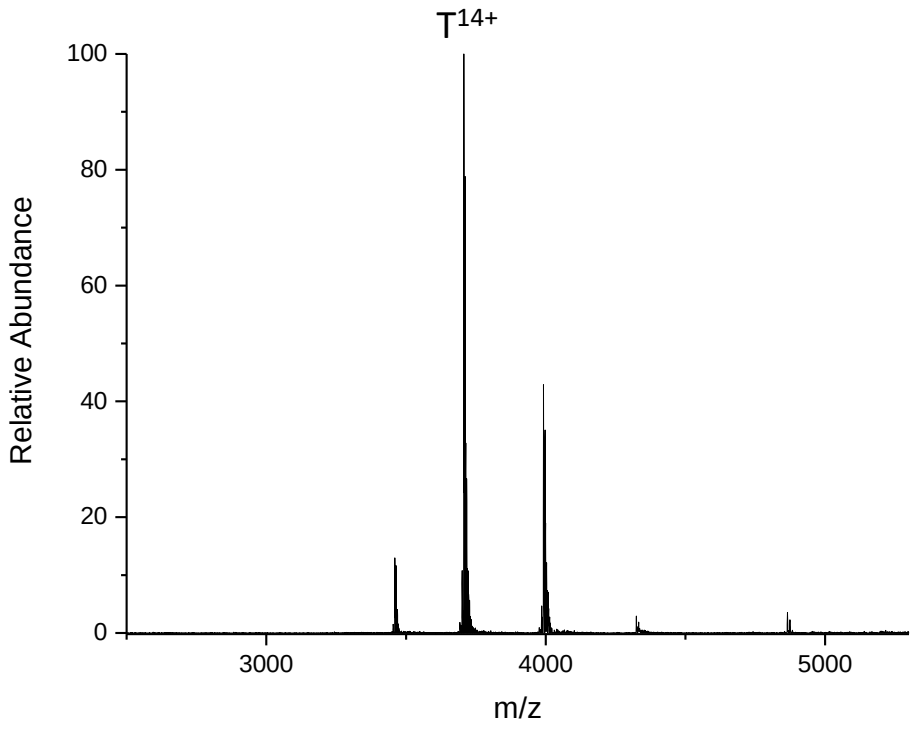

Figure S5. Native mass spectrum of streptavidin tetramer obtained on Orbitrap Ascend Structural Biology Tribrid MS.

References

1. Lössl, P.; van de Waterbeemd, M.; Heck, A. J., The diverse and expanding role of mass spectrometry in structural and molecular biology. *The EMBO Journal* **2016,** *35* (24), 2634-2657.

2. Liko, I.; Allison, T. M.; Hopper, J. T. S.; Robinson, C. V., Mass spectrometry guided structural biology. *Current Opinion in Structural Biology* **2016,** *40*, 136-144.

3. Rostom, A. A.; Robinson, C. V., Detection of the Intact GroEL Chaperonin Assembly by Mass Spectrometry. *Journal of the American Chemical Society* **1999,** *121* (19), 4718-4719.

4. Shoemaker, S. C.; Ando, N., X-rays in the Cryo-Electron Microscopy Era: Structural Biology's Dynamic Future. *Biochemistry* **2018,** *57* (3), 277-285.

5. Panczyk, E. M.; Snyder, D. T.; Ridgeway, M. E.; Somogyi, Á.; Park, M. A.; Wysocki, V. H., Surface-Induced Dissociation of Protein Complexes Selected by Trapped Ion Mobility Spectrometry. *Analytical Chemistry* **2021,** *93* (13), 5513-5520.

6. Li, H.; Wolff, J. J.; Van Orden, S. L.; Loo, J. A., Native Top-Down Electrospray Ionization-Mass Spectrometry of 158 kDa Protein Complex by High-Resolution Fourier Transform Ion Cyclotron Resonance Mass Spectrometry. *Analytical Chemistry* **2014,** *86* (1), 317-320.

7. Lantz, C.; Wei, B.; Zhao, B.; Jung, W.; Goring, A. K.; Le, J.; Miller, J.; Loo, R. R. O.; Loo, J. A., Native Top-Down Mass Spectrometry with Collisionally Activated Dissociation Yields Higher-Order Structure Information for Protein Complexes. *Journal of the American Chemical Society* **2022,** *144* (48), 21826-21830.

8. Zhou, M.; Lantz, C.; Brown, K. A.; Ge, Y.; Paša-Tolić, L.; Loo, J. A.; Lermyte, F., Higher-order structural characterisation of native proteins and complexes by top-down mass spectrometry. *Chemical Science* **2020,** *11* (48), 12918-12936.

9. Zhang, H.; Cui, W.; Wen, J.; Blankenship, R. E.; Gross, M. L., Native Electrospray and Electron-Capture Dissociation FTICR Mass Spectrometry for Top-Down Studies of Protein Assemblies. *Analytical Chemistry* **2011,** *83* (14), 5598-5606.

10. Heck, A. J. R., Native mass spectrometry: a bridge between interactomics and structural biology. *Nature Methods* **2008,** *5* (11), 927-933.

11. Karabacak, N. M.; Li, L.; Tiwari, A.; Hayward, L. J.; Hong, P.; Easterling, M. L.; Agar, J. N., Sensitive and Specific Identification of Wild Type and Variant Proteins from 8 to 669 kDa Using Top-down Mass Spectrometry *^S. *Molecular & Cellular Proteomics* **2009,** *8* (4), 846-856.

12. van Duijn, E., Current limitations in native mass spectrometry based structural biology. *Journal of the American Society for Mass Spectrometry* **2010,** *21* (6), 971-978.

13. Lermyte, F.; Tsybin, Y. O.; O'Connor, P. B.; Loo, J. A., Top or Middle? Up or Down? Toward a Standard Lexicon for Protein Top-Down and Allied Mass Spectrometry Approaches. *Journal of the American Society for Mass Spectrometry* **2019,** *30* (7), 1149-1157.

14. McLuckey, S. A., Principles of collisional activation in analytical mass spectrometry. *Journal of the American Society for Mass Spectrometry* **1992,** *3* (6), 599-614.

15. Zubarev, R. A.; Horn, D. M.; Fridriksson, E. K.; Kelleher, N. L.; Kruger, N. A.; Lewis, M. A.; Carpenter, B. K.; McLafferty, F. W., Electron Capture Dissociation for

Structural Characterization of Multiply Charged Protein Cations. *Analytical Chemistry* **2000,** *72* (3), 563-573.

16. Zubarev, R. A.; Kelleher, N. L.; McLafferty, F. W., Electron Capture Dissociation of Multiply Charged Protein Cations. A Nonergodic Process. *Journal of the American Chemical Society* **1998,** *120* (13), 3265-3266.

17. Good, D. M.; Wirtala, M.; McAlister, G. C.; Coon, J. J., Performance Characteristics of Electron Transfer Dissociation Mass Spectrometry *. *Molecular & Cellular Proteomics* **2007,** *6* (11), 1942-1951.

18. Cooper, H. J.; Håkansson, K.; Marshall, A. G., The role of electron capture dissociation in biomolecular analysis. *Mass Spectrometry Reviews* **2005,** *24* (2), 201-222.

19. Brodbelt, J. S., Photodissociation mass spectrometry: new tools for characterization of biological molecules. *Chemical Society Reviews* **2014,** *43* (8), 2757-2783.

20. Woodin, R. L.; Bomse, D. S.; Beauchamp, J. L., Multiphoton dissociation of molecules with low power continuous wave infrared laser radiation. *Journal of the American Chemical Society* **1978,** *100* (10), 3248-3250.

21. Zenaidee, M. A.; Lantz, C.; Perkins, T.; Jung, W.; Loo, R. R. O.; Loo, J. A., Internal Fragments Generated by Electron Ionization Dissociation Enhance Protein Top-Down Mass Spectrometry. *Journal of the American Society for Mass Spectrometry* **2020,** *31* (9), 1896-1902.

22. Wei, B.; Zenaidee, M. A.; Lantz, C.; Williams, B. J.; Totten, S.; Ogorzalek Loo, R. R.; Loo, J. A., Top-down mass spectrometry and assigning internal fragments for determining disulfide bond positions in proteins. *Analyst* **2023,** *148* (1), 26-37.

23. Zenaidee, M. A.; Wei, B.; Lantz, C.; Wu, H. T.; Lambeth, T. R.; Diedrich, J. K.; Ogorzalek Loo, R. R.; Julian, R. R.; Loo, J. A., Internal Fragments Generated from Different Top-Down Mass Spectrometry Fragmentation Methods Extend Protein Sequence Coverage. *Journal of the American Society for Mass Spectrometry* **2021,** *32* (7), 1752-1758.

24. Zhurov, K. O.; Fornelli, L.; Wodrich, M. D.; Laskay, Ü. A.; Tsybin, Y. O., Principles of electron capture and transfer dissociation mass spectrometry applied to peptide and protein structure analysis. *Chemical Society Reviews* **2013,** *42* (12), 5014-5030.

25. Yin, S.; Loo, J. A., Elucidating the site of protein-ATP binding by top-down mass spectrometry. *Journal of the American Society for Mass Spectrometry* **2010,** *21* (6), 899-907.

26. Compton, P. D.; Zamdborg, L.; Thomas, P. M.; Kelleher, N. L., On the Scalability and Requirements of Whole Protein Mass Spectrometry. *Analytical Chemistry* **2011,** *83* (17), 6868-6874.

27. Huguet, R.; Mullen, C.; Srzentić, K.; Greer, J. B.; Fellers, R. T.; Zabrouskov, V.; Syka, J. E. P.; Kelleher, N. L.; Fornelli, L., Proton Transfer Charge Reduction Enables High-Throughput Top-Down Analysis of Large Proteoforms. *Analytical Chemistry* **2019,** *91* (24), 15732-15739.

28. Anderson, L. C.; English, A. M.; Wang, W.-H.; Bai, D. L.; Shabanowitz, J.; Hunt, D. F., Protein derivatization and sequential ion/ion reactions to enhance sequence coverage produced by electron transfer dissociation mass spectrometry. *International Journal of Mass Spectrometry* **2015,** *377*, 617-624.

29. Stephenson, J. L.; McLuckey, S. A., Ion/Ion Proton Transfer Reactions for Protein Mixture Analysis. *Analytical Chemistry* **1996,** *68* (22), 4026-4032.

30. Stephenson, J. L.; McLuckey, S. A., Ion/Ion Reactions in the Gas Phase: Proton Transfer Reactions Involving Multiply-Charged Proteins. *Journal of the American Chemical Society* **1996,** *118* (31), 7390-7397.

31. Coon, J. J.; Ueberheide, B.; Syka, J. E. P.; Dryhurst, D. D.; Ausio, J.; Shabanowitz, J.; Hunt, D. F., Protein identification using sequential ion/ion reactions and tandem mass spectrometry. *Proceedings of the National Academy of Sciences* **2005,** *102* (27), 9463-9468.

32. Yergey, J.; Heller, D.; Hansen, G.; Cotter, R. J.; Fenselau, C., Isotopic distributions in mass spectra of large molecules. *Analytical Chemistry* **1983,** *55* (2), 353-356.

33. Xie, Y.; Zhang, J.; Yin, S.; Loo, J. A., Top-Down ESI-ECD-FT-ICR Mass Spectrometry Localizes Noncovalent Protein-Ligand Binding Sites. *Journal of the American Chemical Society* **2006,** *128* (45), 14432-14433.

34. Wen, J.; Zhang, H.; Gross, M. L.; Blankenship, R. E., Native Electrospray Mass Spectrometry Reveals the Nature and Stoichiometry of Pigments in the FMO Photosynthetic Antenna Protein. *Biochemistry* **2011,** *50* (17), 3502-3511.

35. Yin, S.; Xie, Y.; Loo, J. A., Mass spectrometry of protein-ligand complexes: Enhanced gas-phase stability of ribonuclease-nucleotide complexes. *Journal of the American Society for Mass Spectrometry* **2008,** *19* (8), 1199-1208.

36. Daggett, V.; Levitt, M., A model of the molten globule state from molecular dynamics simulations. *Proceedings of the National Academy of Sciences* **1992,** *89* (11), 5142-5146.

37. Parthasarathy, S.; Murthy, M. R. N., Protein thermal stability: insights from atomic displacement parameters (B values). *Protein Engineering, Design and Selection* **2000,** *13* (1), 9-13.

38. Sun, Z.; Liu, Q.; Qu, G.; Feng, Y.; Reetz, M. T., Utility of B-Factors in Protein Science: Interpreting Rigidity, Flexibility, and Internal Motion and Engineering Thermostability. *Chemical Reviews* **2019,** *119* (3), 1626-1665.

39. Javanshad, R.; Panth, R.; Venter, A. R., Effects of Amino Acid Additives on Protein Stability during Electrothermal Supercharging in ESI-MS. *Journal of the American Society for Mass Spectrometry* **2024,** *35* (1), 151-157.

40. Green, N. M., AVIDIN. 1. THE USE OF [14C]BIOTIN FOR KINETIC STUDIES AND FOR ASSAY. *Biochemical Journal* **1963,** *89* (3), 585-591.

41. Green, N. M., Thermodynamics of the binding of biotin and some analogues by avidin. *Biochemical Journal* **1966,** *101* (3), 774-780.

42. Bykhovski, A.; Zhang, W.; Jensen, J.; Woolard, D., Analysis of Electronic Structure, Binding, and Vibrations in Biotin–Streptavidin Complexes Based on Density Functional Theory and Molecular Mechanics. *The Journal of Physical Chemistry B* **2013,** *117* (1), 25-37.

43. Young, T.; Abel, R.; Kim, B.; Berne, B. J.; Friesner, R. A., Motifs for molecular recognition exploiting hydrophobic enclosure in protein–ligand binding. *Proceedings of the National Academy of Sciences* **2007,** *104* (3), 808-813.

44. Stenkamp, R. E.; Trong, I. L.; Klumb, L.; Stayton, P. S.; Freitag, S., Structural studies of the streptavidin binding loop. *Protein Science* **1997,** *6* (6), 1157-1166.

Chapter 4: Native Top-Down Mass Spectrometry Aids Cryo-Electron Microscopy to Reveal the Three-Dimensional Structure for a Potential Human E3 Ligase

Boyu Zhao[1], Eric Z. Pang[1], Cameron Flowers[1], Steven G. Clarke[1], Jose A. Rodriguez[1], Joseph A. Loo[1,2]

[1]Department of Chemistry and Biochemistry, [2]Department of Biological Chemistry, University of California Los Angeles, Los Angeles, CA

Abstract

Native top-down mass spectrometry (nTD-MS) provides critical information on sequence, post-translational modifications, ligand-binding stoichiometry, and potentially higher-order structure for protein complexes. Single particle cryo-electron microscopy (cryo-EM) is a powerful tool for solving the three-dimensional (3D) structures of protein complexes; however, it is still challenging to yield atomic level resolution for all proteins. In this study, we describe the complementarity of an integrated nTD-MS and cryo-EM strategy to analyze a protein complex that has yet been characterized. Native MS was used to identify protein-ligand binding events. From the cryo-EM derived structure, the quaternary structures determined by the gas-phase MS measurements are retained from the solution-phase origin. The information provided by nTD-MS can be used to aid solving high-resolution structures from cryo-EM data and highlights the potential of native MS to be integrated with cryo-EM for structural biology studies.

Introduction

Protein carboxyl methyltransferase domain-containing protein 1 (PCMTD1) may be the substrate adaptor protein of a potential E3 ubiquitin ligase that ubiquitylates proteins harboring isoaspartyl damage for proteasomal degradation. The potential role of PCMTD1 in isoaspartyl maintenance was predicted from its sequence similarity to protein-L-isoaspartyl (D-aspartyl) O-methyltransferase (PCMT1), as both enzymes share binding motifs for L-isoaspartate substrates and the methyl donor cofactor, S-adenosylmethionine (SAM). However, despite PCMTD1's ability to site-specifically engage SAM[1], PCMTD1 lacks methylation activity against known damaged substrates to PCMT1. But PCMTD1 was shown to multimerize with cullin-RING ligase (CRL) components to form the putative CRL: CRL5-PCMTD1 complex in vitro and in cultured cells[1]. This implies some functional role for the assembly of PCMTD1 into a CRL in the regulation of isoaspartyl damages through targeted proteolysis.

Currently, it is unknown how PCMTD1 may have lost its methylation activity despite its high sequence homology with PCMT1. If PCMTD1 indeed lacks methylation activity, the functional role of SAM as a cofactor remains a mystery. Other features found in the PCMTD1 sequence are also unexplored, such as a novel extended linker region found flanked between its suppressors of cytokine signaling (SOCS)-box domains. While SOCS-box domains are conserved among CRL substrate adaptor proteins, which facilitate multimerization into a CRL, the PCMTD proteins are the only SOCS-box proteins that harbor an extended low-complexity domain between the SOCS-box domains whose current function is unknown[2]. We aim to structurally characterize PCMTD1 as a CRL,

CRL5-PCMTD1, to answer such questions and to elucidate its structure-activity relationship as a multimeric protein.

Our chosen methodology for structurally characterizing CRL5-PCMTD1 takes into consideration that structural dynamics of CRLs are important for ubiquitylation activity. Cullin scaffold proteins and E2~Ub recruiting Rbx proteins are flexible bodies that promote ubiquitin transfer from E2 to substrates[3]. Experimental structures of CRLs, obtained by x-ray crystallography and cryo-electron microscopy (cryo-EM), are typically limited to static structures and fail to capture the dynamics involved in substrate tagging. To address these issues in our characterization efforts of CRL5-PCMTD1, we have established a platform for characterizing the structural dynamics of CRL5-PCMTD1 complexes using single particle cryo-EM and nano electrospray ionization (nESI)-native top-down mass spectrometry (nTD-MS). This platform offers full biochemical control as we work with a fully recombinantly assembled CRL, CRL5-PCMTD1, and any subcomplex of that CRL. Dynamics will be uncovered by using heterogenous refinement strategies to capture differential conformations that may exist in this system, and pairing this information with predictive AI models AlphaFold[4] and nTD-MS to determine the stoichiometric makeup and facilitate the identification of direct protein-protein interfaces and solvent accessible surfaces in this putative CRL.

Native top-down mass spectrometry has been a useful technique for characterizing native protein complexes with noncovalent interactions[5, 6], obtaining sequence, modification and higher-order structure information[5, 7-9], probing substrate/ligand binding events[10, 11], and providing complementary information to data supplied by conventional structural analysis methods, such as, NMR[12], x-ray crystallography[13], and cryo-EM[14]. To confidently obtain

the higher-order structure information of protein complexes, nESI-MS is optimized to gently ionize and transfer protein complexes from solution into the gas-phase[15], while preserving the native-like structures of protein complexes and protein-ligand complexes[16, 17], and measuring their masses with high accuracy[6].

Top-down mass spectrometry can be coupled with native MS to obtain structural information. Various fragmentation methods can be used with TD-MS, such as collision-, electron-, or photon-based dissociation for protein sequencing[18], modification localization[19], and structure information characterization[5, 7-9]. It has been found that an Orbitrap-based MS equipped with high energy C-trap dissociation (HCD)[7], a type of collision induced dissociation (CID), which happens on a shorter timescale than conventional CID, and EChcD (as described in Chapter 2 and 3), electron capture dissociation with supplement HCD, which has the capacity cleaving peptide backbones while preserving labile bonds and noncovalent interactions[11, 20, 21], can generate fragments directly from protein complexes. Therefore, native top-down mass spectrometry with HCD and EChcD enables us to obtain structure information by fragmenting the intact gas-phase protein complexes and subcomplexes. Complex-down MS (pseudo-MS^3)[22], where a subunit is ejected from the native protein complex using in-source CID (ISD) and subsequently subjected to fragmentation, can reflect the stoichiometry of the protein complex, and provide sequence information for each subunit. Structure information, such as helping to define solvent accessible regions, can be obtained by a combination of nTD-MS and complex-down MS.

In this study, we show that nMS and complex-down MS with HCD and EChcD analysis of CRL5-PCMTD1 heteropentamer and its subcomplexes confirm the sequence,

stoichiometry, and substrate binding events. Moreover, nTD-MS with HCD and EChcD analysis of the heteropentamer elucidate its higher-order structure, and confirms the 3D structure derived by cryo-EM measurements.

Experimental

Sample preparation. PCMTD1-eloBC heterotrimer (65 kDa), Cul5-Rbx2 heterodimer (104 kDa), and CRL5-PCMTD1 heteropentamer (169 kDa) were purified from *E. coli* expression systems described previously[1]. Either β-mercaptoethanol (βME) or dithiothreitol (DTT) was added in the lysis buffer. The His-TEV-tag on the Cul5 subunit and TEV-tag on the PCMTD1 subunit were cleaved, except when explicitly mentioned. Proteins were buffer exchanged using 50 kDa or 100 kDa Millipore Amicon Ultra filters (Sigma-Aldrich, St. Louis, MO, USA) into 200 mM ammonium acetate and diluted to a final concentration of 20 μM. Peptides were ordered from GenScript Biotech (Piscataway, NJ, USA). The peptides were dissolved in MS-grade water to a final concentration of 50 μM. S-Adenosyl methionine (SAM) were dissolved in MS-grade water to a final concentration of 50 μM.

Native Top-Down and Complex-Down HCD and EChcD MS. Both HCD and electron capture dissociation with supplement HCD (EChcD) experiments were performed on a Thermo Fisher Scientific Q Exactive Ultra-High Mass Range (UHMR) Orbitrap mass spectrometer with an ExD cell developed by e-MSion (Corvallis, OR, USA). Protein solutions were loaded into Pt-coated borosilicate capillaries on a nanospray ionization source and sprayed at 0.8-1.5 kV, 175 ℃. The S-lens RF was set at 100 V. In-source CID was set over a range of 30-150 eV for monomer ejection experiments. A single charge state

was isolated by the quadrupole for protein complex and subcomplexes. In EChcD experiments, the precursor ions were transferred into the ECD cell, where they were subject to electron capture, then into the HCD cell for post-ECD collisional activation. The ECD filament current was set at 2.23 A. The HCD collision energy was optimized to minimize the generation of b/y fragment ions. Additional details of ExD cell (Figure S1) and tuning parameters are provided in the Supporting Information (Table S1). All top-down mass spectra were acquired at 100,000 resolution (*m/z* 400) with a noise threshold set to 3. Each spectrum was a result of 500 averaged scans.

Denatured Protein MS. Protein were denatured with formic acid (final concentration 0.5%). Denatured protein sample was injected to an Agilent 1260 Infinity LC equipped with a 50 mm x 2.1 mm analytical column (PLRP-S 100Å, 5 μm, Agilent Technologies). The LC gradient was 1% solvent B (A= H_2O with 0.1% formic acid; B = acetonitrile with 0.1% formic acid) in 2 min and from 1 – 95% in 10 min at flow rate 0.8 mL/min. All denatured spectra were collected on an Agilent Q-TOF 6530 MS. The ESI voltage was set at 1.5 kV, and the capillary temperature was set at 300°C. Full spectra (*m/z* 100 - 3000) were acquired in profile mode.

Bottom-up Proteomics for Sequence Verification. Proteins was exchanged into 8 M urea buffer using a 10 kDa Microcon ultrafiltration unit (Millipore). Proteins were alkylated with 17 mM iodoacetamide and digested overnight at 37°C with a 1:100 ratio of trypsin:protein. Peptides were dried, resuspended in 0.1% formic acid, desalted with STAGE tips, as described earlier[23]. Desalted peptide-containing samples were resuspended in LC–MS injection buffer (buffer A, 0.1% formic acid) and analyzed on a quadrupole

Orbitrap mass spectrometer (Q-Exactive Plus, ThermoFisher Scientific, Waltham, USA) using liquid chromatography–tandem mass spectrometry (LC–MS/MS).

Protein (1.0 μg) was injected to an Ultimate 3000 nano LC, which was equipped with a 75μm x 2 cm trap column packed with C18 3μm bulk resins (Acclaim PepMap 100, ThermoFisher Scientific) and a 75μm x 15 cm analytical column with C18 2μm resins (Acclaim PepMap RSLC, ThermoFisher Scientifc). The nanoLC gradient was 3 - 35% solvent B (A = H_2O with 0.1% formic acid; B = acetonitrile with 0.1% formic acid) over 40 min and from 35% - 85% solvent B in 5 min at flow rate 300 nL/min. The nanoLC was coupled with a Q Exactive Plus orbitrap mass spectrometer (Thermo Fisher Scientific, San Jose, CA). The ESI voltage was set at 1.9 kV, and the capillary temperature was set at 275°C. Full spectra (m/z 350 - 2000) were acquired in profile mode with resolution 70,000 at *m/z* 200 with an automated gain control (AGC) target of 3E6. The most abundance 15 ions were subjected to fragmentation by high energy C-trap dissociation (HCD) with a normalized collisional energy of 25%. Dynamic exclusion was applied for 45 s over ±10 ppm. MS/MS scans were collected with a first fixed mass of *m/z* 100, 2 *m/z* isolation window, 17,500 orbitrap resolution, and normalized AGC target of 100%.

Data Analysis. Native and denatured spectra were deconvoluted by UniDec[24]. All MS/MS spectra were deconvoluted with BioPharma Finder 5.0 (ThermoFisher Scientific, Waltham, USA). Deconvolved peaks were assigned by ClipsMS 2.0.035 with an error tolerance of 5 ppm. Sequence assignment accommodated the major ECD (c, c+H, c-H, z, z+H, z-H) and HCD (b, y) ion types without annotating neutral losses ions, except when explicitly mentioned. Terminal fragments were manually validated by confirming the isotopic distributions.

Raw data from bottom-up proteomics was searched again UniProt human database by Proteome Discovered version 2.5. Following parameters were set: precursor mass tolerance ±10 ppm, fragment mass tolerance ±0.02 Th for HCD, up to two miscleavages by semi trypsin, methionine oxidation as variable modification, and cysteine carbamidomethylation as static modification. False discovery rate was at 1.0% and minimum of 1 peptide was required for protein identification.

Results and Dissociation

Determining Molecular Mass and Stoichiometry for CRL5-PCMTD1 Complex

Native and denatured MS analyses of the putative CRL5-PCMTD1 heteropentamer complex, subcomplexes and individual subunits provide a comprehensive overview of the composition and stoichiometry of the overall assembly. A relative narrow charge state distribution from 30+ to 23+ corresponding to the heteropentamer was observed (Figure 1A). The same sample was measured after a month of storage at -80 ℃. The resultant spectrum revealed subcomplexes and subunits, thus confirming the stoichiometry of CRL5-PCMTD1 complex. Moreover, at a mass resolution of 100,000 (at *m/z* 400), the 6+ eloB monomer peak and 4+ eloC monomer peak were isotopically resolved (Figure S2B and C). The calculated isotopic masses for eloB and eloC are 13125.599 Da, and 10957.488 Da, respectively and within 6 ppm mass accuracy from the theoretical mass. The mass of the Rbx2 subunit was measured by performing denatured MS, and the resultant spectrum (Figure S2A) indicates the accurate mass of Rbx2 subunit and the presence of 1 and 2 βME bound forms. Therefore, the proteins were purified with a different reducing agent, DTT, to eliminate the heterogeneity caused by the addition of βME for following experiments.

The sequences of Cul5 and PCMTD1 subunits were confirmed by bottom-up proteomics (Figure S3).

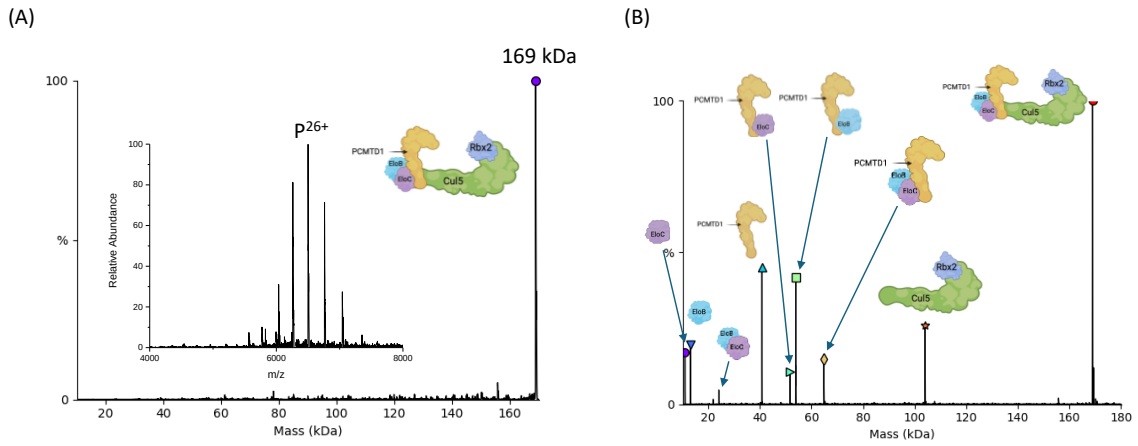

Figure 1. (A) Native deconvolved mass spectrum of CRL5-PCMTD1 heteropentamer, (B) and deconvolved spectrum of CRL5-PCMTD1 heteropentamer after one month storage at -80 ℃; the observation of monomers, heterodimers and heterotrimers confirm the stoichiometry of CRL5-PCMTD1 complex.

Native Top-Down HCD and EChcD of CRL5-PCMTD1 Complex and Subcomplexes

We first performed nTD-MS HCD on the 23+ charge state of Cul5-Rbx2 heterodimer. This generated N-terminal *b*-fragments from the Cul5 subunit, and C-terminal *y*-fragments from the Rbx2 subunit. From previous nTD-MS HCD studies from our lab[7], this suggests that the Cul5 N-terminus and the Rbx2 C-terminus are solvent exposed. The data also suggests that C-terminus of Cul5 subunit and N-terminus of Rbx2 subunit should be close to the Cul5-Rbx2 monomer interfaces. Due to the ISD energy upper limit, we were not able to detach the Cul5-Rbx2 monomers from each other.

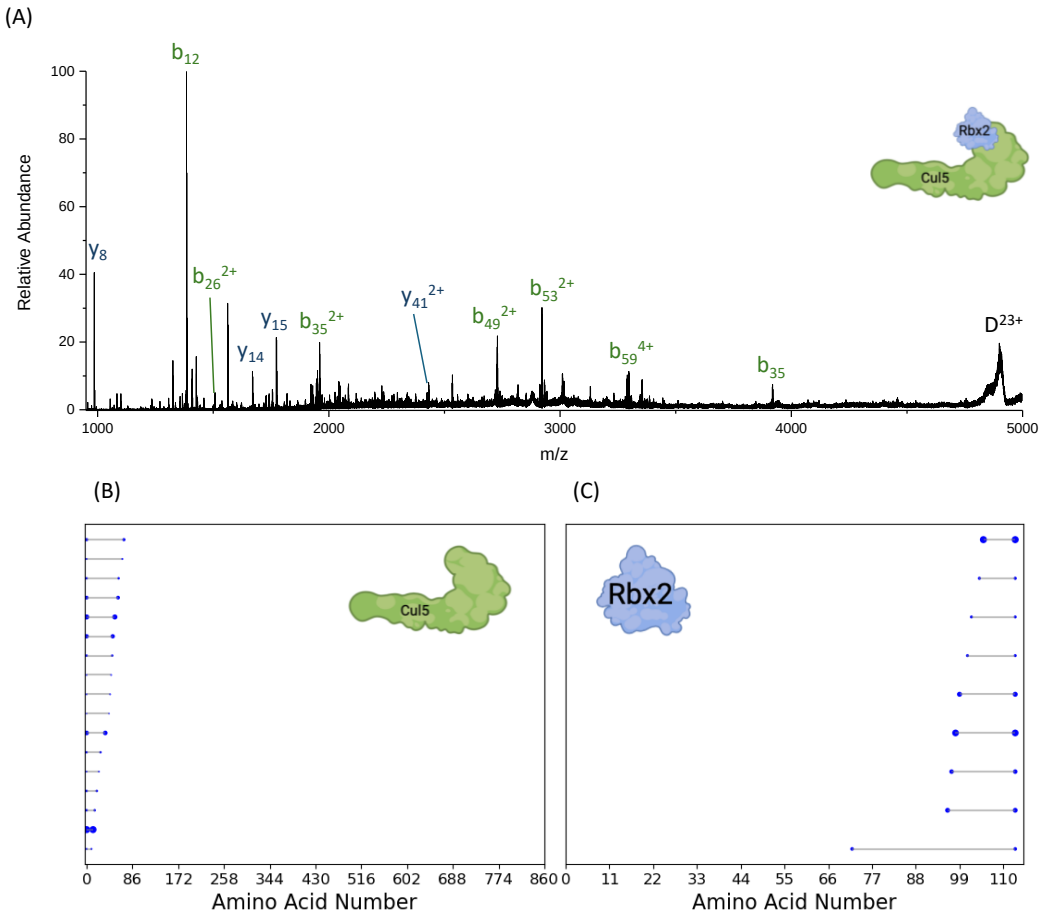

Figure 2. (A) Native top-down HCD MS of the 23+ charge state of His-TEV-Cul5-Rbx2 heterodimer, with fragments ions from the Cul5 subunit labeled in green, and fragment ions from the Rbx2 subunit labeled in dark blue; fragmentation location map of (B) His-TEV-Cul5 subunit, and (C) Rbx2 subunit.

In addition, we performed nTD-MS using both HCD and EChcD on the eloB-eloC-PCMTD1 heterotrimer. Dissociation of the heterotrimer into its monomer components was observed at low HCD energy without generating sequence-bearing product ions. Instead, nTD-MS with EChcD was performed to prevent monomer ejection prior to direct fragmentation of the heterotrimer. Although ejected eloB and eloC monomers were observed with EChcD (Figure 3A), fragment ions that appear to provide higher-order structure information from each monomer were observed. The fragment location maps of

eloB and eloC subunits (Figures 3B and C) show mainly N-terminal *c*-fragments generated from each subunit, suggesting that the N-termini of eloB and eloC are more solvent exposed in the heterotrimer, whereas the C-termini of both subunits may be involved in biding to PCMTD1. There were only 3 C-terminal *z*-fragments assigned to the PCMTD1 subunit. Thus, due to the limited number of fragments, we are not able to conclude the monomer interface on PCMTD1 subunit.

To gain more information on the monomer binding interfaces, we performed complex-down HCD experiments on the eloB (Figure S4A and B) and eloC (Figure S4C and D) subunits separately. The resultant MS/MS spectra reveal both N-terminal *b*-fragments and C-terminal *y*-fragments of both subunits. The presence of near equal proportions of *b*- and *y*- fragments from complex-down MS indicates that both termini of both subunits are accessible by HCD. Therefore, each subunit released by ISD retain little higher-order structure information about the native heterotrimer. However, by comparing the fragmentation patterns between nTD-MS and complex-down for each subunit, we were able to confidently confirm the monomer binding interfaces for the eloB-eloC-PCMTD1 heterotrimer.

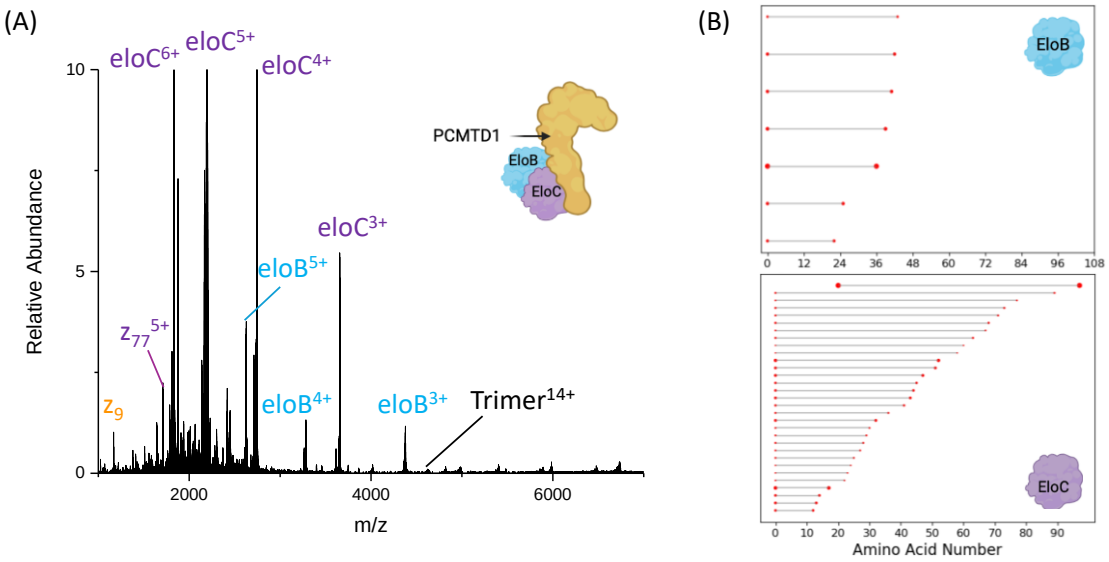

Figure 3. (A) Native top-down EChcD MS of (A) the 14+ charge state of eloB-eloC-PCMTD1 trimer, with eloB subunit ions labeled in cyan, eloC subunit and its fragments labeled in purple, and fragments from PCMTD1 labeled in yellow, and (B) the corresponding fragment location maps for eloB and eloC subunits.

ECD and EChcD have the capability for preserving labile bonding and noncovalent interactions during the protein backbone cleavage process[11, 20, 21]. Moreover, our previous study (shown in Chapter 2) has shown that EChcD has enhanced fragmentation efficiency, compared to HCD alone. EChcD of the native fully intact CRL5-PCMTD1 heteropentamer revealed numerous peaks at fragmentation region (*m/z* 1000-4000) as well as charge reduced intact species. However, only c-fragments from the Cul5 subunit can be mapped back to the sequence (Figure 4B), which indicates that N-terminus of Cul5 subunit may be at the solvent exposed region, and not directly in contact with other the subunits. The limited number of fragments assigned might be due to the complexity of spectrum at the fragment-rich region. As the number of fragments increases, more overlapped peaks can be observed, which makes the deconvolution of a fragmentation spectrum challenging. Therefore, the deconvoluted masses may not be accurate, resulting in less matched

fragments for a given mass accuracy. To address this issue, we also performed native top-down HCD MS of the native CRL5-PCMTD1 heteropentamer. Although HCD of the pentamer resulted in the release of eloB, HCD generated N-terminal b-fragments from Cul5, N-terminal b-fragments from eloB, C-terminal y-fragments from Rbx2, and C-terminal y-fragments from PCMTD1. This result is consistent with fragmentation patterns revealed by top-down of the Cul5-Rbx2 heterodimer, eloBC-PCMTD1 heterotrimer, and CRL5-PCMTD1 heteropentamer, and confirms the subunit-subunit interfaces suggested from the nTD-MS of the subcomplexes. (It should be noted that CRL5-PCMTD1 heteropentamer in the HCD experiment has a His-TEV tag on Cul5 N-terminus, and a TEV tag on PCMTD1 N-terminus.)

Moreover, the results from native TD-MS are consistent with the 3D structure obtained from cryo-EM at 4.38 Å resolution at the Fourier shell correlation (FSC) threshold of 0.143 (Figure S5). The cryo-EM structure shows that a region of the the N-terminus of Cul5 is solvent exposed, which are easily accessed by HCD and EChcD MS experiments.

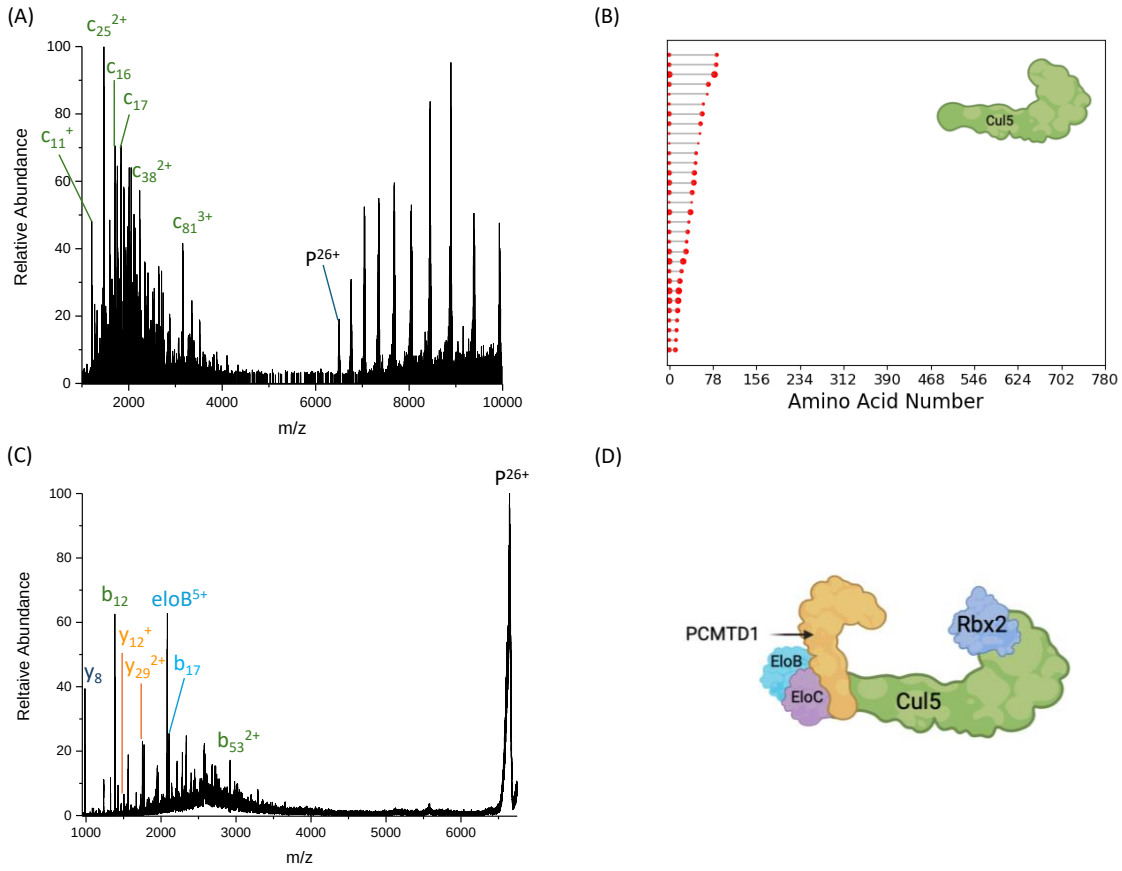

Figure 4. Native top-down (A) EChcD MS of the 26+ charge state of CRL5-PCMTD1 without tags on both Cul5 and PCMTD1 subunits, with fragments from the Cul5 subunit labeled in green, and (B) corresponding fragmentation map for Cul5 subunit. (C) HCD MS of the 26+ charge state of CRL5-PCMTD1 heteropentamer with His-TEV-tag on Cul5 and TEV-tag on PCMTD1 subunit, with fragments from the Cul5 subunit labeled in green, fragments from Rbx2 subunit labeled in dark blue, fragments from the PCMTD1 subunit labeled in yellow, and the eloB monomer and fragment from eloB subunit labeled in cyan. (D) Proposed CRL5-PCMTD1 heteropentamer higher-order structure.

Native MS Probes Subcomplex-Ligand Binding Event

Structural characterization via single particle cryo-EM on PCMTD1 multimerized in a pentameric assembly, CRL5-PCMTD1, yielded resolution sufficient for investigating its domain-level architecture but not atomic features. Sub-optimal structural resolution may be due to known dynamics in CRLs, which help facilitate their enzymatic functions. To

obtain higher resolution information for PCMTD1 by cryo-EM, we reconstituted a variant of CRL5-PCMTD1 where PCMTD1 is multimerized into a tetramer with eloBC and a N-terminal domine of Cul5 to further stabilize PCMTD1. We envision this new preparation will provide greater structural details for PCMTD1 to elucidate its structure-function relationship. We also aimed to characterize potential iso-aspartic acid (isoD) peptide binding for this new heterotetramer preparation with cryo-EM and nTD-MS where high resolution information on where PCMTD1 engages isoD residues could be achieved.

Native MS experiments were performed on eloB-eloC-PCMTD1-Cul5 N-terminal domain (NTD) heterotetramer, and the heterotetramer with excess SAM, excess GGGVYPisoDLA (isoP1), and excess GGGKASAisoDLAKY (isoP2). Figure 5A shows two charge state distributions corresponding to apo-tetramer and tetramer with SAM (holo-tetramer), suggesting that that presence of SAM is not critical for forming the tetramer. With the addition of excess SAM, only holo-tetramer was observed (Figure 5B). With the addition of isoD peptide 1 (no SAM added), three charge state distributions were observed in the spectrum corresponding to apo-tetramer, holo-tetramer (with SAM), and tetramer bound to both SAM and the isoD peptide (Figure 5C). No tetramer bound to the isoD peptide but without SAM-bound was observed. This result suggests that the presence of SAM is critical for tetramer-isoD peptide binding. Similar result was observed with the addition of isoD peptide 2 (Figure 5D).

To confirm that isoD is also a key factor for tetramer-peptide binding, we performed nMS experiments with the addition of normal peptides (*i.e.*, non-isoAsp) with the same sequence as the isoD peptides. Only the apo- and holo-tetramer (with SAM) were observed (Figure

S6). This result supports our hypothesis that only peptides with isoD are the substrates of the tetramer.

To investigate the isoD peptide binding site(s) on PCMTD1 subunit, we performed nTD-MS with HCD and EChcD; however, isoD peptides were released at low energy before generating any fragments that retains peptide binding.

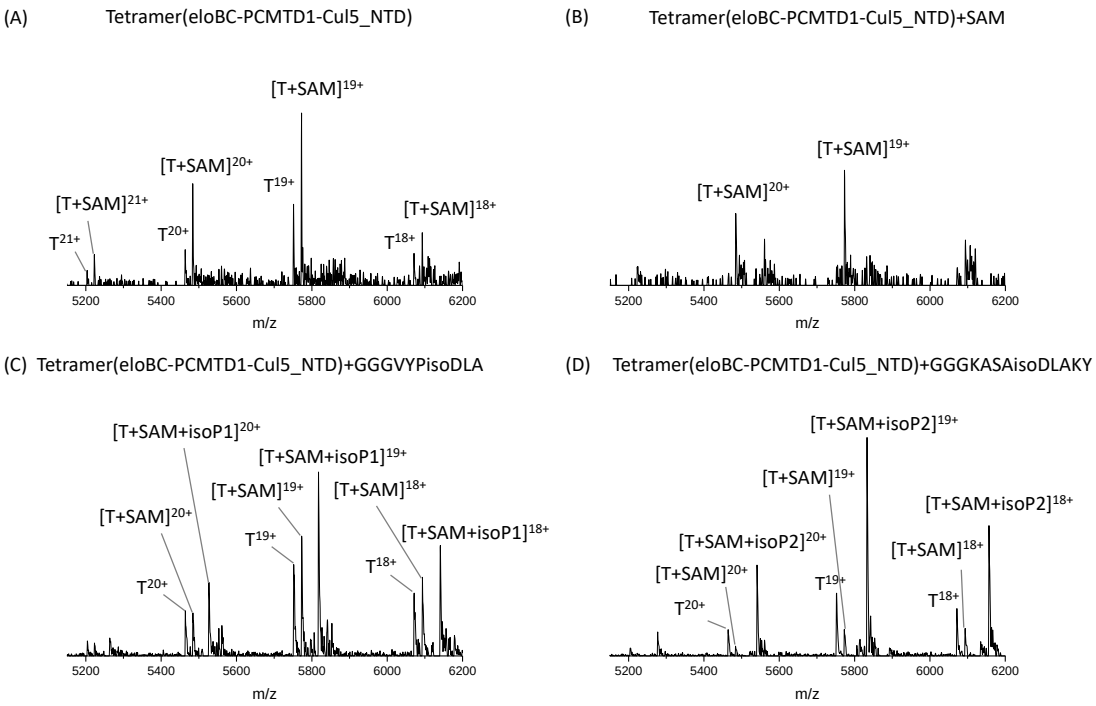

Figure 5. Native mass spectrum of (A) eloB-eloC-PCMTD1-Cul5_NTD heterotetramer, (B) eloB-eloC-PCMTD1-Cul5_NTD heterotetramer with 50 μM SAM, (C) eloB-eloC-PCMTD1-Cul5_NTD heterotetramer with peptide GGGVYPisoDLA (isoP1) (with a 1:5 ratio of tetramer:peptide), and (D) eloBC-PCMTD1-Cul5_NTD heterotetramer with peptide GGGKASAisoDLAKY (isoP2) (with a 1:5 ratio of tetramer:peptide).

Conclusion

Here we report the combination of cryo-EM and nTD-MS for the characterization of a potential human E3 ligase with an unknown structure. The results demonstrate that near-native structures can be retained in the gas phase (by MS), therefore, enabling the MS experiments to reveal higher order structure information for protein complexes and to obtain 3D structure information that can be coupled with cryo-EM results. Moreover, the native MS probing of protein-substrate binding events reveal important functional information of the PCMTD1 complex, and this can be followed-up with subsequent cryo-EM studies. It also underscores the utility of native MS to identify experimental conditions for subsequent structural studies.

Chapter 4: Supporting Information

Supplementary Figures

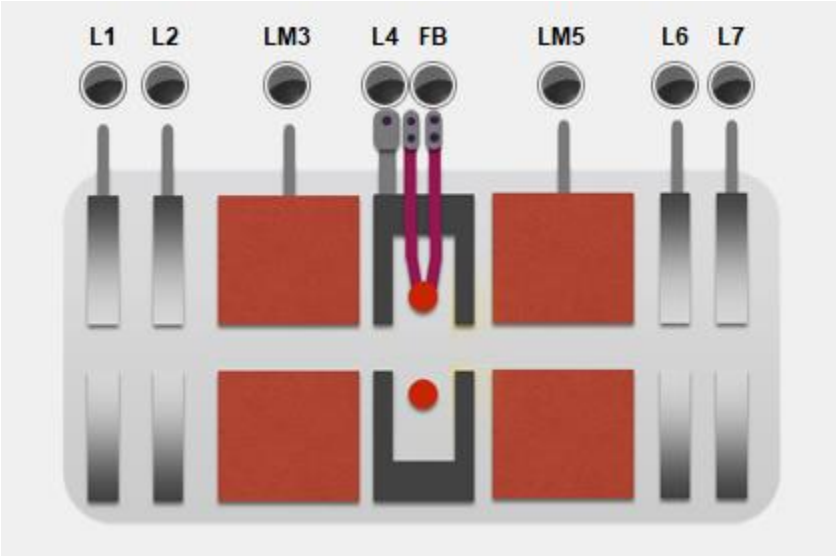

Figure S1. Schematic of the electromagnetostatic ExD cell.[1]

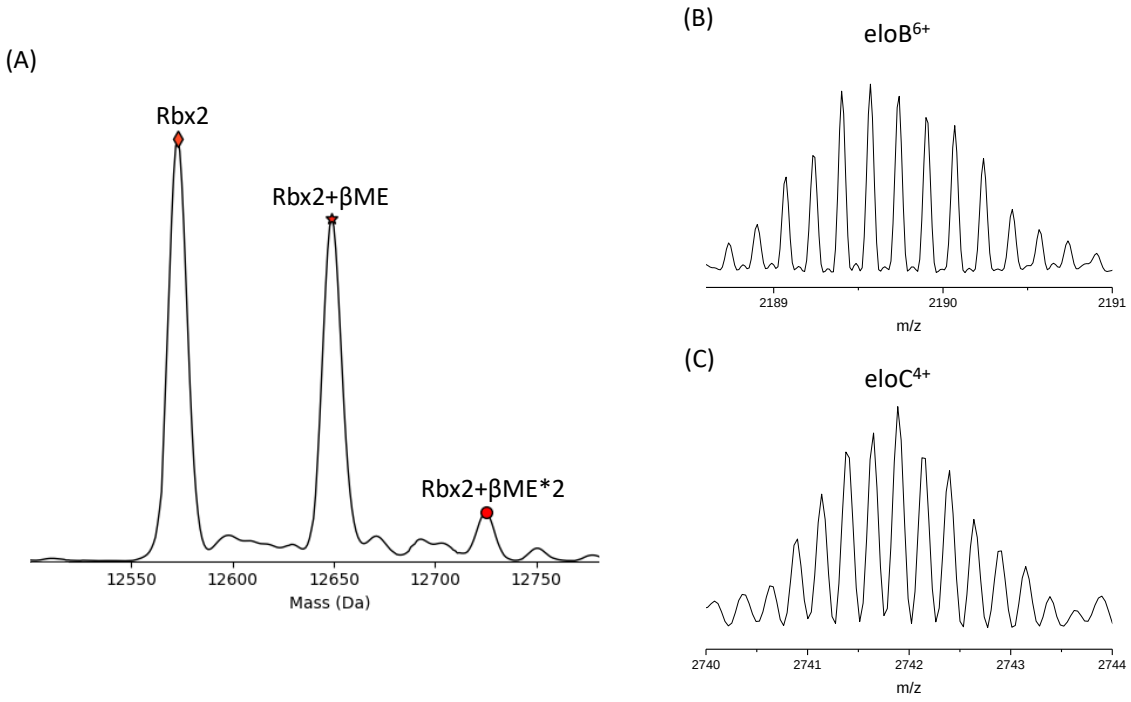

Figure S2. (A) Deconvoluted spectrum of Rbx2 subunit and Rbx2 with βME bound forms. Isotopically resolved mass spectra of (B) eloB subunit, and (C) eloC subunit.

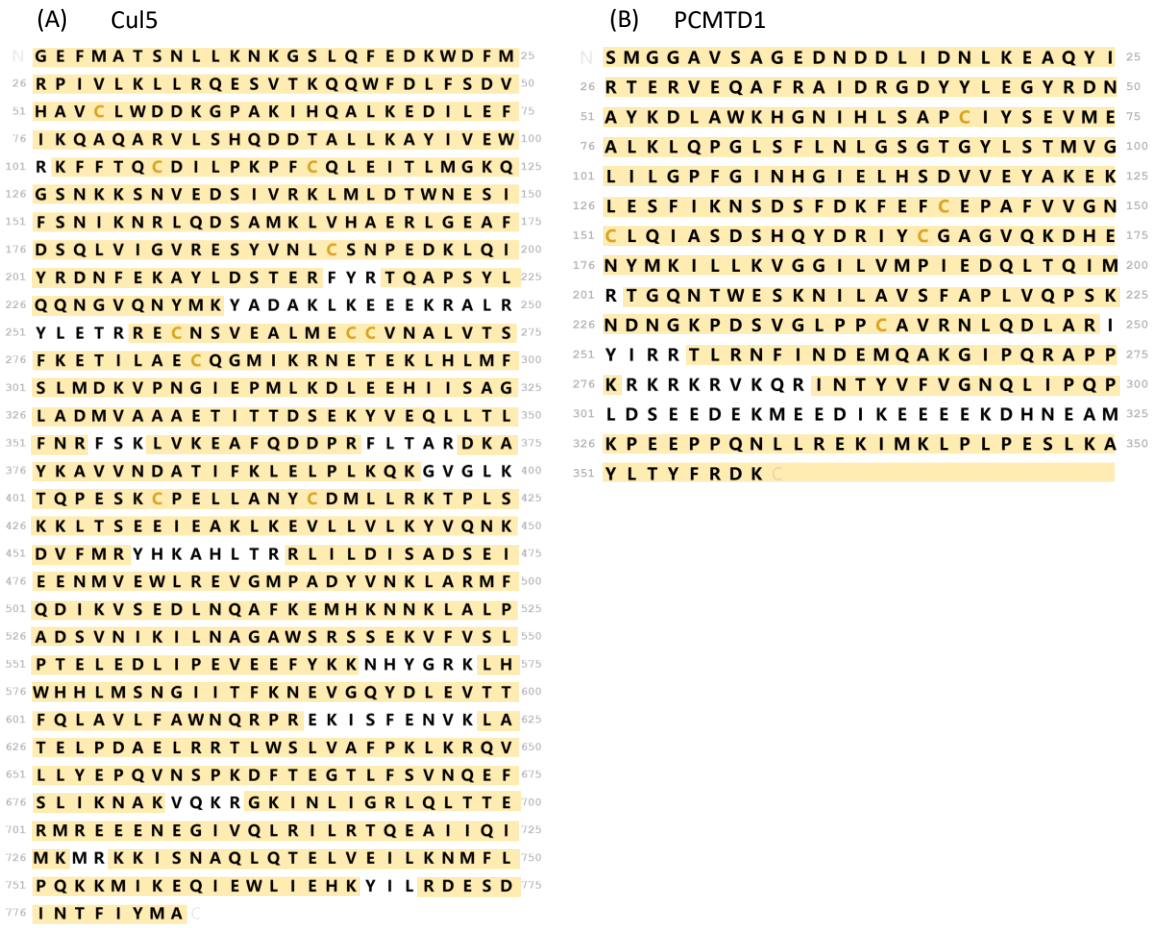

Figure S3. Protein sequence identification maps for Cul5 subunit (left panel) and PCMTD1 subunit (right panel) by bottom-up proteomics.

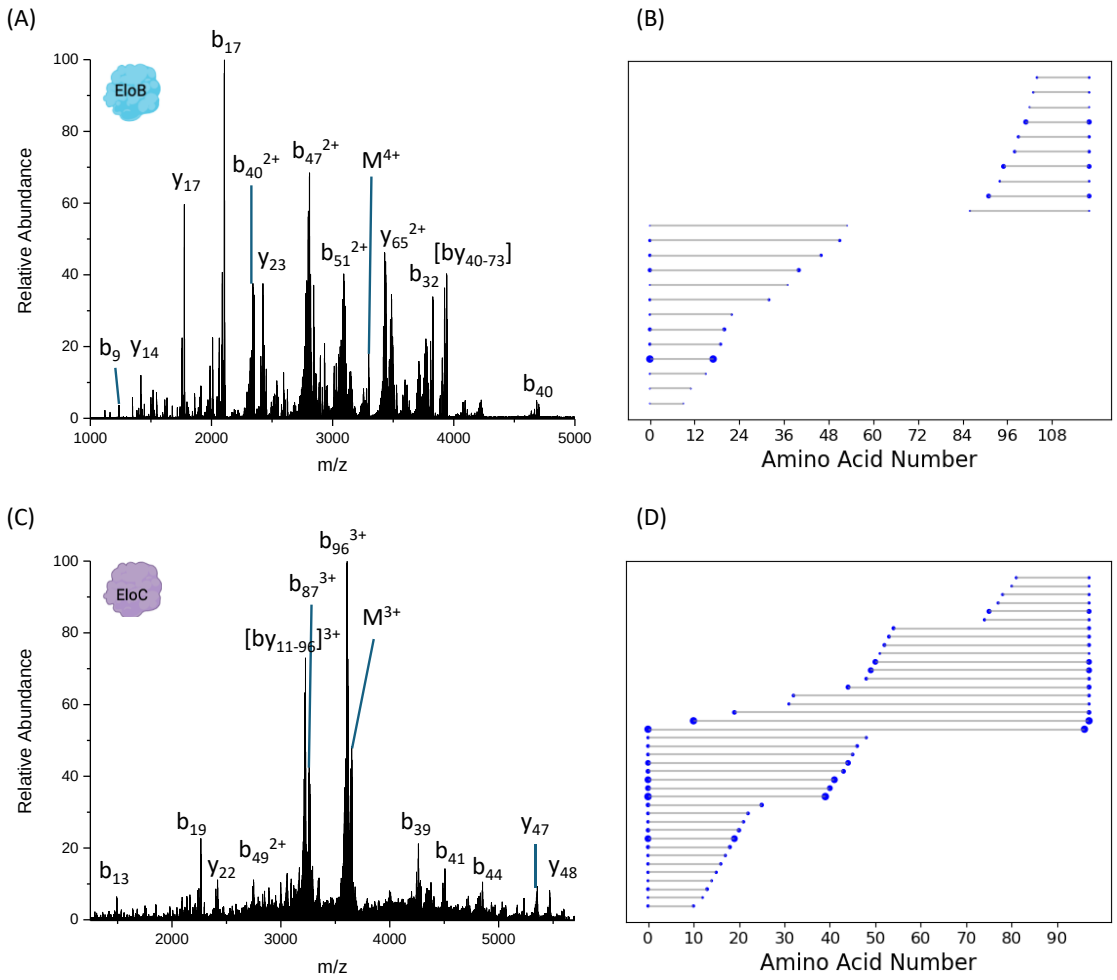

Figure S4. (A) Native top-down HCD mass spectrum of the 4+ charge state of eloB subunit, and (B) corresponding fragmentation location. (C) Native top-down HCD spectrum of the 3+ charge state of eloC subunit, and (D) corresponding fragmentation location map.

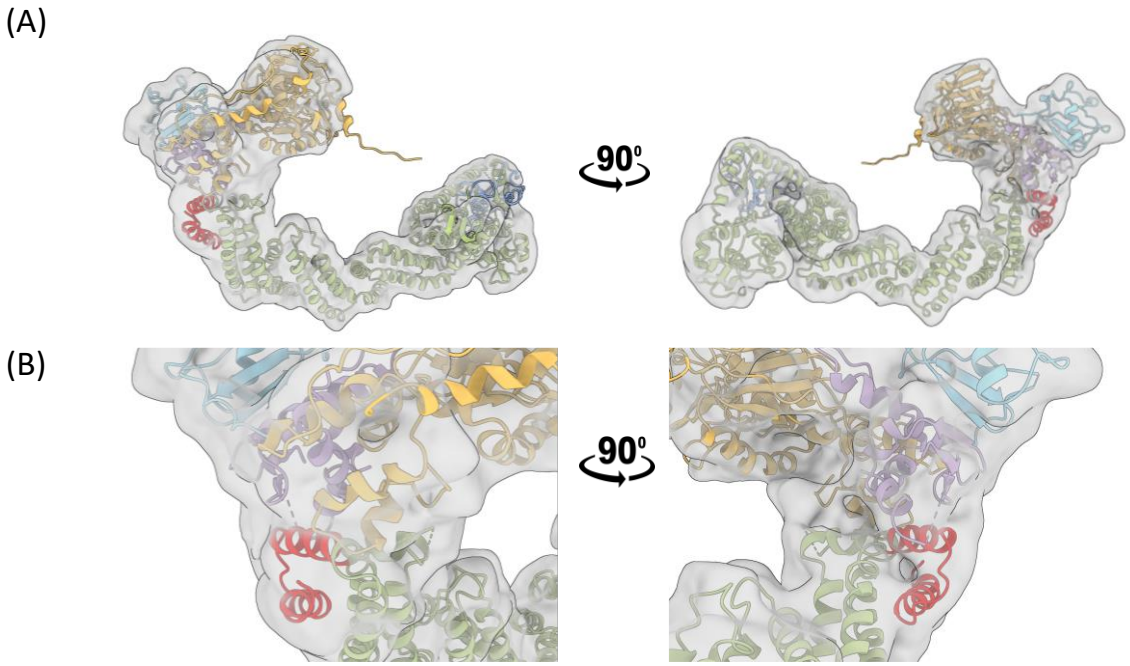

Figure S5. (A) CRL5-PCMTD1 complex structure fitted into Cryo-EM density; N-terminal fragments generated by EChcD labeled in red, the rest of Cul5 subunit labeled in green, Rbx2 subunit labeled in blue, eloB subunit labeled in cyan, and PCMTD1 subunit labeled in yellow. (B) Expanded structure for Cul5 N-terminus shows that Cul5 N-terminus is at the solvent exposed region. Cryo-EM images were collected by Eric Pang.

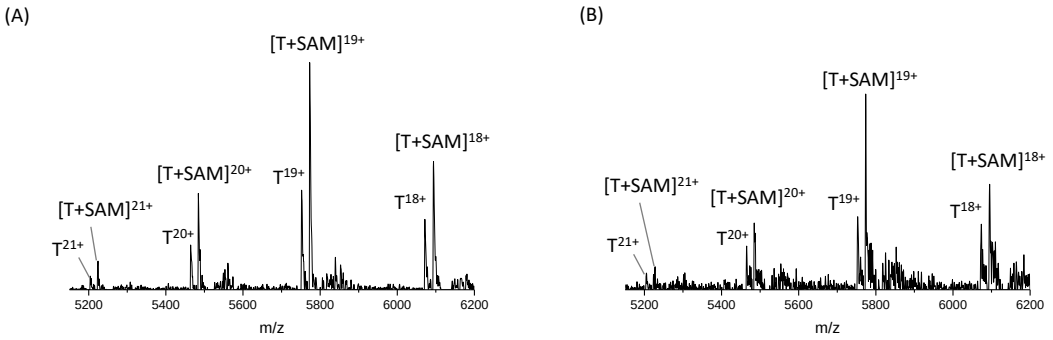

Figure S6. Native mass spectra of (A) eloB-eloC-PCMTD1-Cul5_NTD heterotetramer with peptide GGGVYPDLA (P1), and (B) eloB-eloC-PCMTD1-Cul5_NTD heterotetramer with peptide GGGKASADLAKY (P2). No peptide bound form were detectred.

Supplementary Tables

Table S1. ExD cell parameters for the protein complexes analyzed in the study.

Protein Complex	L1	L2	LM3	L4	FB	LM5	L6
eloB-eloC-PCMTD1 heterotrimer	-0.82	-40.0	1.0	4.11	-8.0	1.0	-40.0
CRL5-PCMTD1 heteropentamer	-1.27	-52.0	4.7	12.2	0.8	4.7	-52.0

Table S2. Theoretical and measured masses for monomers, subcomplexes, and the full complex. Average masses are shown in the table, unless stated otherwise.

Proteins	Theoretical mass (Da)	Measured mass (Da)
eloC monomer	10,963.54 (monoisotopic)	10,957.488 (monoisotopic)
eloB monomer	13,125.548 (monoisotopic)	13,125.599 (monoisotopic)
PCMTD1 monomer (w/o tag)	40,761.03	40,761.21
Rbx2 monomer	12,576.29	12,573.57
Cul5 monomer (w/o tags)	91,306.95	N/A
eloB-eloC heterodimer	24,096.21	24,097.37
eloB-PCMTD1 heterodimer	53,893.70	53,891.129
eloC-PCMTD1 heterometer	51,724.57	51,721.921
eloB-eloC-PCMTD1 heterotrimer	64,857.24	64,857.461
Cul5-Rbx2 heterodimer	104,014.36	104,070.875
CRL5-PCMTD1 heteropentamer	168,871.6	168,960.234

Reference

1. Shaw, J. B.; Malhan, N.; Vasil'ev, Y. V.; Lopez, N. I.; Makarov, A.; Beckman, J. S.; Voinov, V. G., Sequencing Grade Tandem Mass Spectrometry for Top–Down Proteomics Using Hybrid Electron Capture Dissociation Methods in a Benchtop Orbitrap Mass Spectrometer. *Analytical Chemistry* **2018,** *90* (18), 10819-10827.

References

1. Warmack, R. A.; Pang, E. Z.; Peluso, E.; Lowenson, J. D.; Ong, J. Y.; Torres, J. Z.; Clarke, S. G., Human Protein-l-isoaspartate O-Methyltransferase Domain-Containing Protein 1 (PCMTD1) Associates with Cullin-RING Ligase Proteins. *Biochemistry* **2022,** *61* (10), 879-894.

2. Mahrour, N.; Redwine, W. B.; Florens, L.; Swanson, S. K.; Martin-Brown, S.; Bradford, W. D.; Staehling-Hampton, K.; Washburn, M. P.; Conaway, R. C.; Conaway, J. W., Characterization of Cullin-box Sequences That Direct Recruitment of Cul2-Rbx1 and Cul5-Rbx2 Modules to Elongin BC-based Ubiquitin Ligases*. *Journal of Biological Chemistry* **2008,** *283* (12), 8005-8013.

3. Lumpkin, R. J.; Baker, R. W.; Leschziner, A. E.; Komives, E. A., Structure and dynamics of the ASB9 CUL-RING E3 Ligase. *Nature Communications* **2020,** *11* (1), 2866.

4. Jumper, J.; Evans, R.; Pritzel, A.; Green, T.; Figurnov, M.; Ronneberger, O.; Tunyasuvunakool, K.; Bates, R.; Žídek, A.; Potapenko, A.; Bridgland, A.; Meyer, C.; Kohl, S. A. A.; Ballard, A. J.; Cowie, A.; Romera-Paredes, B.; Nikolov, S.; Jain, R.; Adler, J.; Back, T.; Petersen, S.; Reiman, D.; Clancy, E.; Zielinski, M.; Steinegger, M.; Pacholska, M.; Berghammer, T.; Bodenstein, S.; Silver, D.; Vinyals, O.; Senior, A. W.; Kavukcuoglu, K.; Kohli, P.; Hassabis, D., Highly accurate protein structure prediction with AlphaFold. *Nature* **2021,** *596* (7873), 583-589.

5. Li, H.; Nguyen, H. H.; Ogorzalek Loo, R. R.; Campuzano, I. D. G.; Loo, J. A., An integrated native mass spectrometry and top-down proteomics method that connects sequence to structure and function of macromolecular complexes. *Nature Chemistry* **2018,** *10* (2), 139-148.

6. Li, H.; Wolff, J. J.; Van Orden, S. L.; Loo, J. A., Native Top-Down Electrospray Ionization-Mass Spectrometry of 158 kDa Protein Complex by High-Resolution Fourier Transform Ion Cyclotron Resonance Mass Spectrometry. *Analytical Chemistry* **2014,** *86* (1), 317-320.

7. Lantz, C.; Wei, B.; Zhao, B.; Jung, W.; Goring, A. K.; Le, J.; Miller, J.; Loo, R. R. O.; Loo, J. A., Native Top-Down Mass Spectrometry with Collisionally Activated Dissociation Yields Higher-Order Structure Information for Protein Complexes. *Journal of the American Chemical Society* **2022,** *144* (48), 21826-21830.

8. Heck, A. J. R., Native mass spectrometry: a bridge between interactomics and structural biology. *Nature Methods* **2008,** *5* (11), 927-933.

9. Zhou, M.; Lantz, C.; Brown, K. A.; Ge, Y.; Paša-Tolić, L.; Loo, J. A.; Lermyte, F., Higher-order structural characterisation of native proteins and complexes by top-down mass spectrometry. *Chemical Science* **2020,** *11* (48), 12918-12936.

10. Xie, Y.; Zhang, J.; Yin, S.; Loo, J. A., Top-Down ESI-ECD-FT-ICR Mass Spectrometry Localizes Noncovalent Protein-Ligand Binding Sites. *Journal of the American Chemical Society* **2006,** *128* (45), 14432-14433.

11. Yin, S.; Loo, J. A., Elucidating the site of protein-ATP binding by top-down mass spectrometry. *Journal of the American Society for Mass Spectrometry* **2010,** *21* (6), 899-907.

12. Clore, G. M.; Gronenborn, A. M., Structures of Larger Proteins in Solution: Three- and Four-Dimensional Heteronuclear NMR Spectroscopy. *Science* **1991,** *252* (5011), 1390-1399.

13. Garman, E. F., Developments in X-ray Crystallographic Structure Determination of Biological Macromolecules. *Science* **2014,** *343* (6175), 1102-1108.

14. Bai, X.-c.; McMullan, G.; Scheres, S. H. W., How cryo-EM is revolutionizing structural biology. *Trends in Biochemical Sciences* **2015,** *40* (1), 49-57.

15. Ogorzalek Loo, R. R.; Lakshmanan, R.; Loo, J. A., What Protein Charging (and Supercharging) Reveal about the Mechanism of Electrospray Ionization. *Journal of the American Society for Mass Spectrometry* **2014,** *25* (10), 1675-1693.

16. Lössl, P.; van de Waterbeemd, M.; Heck, A. J. R., The diverse and expanding role of mass spectrometry in structural and molecular biology. *The EMBO Journal* **2016,** *35* (24), 2634-2657-2657.

17. Liko, I.; Allison, T. M.; Hopper, J. T. S.; Robinson, C. V., Mass spectrometry guided structural biology. *Current Opinion in Structural Biology* **2016,** *40*, 136-144.

18. Zenaidee, M. A.; Wei, B.; Lantz, C.; Wu, H. T.; Lambeth, T. R.; Diedrich, J. K.; Ogorzalek Loo, R. R.; Julian, R. R.; Loo, J. A., Internal Fragments Generated from Different Top-Down Mass Spectrometry Fragmentation Methods Extend Protein Sequence Coverage. *Journal of the American Society for Mass Spectrometry* **2021,** *32* (7), 1752-1758.

19. Nshanian, M.; Lantz, C.; Wongkongkathep, P.; Schrader, T.; Klärner, F.-G.; Blümke, A.; Despres, C.; Ehrmann, M.; Smet-Nocca, C.; Bitan, G.; Loo, J. A., Native Top-Down Mass Spectrometry and Ion Mobility Spectrometry of the Interaction of Tau Protein with a Molecular Tweezer Assembly Modulator. *Journal of the American Society for Mass Spectrometry* **2019,** *30* (1), 16-23.

20. Zhang, H.; Cui, W.; Wen, J.; Blankenship, R. E.; Gross, M. L., Native Electrospray and Electron-Capture Dissociation FTICR Mass Spectrometry for Top-Down Studies of Protein Assemblies. *Analytical Chemistry* **2011,** *83* (14), 5598-5606.

21. Zhurov, K. O.; Fornelli, L.; Wodrich, M. D.; Laskay, Ü. A.; Tsybin, Y. O., Principles of electron capture and transfer dissociation mass spectrometry applied to peptide and protein structure analysis. *Chemical Society Reviews* **2013,** *42* (12), 5014-5030.

22. Lermyte, F.; Tsybin, Y. O.; O'Connor, P. B.; Loo, J. A., Top or Middle? Up or Down? Toward a Standard Lexicon for Protein Top-Down and Allied Mass Spectrometry Approaches. *Journal of the American Society for Mass Spectrometry* **2019,** *30* (7), 1149-1157.

23. Rappsilber, J.; Mann, M.; Ishihama, Y., Protocol for micro-purification, enrichment, pre-fractionation and storage of peptides for proteomics using StageTips. *Nature Protocols* **2007,** *2* (8), 1896-1906.

24. Marty, M. T.; Baldwin, A. J.; Marklund, E. G.; Hochberg, G. K. A.; Benesch, J. L. P.; Robinson, C. V., Bayesian Deconvolution of Mass and Ion Mobility Spectra: From Binary Interactions to Polydisperse Ensembles. *Analytical Chemistry* **2015,** *87* (8), 4370-4376.

Chapter 5: Conclusion

Identifying and characterizing the structure of protein complexes are important for understanding how they function in biological processes at the molecular level. This work addresses several experimental issues to increase the applicability of native top-down mass spectrometry (nTD-MS) for elucidating information on the primary (*i.e.*, sequence) and higher-order structures of protein complexes and their individual subunit components.

TD-MS fragmentation efficiency is largely dependent on the abundance and charge of the precursor ion. Increasing the precursor charge state enhances the efficiency of collision- and electron-based fragmentation. The new supercharging agents tested in this work (Appendix), 3-nitrophenylacetonitrile, 4-nitrophenylacetonitrile and 3-nitribenzontrile, showed the capabilities of a 19% to 38% increase of the average charge state for denatured lysozyme. The discovery of supercharging agents can provide the ability to extract more information out of a protein in top-down MS experiments. Because the increase of charges on a protein promises an increase in efficiency of fragmentation, a higher sequence coverage (*i.e.*, more unique protein backbone cleavage sites) can be returned to provide more information on the sequence, locations of modifications, and even reveal information for the native protein structure. However, due to the insolubility of the three new supercharging agents in aqueous solutions, they were not tested in nTD-MS experiments.

The gas phase stability affects the fragmentation pattern of nTD-MS. In this work, we used the streptavidin tetramer (52 kDa) as an example to show that complex-down MS and nTD-MS with HCD of the intact complex returned the same fragmentation pattern, consistent with its weak noncovalent interactions between monomers in the gas-phase. The addition

of both L-proline, an adduct previously reported to stabilize intra-molecular noncovalent interactions, and biotin, which has a high binding affinity to streptavidin in the solution phase, shows *no* stabilization effect on noncovalent interactions among subunits. Therefore, fragments generated by electron capture-high collision energy dissociation (EChcD) did *not* return any higher-order structure information for the tetramer. However, electron transfer dissociation (ETD) showed the ability to release fragments mainly from the tetramer and therefore, provided the higher-order structure information of streptavidin tetramer. This aspect of ETD should be explored in the future.

A recently developed ExD cell have provided us an option to perform electron-based fragmentation on an Orbitrap system, which has traditionally been coupled to Q-TOF and FT-ICR MS. In this work, we described how the electron capture dissociation coupled with HCD (EChcD) can reveal quaternary structure information on most of the protein complexes by directly fragmenting the complexes. Additionally, Orbitrap-based ECD fragmentation efficiency is comparable or higher than FT-ICR ECD fragmentation efficiency in terms of the sequence coverage of large protein complexes, such as aldolase homotetramer and glutamate dehydrogenase homohexamer.

PCMTD1 was shown to multimerize with cullin-RING ligase components. Predicted from a previously characterized E3 ligase structure, the complex CRL5-PCMTD1 might be a potential E3 ubiquitin ligase, and is thought to play a role in isoaspartyl maintenance. Structure characterization of CRL5-PCMTD1 is critical to understand its biological activities, but the dynamics involved in substrate tagging makes it challenging to analyze by X-ray crystallography and cryo-EM. This work shows that mass spectrometry can provide relevant information on CRL5-PCMTD1 complex including its quaternary

structure information and iso-aspartic acid peptide binding activity. This data can be used to provide information on the substrate binding sites. Although the mass spectrometry result did not provide high resolution 3D structure, the combination of cryo-EM and nTD-MS results elucidates the 3D structure of this CRL5-PCMTD1 complex. It is possible that the combination of cryo-EM and nTD-MS results can also probe its substrate binding sites and uncover its biological function.

Appendix A: Native Top-Down Mass Spectrometry with Collisionally Activated Dissociation Yields Higher-Order Structure Information for Protein Complexes

Reprinted with permission from

Lantz, C.; Wei, B.; Zhao, B.; Jung, W.; Goring, A. K.; Le, J.; Miller, J.; Loo, R. R. O.; Loo, J. A., Native Top-Down Mass Spectrometry with Collisionally Activated Dissociation Yields Higher-Order Structure Information for Protein Complexes. *Journal of the American Chemical Society* **2022**, *144* (48), 21826-21830. DOI: https://doi.org/10.1021/jacs.2c06726.

Carter Lantz[1], Benqian Wei[1], Boyu Zhao[1], Wonhyeuk Jung[1], Andrew K. Goring[1], Jessie Le[1], Justin Miller[3], Rachel R. Ogorzalek Loo[1,2,3], Joseph A. Loo[1,2,3,4*]

[1]Department of Chemistry and Biochemistry, University of California-Los Angeles, Los Angeles, CA, USA

[2]UCLA-DOE Institute, University of California-Los Angeles, Los Angeles, CA, USA

[3]Molecular Biology Institute, University of California-Los Angeles, Los Angeles, CA, USA

[4]Department of Biological Chemistry, University of California-Los Angeles, Los Angeles, CA, USA

***Corresponding Author**

Joseph A. Loo

University of California-Los Angeles, Los Angeles, CA, United States

Email: jloo@chem.ucla.edu

Abstract

Native mass spectrometry (MS) of proteins and protein assemblies reveals size and binding stoichiometry, but elucidating structures to understand their function is more challenging. Native top-down MS (nTDMS), *i.e.*, fragmentation of the gas-phase protein, is conventionally used to derive sequence information, locate post-translational modifications (PTMs), and pinpoint ligand binding sites. nTDMS also endeavors to dissociate covalent bonds in a conformation-sensitive manner, such that information about higher-order structure can be inferred from the fragmentation pattern. However, the activation/dissociation method used can greatly affect the resulting information on protein higher-order structure. Methods such as electron capture/transfer dissociation (ECD and ETD, or ExD) and ultraviolet photodissociation (UVPD) can produce product ions that are sensitive to structural features of protein complexes. For multi-subunit complexes, a long-held belief is that collisionally activated dissociation (CAD) induces unfolding and release of a subunit, and thus is not useful for higher-order structure characterization. Here we show not only that sequence information can be obtained directly from CAD of native protein complexes but that the fragmentation pattern can deliver higher-order structural information about their gas- and solution-phase structures. Moreover, CAD-generated internal fragments (*i.e.*, fragments containing neither N-/C-termini) reveal structural aspects of protein complexes.

Main Text

Native top-down mass spectrometry (nTDMS) of gas-phase proteins yields product ions that can provide information on amino acid sequence,[1, 2] sites of modifications,[3-5] and even higher-order structure.[6] Performing nTDMS with electron-based techniques such as electron capture dissociation (ECD) and electron transfer dissociation (ETD)[7-11] and photon-based techniques such as infrared multiphoton dissociation (IRMPD) and ultraviolet photodissociation (UVPD)[8, 12-14] is generally favored, as it fragments the complex directly without disrupting the overall complex structure. In contrast, it has been generally assumed that collision-based fragmentation does not reveal higher-order structural information, as unfolding and ejection of monomer subunits (and ligands) occurs. However, we have found that direct fragmentation of native protein complexes with Orbitrap-based high-energy C-trap dissociation (HCD),[15] a collision-based fragmentation technique performed with higher energy on a faster time scale than conventional collisionally activated dissociation (CAD), can uncover aspects of protein higher-order structure. For a variety of protein complexes, we show here that HCD can generate b-/y-type product ions that provide information on solvent-exposed regions and subunit interfaces.

To investigate HCD fragmentation of protein complexes,[16] complex-down MS (pseudo-MS^3)[17, 18] and nTDMS (Scheme 1) of yeast alcohol dehydrogenase (ADH) homotetramer (147 kDa) were compared. Complex-down MS was performed by using in-source CAD to detach a monomer from the tetramer and to subsequently activate the 12+ charged monomer with HCD. The resultant MS/MS spectrum revealed both N-terminal b-fragments and C-terminal y-fragments of ADH (Figure S1A); 24 b-fragments and 18 y-

fragments resulted in 11.8% total sequence coverage (Figure 1A). The fragmentation pattern also revealed the presence of N-terminal acetylation, a V58T proteoform, and Zn^{2+} binding. The presence of near equal numbers of abundant b- and y-fragments from the complex-down MS workflow suggests that both termini of the ADH monomer subunit are easily accessed by HCD fragmentation, *i.e.*, the in-source CAD process releases a low-structured monomer such that subsequent HCD products yield little information about the 3D structure of the native tetramer.

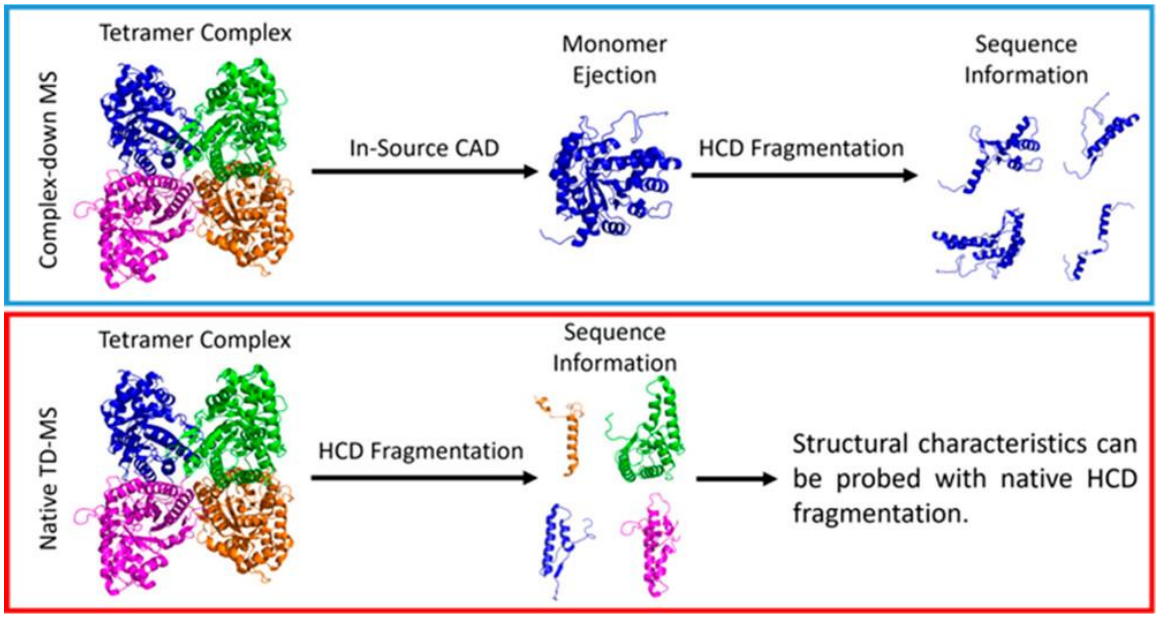

Scheme 1. Complex-Down MS and nTDMS Workflows Used in This Study.

For comparison, nTDMS results from HCD of the 25+ charged ADH tetramer were examined. Primarily b-products and surprisingly few peaks corresponding to released ADH monomers (Figure 1B, Figure S1B) were detected. We speculate that monomers were not ejected from the tetramer complex prior to covalent bond cleavage, *i.e.*, the tetramer fragmented directly. To further support this claim, broadband fragmentation (of all ADH tetramer charge states) with a range of HCD energies did not yield significant levels of

released monomer signals (Figure S2). nTDMS of ADH yielded 60 N-terminal b-fragments, but only three C-terminal y-fragments (17.6% sequence coverage) (Figure 1B). Numerous abundant N-terminal fragments produced by HCD resemble nTDMS products from electron-based[7, 8] and photodissociation techniques.[8, 12] Mapping the fragments onto the crystal structure of ADH shows that the N-terminal region is more solvent exposed than the C-terminal region, with the latter forming subunit–subunit interfaces of the complex (Figure S3). Our analysis indicates that fragments that cut at the interface of the tetramer (residues 240–310) accounted for only 8% of the fragment ion current.

To further examine how collision-based fragmentation can reveal structural information from protein complexes, intact (rabbit) aldolase homotetramer (157 kDa) was fragmented with HCD. Much like ADH, aldolase did not release monomers upon HCD, but rather y-fragments including an especially abundant y_{74} ion (2+ to 5+ charged) (Figure S4). At low HCD energies, a large complementary fragment corresponding to the mass of the intact tetramer losing a y_{74}-fragment, *i.e.*, (4M – y_{74}), was observed (Figure S5 and Table S1), indicating direct fragmentation of the tetramer. nTDMS yielded 35 C-terminal y-fragments but only eight N-terminal b-fragments (11.0% sequence coverage) (Figure 2). This result differs from the complex-down mass spectrum of aldolase, which shows a nearly equal proportion of N-terminal b-fragments[19] and C-terminal y-fragments[16] (Figure S6).

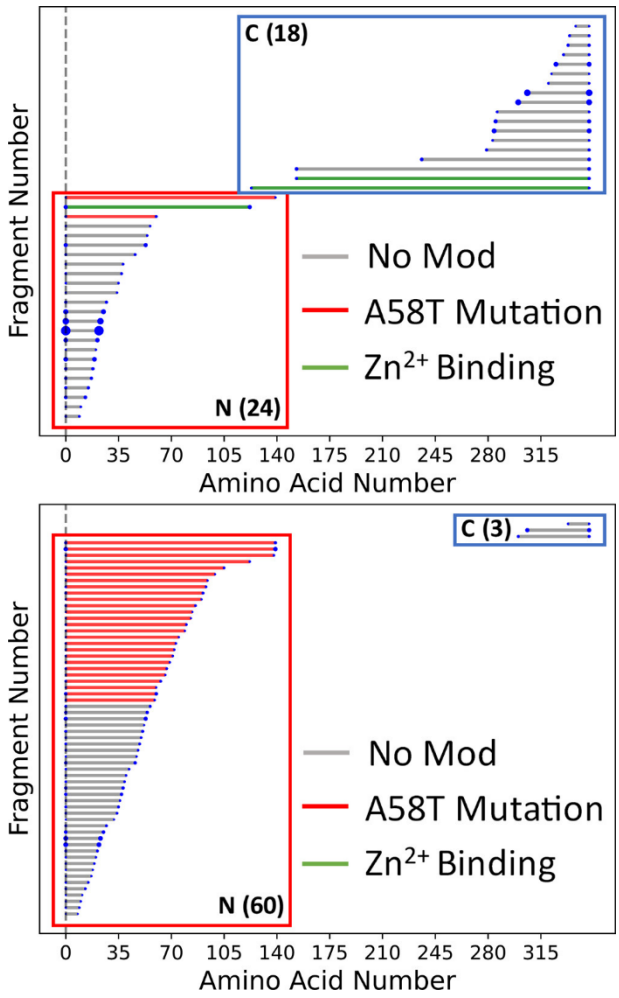

Figure 1. Fragment location maps for ADH representing b-/y-product ions measured by (top) complex-down MS and (bottom) nTDMS with HCD. Red lines indicate V58T mutation, green lines indicate Zn^{2+} binding, the vertical dotted line indicates N-terminal acetylation, and the size of the blue dots indicates the relative intensity of each fragment. Numbers in parentheses indicate the number of product ions detected.

The HCD fragments from the aldolase tetramer mainly cover the solvent-exposed C-terminus and are absent from the interface forming N-terminus (Figure 2). Our analysis indicates that fragments that cut at the interface of the tetramer (residues 110–224) accounted for only 1% of the fragment ion current. The relatively high proportion of C-terminal fragments present in the native HCD spectrum of aldolase is similar to that

measured by ECD previously[19] and further suggests that direct HCD fragmentation of some protein complexes can reveal regions of solvent accessibility.

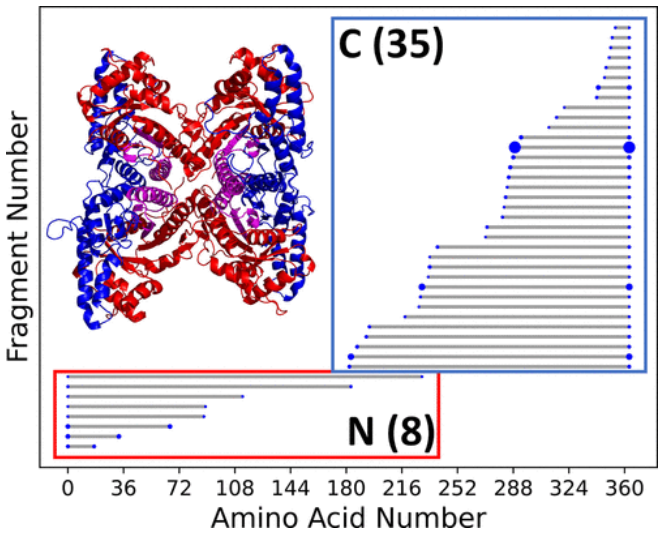

Figure 2. Fragment location map for nTDMS products of the 25+ charged precursor of aldolase homotetramer, with the size of the blue dots corresponding to the relative intensity of the fragments The crystal structure shows that most cleavage sites lie on the solvent-exposed C-terminus (blue), rather than the interface forming N-terminus (red). The purple region is covered by both N-terminal and C-terminal fragments.

nTDMS with HCD was performed on several other protein complexes. Complex-down fragmentation of the glutathione S-transferase A1 (GSTA1) dimer revealed 25 N-terminal b-fragments and 20 C-terminal y-fragments (Figure S7A). In contrast, the native fragmentation spectrum of GSTA1 reveals five N-terminal b-fragments and 19 C-terminal y-fragments (Figure S7B), consistent with the GSTA1 crystal structure showing that the C-terminus is more solvent exposed than the N-terminus (Figure S7B). For the yeast enolase dimer, 27 b-fragments along with 18 y-fragments were measured by complex-down MS (Figure S8A). nTDMS revealed 48 N-terminal b-fragments along with 51 C-terminal y-fragments without the appearance of abundant monomer ions (Figure S8B). The crystal structure of enolase (Figure S8B) indicates that both N-/C-termini are solvent

exposed and are not involved in forming the dimer interface, consistent with the near equal proportion of b-/y-products measured by nTDMS.

Some complexes did not release monomers from in-source CAD for complex-down fragmentation; however, HCD of the native complexes still returned structural information. Native HCD of the creatine kinase dimer revealed nine b- and 38 y-fragments, which suggests that the C-terminus is solvent exposed and the N-terminus forms the interface of the dimer; this aligns well with the crystal structure of creatine kinase (Figure S9). Similarly, HCD of 6-phosphogluconate dehydrogenase (GND1) dimer generated 23 b-fragments but only six y-fragments, consistent with the GND1 crystal structure showing the N-termini to be solvent exposed and the C-termini forming the dimer interface (Figure S10).

There are some exceptions to this pattern of b-/y-product formation directly from intact native complexes under HCD. For example, HCD of the native membrane protein, aquaporin Z (AqpZ) homotetramer,[20-22] yielded abundant monomer, dimer, and trimer products released from the intact complex (Figure S11A). This observation can be attributed to the weak hydrophobic binding interface between the monomer subunits of the AqpZ tetramer. Complexes such as aldolase and ADH are stabilized somewhat by salt bridges that strengthen greatly in the gas phase,[23, 24] potentially preventing monomer ejection during HCD (Figure S12). That monomer products are released when HCD is applied to native AqpZ complexes suggests that structural information (such as the locations of solvent-exposed regions and the tetramer interface) cannot be inferred from the resulting b-/y-fragments, at least assuming that the monomers likely eject before covalent bonds cleave. This suggestion is supported by the fact that the nTDMS

fragmentation pattern of AqpZ tetramers (65 b-fragments, 62 y-fragments, 38.4% sequence coverage; Figure S11A) does not differ significantly from the complex-down fragmentation pattern of isolated monomers (63 b-fragments, 60 C-terminal y-fragments, 34.6% sequence coverage; Figure S11B). Although HCD fragmentation of native AqpZ does not reveal significant higher-order structural information, it does suggest that the interaction between complex monomers in the gas phase is relatively weak.

Monomer releases during HCD are not limited to membrane protein complexes. HCD fragmentation of the hemoglobin (Hb) tetramer revealed monomer and trimer peaks in addition to 10 b-fragments and eight y-fragments from the α-subunit and seven b-fragments and seven y-fragments from the β-subunit (Figure S13A). Fragmentation of the Hb dimer also revealed released monomer peaks in addition to 11 b-fragments and 16 y-fragments from the α-subunit and 10 b-fragments and four y-fragments from the β-subunit (Figure S13B). A similar HCD fragmentation pattern can be observed from complex-down MS of individual subunits (nine b- and 10 y-fragments and six b- and five y-fragments from the α- and β-subunits, respectively) (Figure S13C). Similarly, nTDMS of human transthyretin (TTR) tetramers by HCD releases monomer products in addition to two b- and 38 y-fragments (Figure S14A). The relative proportion of b-/y-product ions between the tetramer and monomer TTR is similar, with complex-down of the TTR monomer yielding three b-fragments and 41 y-fragments (Figure S14B). The HCD results for all of the complexes included in the study are listed in Table S2.

Lastly, we investigated the utility of internal fragments (i.e., product ions containing neither N-/C-termini that result from at least two bond cleavage events)[1, 25-30] for structure determination of protein complexes. Preliminary data show that HCD fragmentation of

ADH tetramers reveals numerous internal fragments spanning residues 178–236 (Figure S15A), which correspond to a solvent-exposed region (Figure S15B). More work will extend this concept further, but it demonstrates that HCD-derived internal fragments can deliver structural information on protein assemblies.

Although other studies have noted the detection of b-/y-products with concurrent subunit release from CAD[31] and HCD[16] of protein complexes, we have found that collision-based fragmentation with HCD can reveal higher-order structure information for several multi-subunit protein complexes that appear to be stabilized through the presence of salt bridges.[23] These complexes fragment directly by HCD without significant monomer release. The resulting products map to solvent-exposed areas, while regions delivering fewer fragments likely comprise subunit interfaces. Other weak gas-phase complexes eject monomers upon HCD. Nonetheless, it is currently unclear what differences between HCD and other beam-type CAD experiments are responsible for the unique fragmentation behavior.

An assumption carried over from small-molecule dissociation studies to macroion decompositions is that, on the experimental time scale, activation from collisions always randomizes fully to steer collision-induced decompositions along the lowest energy pathways. However, those assumptions fail to consider that entropically demanding, slow rearrangements might be essential to releasing a subunit, *e.g.*, to reposition salt bridges tethering one subunit to others.[23] In cases where the number of collisions and/or energy per collision are insufficient to stumble on the rare configuration ejecting a subunit within the experimental time frame, alternative rearrangements to eject smaller polypeptide fragments (with fewer tethers) may be competitive. Nevertheless, we show that HCD can be a

powerful biophysical tool to probe the structure of proteins without the need for other electron- and photon-based activation/dissociation methods.

Associate Content

The Supporting Information is available free of charge at:

https://doi.org/10.1021/jacs.2c06726.

Materials and methods; supplementary figures (Figures S1−S15) showing nTDMS and complex-down MS spectra, data, and protein structures of those studied; Table S1, listing information for all proteins studied (PDF).

Author Information

Corresponding Author

Joseph A. Loo - Department of Chemistry and Biochemistry, University of California-Los Angeles, Los Angeles, California 90095, United States; Department of Biological Chemistry, UCLA-DOE Institute, and Molecular Biology Institute, University of California-Los Angeles, Los Angeles, California 90095, United States; https://orcid.org/0000-0001-9989-1437; Email: jloo@chem.ucla.edu

Authors

Carter Lantz - Department of Chemistry and Biochemistry, University of California-Los Angeles, Los Angeles, California 90095, United States.

Benqian Wei - Department of Chemistry and Biochemistry, University of California-Los Angeles, Los Angeles, California 90095, United States; https://orcid.org/0000-0003-4853-4848.

Boyu Zhao - Department of Chemistry and Biochemistry, University of California-Los Angeles, Los Angeles, California 90095, United States.

Wonhyeuk Jung - Department of Chemistry and Biochemistry, University of California-Los Angeles, Los Angeles, California 90095, United States.

Andrew K. Goring - Department of Chemistry and Biochemistry, University of California-Los Angeles, Los Angeles, California 90095, United States.

Jessie Le - Department of Chemistry and Biochemistry, University of California-Los Angeles, Los Angeles, California 90095, United States.

Justin Miller - Molecular Biology Institute, University of California-Los Angeles, Los Angeles, California 90095, United States.

Rachel R. Ogorzalek Loo - Department of Chemistry and Biochemistry, University of California-Los Angeles, Los Angeles, California 90095, United States; UCLA-DOE Institute, University of California−Los Angeles, Los Angeles, California 90095, United States; Molecular Biology Institute, University of California−Los Angeles, Los Angeles, California 90095, United States; https://orcid.org/0000-0002-0580-2833.

Complete contact information is available at:

https://doi.org/10.1021/jacs.2c06726.

Notes:

The authors declare no competing financial interest.

Acknowledgements

J.A.L. and R.R.O.L. acknowledge support from the US National Institutes of Health (R01GM103479, R35GM145286), the US National Science Foundation (NSF) (CHE1808492), and the US Department of Energy (DE-FC02-02ER63421). C.L. acknowledges support from the Ruth L. Kirschstein National Research Service Award program (GM007185). A.G. acknowledges support from the National Institute of Dental & Craniofacial Research (T90DE030860).

Appendix A: Supporting Information

Materials and Methods

Commerically available protein samples were obtained from Sigma Aldrich (St. Louis, MO, USA), and dissolved in 200mM ammonium acetate, and desalted with 10K Amicon filters from Sigma Aldrich. Aquaporin Z (AqpZ; from Pascal Egea, UCLA)[1] and human hemoglobin (Hb; from Robert Clubb, UCLA)[2] were isolated and prepared as described previously. The samples were then diluted to 10μM and sprayed on a Thermo UHMR (Thermo Fisher Scientific, San Jose, CA) with voltages of 1-2kV. To fragment native complexes, HCD energies of 125-280V were applied. Lower voltages were applied for select applications. Complex-down MS experiments were performed by applying 5-150V of in-source CAD or -60V of desolvation voltage to eject monomers and then applying 100V-177V of HCD energy to subsequently activate those monomers. For internal fragment analysis, the ADH the tetramer was fragmented with 215V of collision energy with argon as the collision gas.

Deconvolution was performed with BioPharma Finder 3.2 and the resulting deconvoluted peak list was run through ClipsMS.[3] b- and y-fragments were matched to protein sequences with an error tolerance of 5ppm and unlocalized modifications included the addition of a hydrogen atom and the abstraction of a water molecule were added to the theoretical masses. For ADH, additional modifications including an N-terminal acetylation, a V58T mutation, and a Zn2+ ion were added to theoretical fragments. by internal fragments of ADH were searched with ClipsMS with an error tolerance of 5ppm. To deconvolute large complementary fragments, UniDec was used.[4] Fragments were mapped onto crystal

structures of protein complexes using Pymol 2.5.4. The ADH pymol code used was 4W6Z, the aldolase pymol code used was 1ADO, the enolase pymol code used was 1EGB, the GSTA1 pymol code used was 1GSD, and the creatine kinase pymol code used was 1U6R, and the aquaporin Z pymol code used was 1RC2.

References

1. Lippens, J. L.; Nshanian, M.; Spahr, C.; Egea, P. F.; Loo, J. A.; Campuzano, I. D. G., Fourier Transform-Ion Cyclotron Resonance Mass Spectrometry as a Platform for Characterizing Multimeric Membrane Protein Complexes. *Journal of the American Society for Mass Spectrometry* **2018,** *29* (1), 183-193.

2. Spirig, T.; Malmirchegini, G. R.; Zhang, J.; Robson, S. A.; Sjodt, M.; Liu, M.; Krishna Kumar, K.; Dickson, C. F.; Gell, D. A.; Lei, B.; Loo, J. A.; Clubb, R. T., Staphylococcus aureus Uses a Novel Multidomain Receptor to Break Apart Human Hemoglobin and Steal Its Heme*. *Journal of Biological Chemistry* **2013,** *288* (2), 1065-1078.

3. Lantz, C.; Zenaidee, M. A.; Wei, B.; Hemminger, Z.; Ogorzalek Loo, R. R.; Loo, J. A., ClipsMS: An Algorithm for Analyzing Internal Fragments Resulting from Top-Down Mass Spectrometry. *J Proteome Res* **2021,** *20* (4), 1928-1935.

4. Marty, M. T.; Baldwin, A. J.; Marklund, E. G.; Hochberg, G. K. A.; Benesch, J. L. P.; Robinson, C. V., Bayesian Deconvolution of Mass and Ion Mobility Spectra: From Binary Interactions to Polydisperse Ensembles. *Analytical Chemistry* **2015,** *87* (8), 4370-4376.

Supplementary Figures

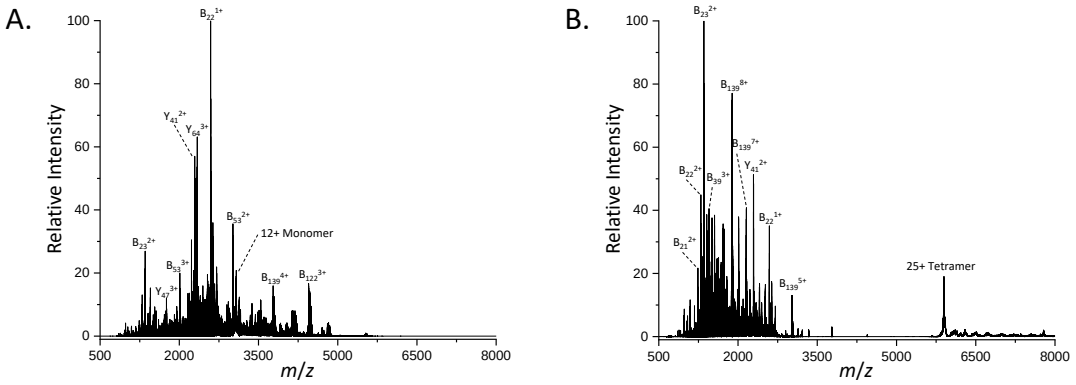

Figure S1. (A) A complex-down fragmentation spectrum and (B) a native TD-MS spectrum of ADH.

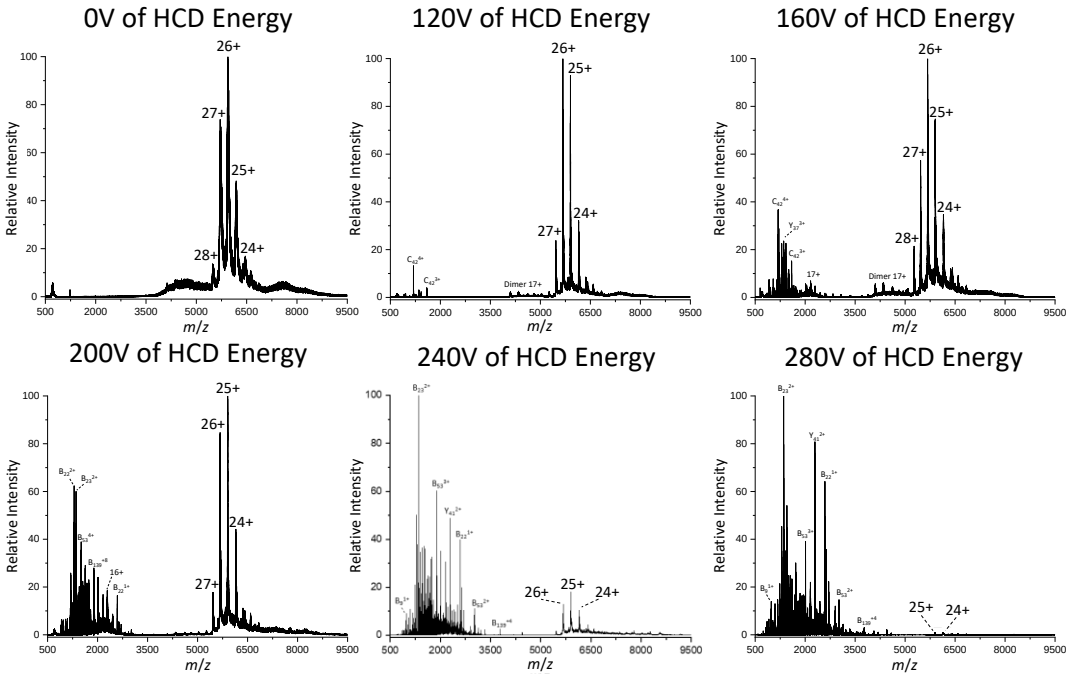

Figure S2. Broadband nTD-MS spectra of ADH at various voltages. Notice how intense monomer peaks do not appear at any voltage that was applied.

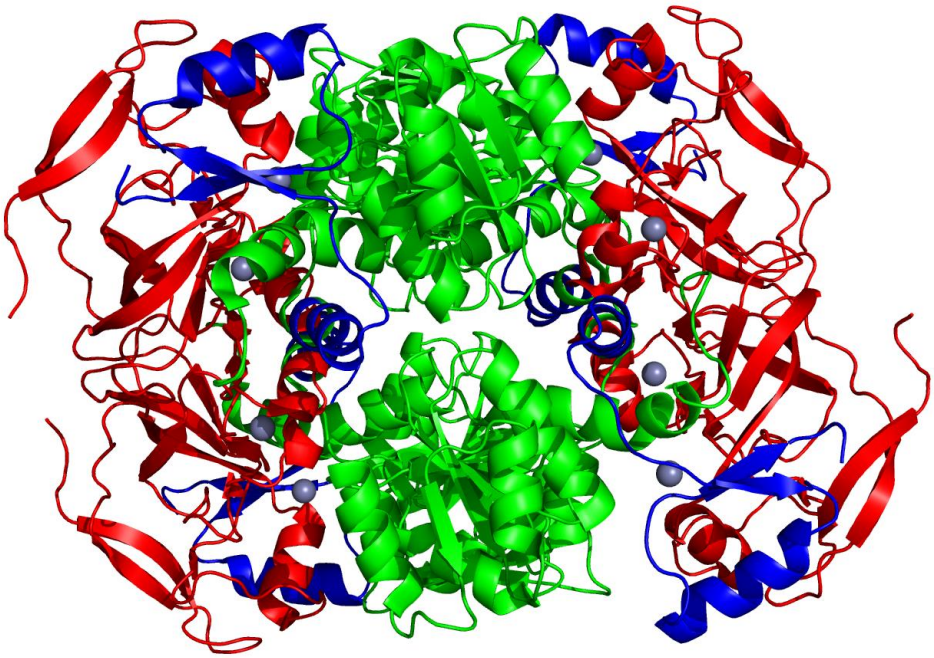

Figure S3. The structure of ADH with the region covered by the N-terminal fragments labeled in red and the region covered by the C-terminal fragments labeled in blue. Notice how fragments do not stem from the interface forming region of the tetramer (green).

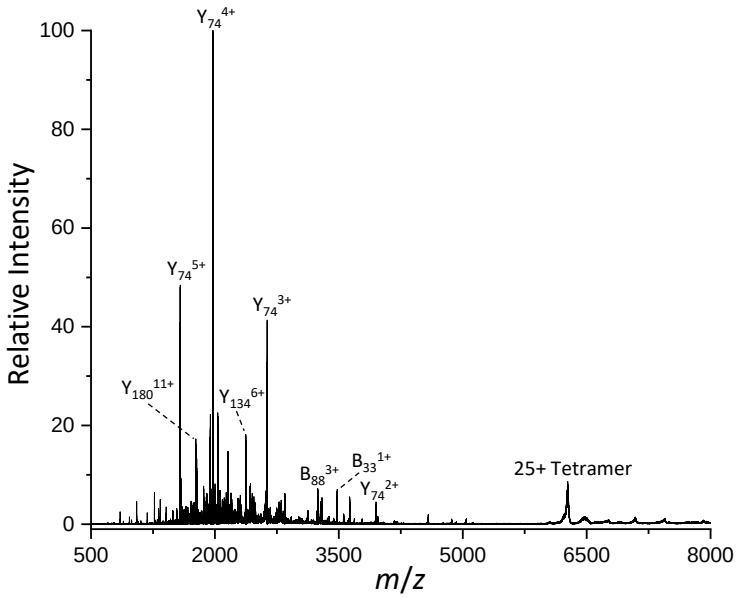

Figure S4. A native top-down mass spectrum of the aldolase homotetramer.

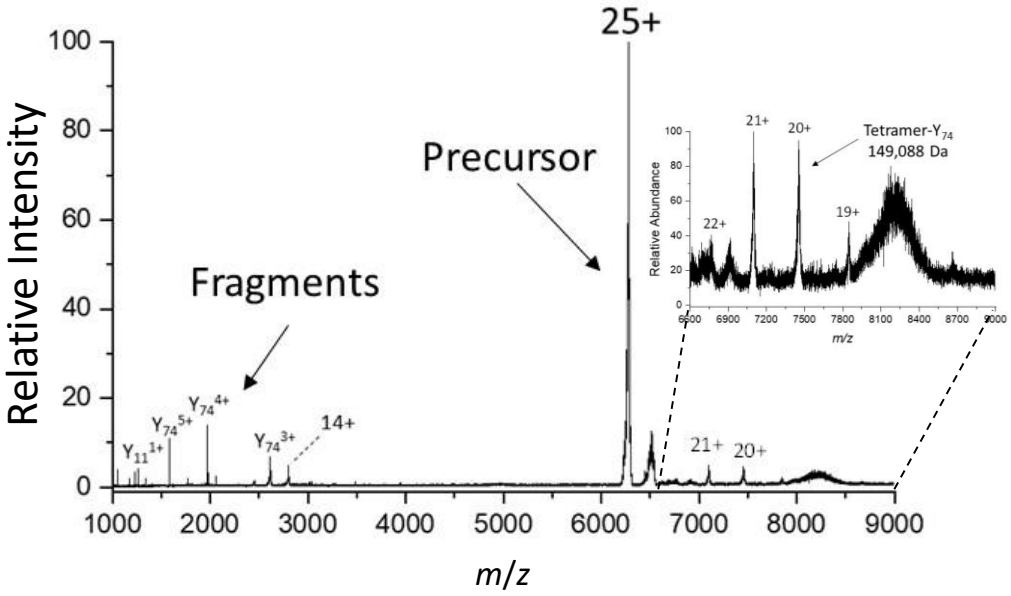

Figure S5. A native top-down mass spectrum of the 25+ charge state of the aldolase homotetramer showing multiple charge states of an abundant y_{74} fragment and high *m/z* peaks corresponding to charge states of the tetramer-y_{74}.

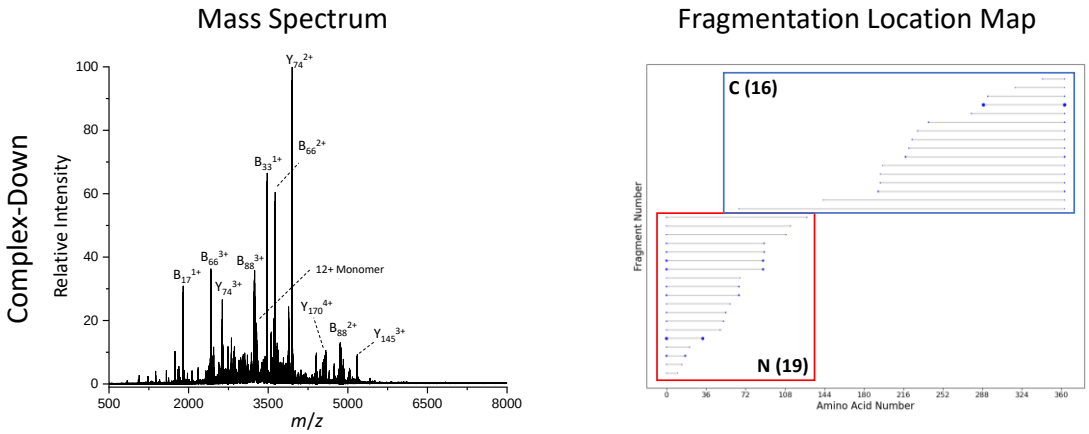

Figure S6. A complex-down spectrum and the corresponding fragment location map for the aldolase homotetramer.

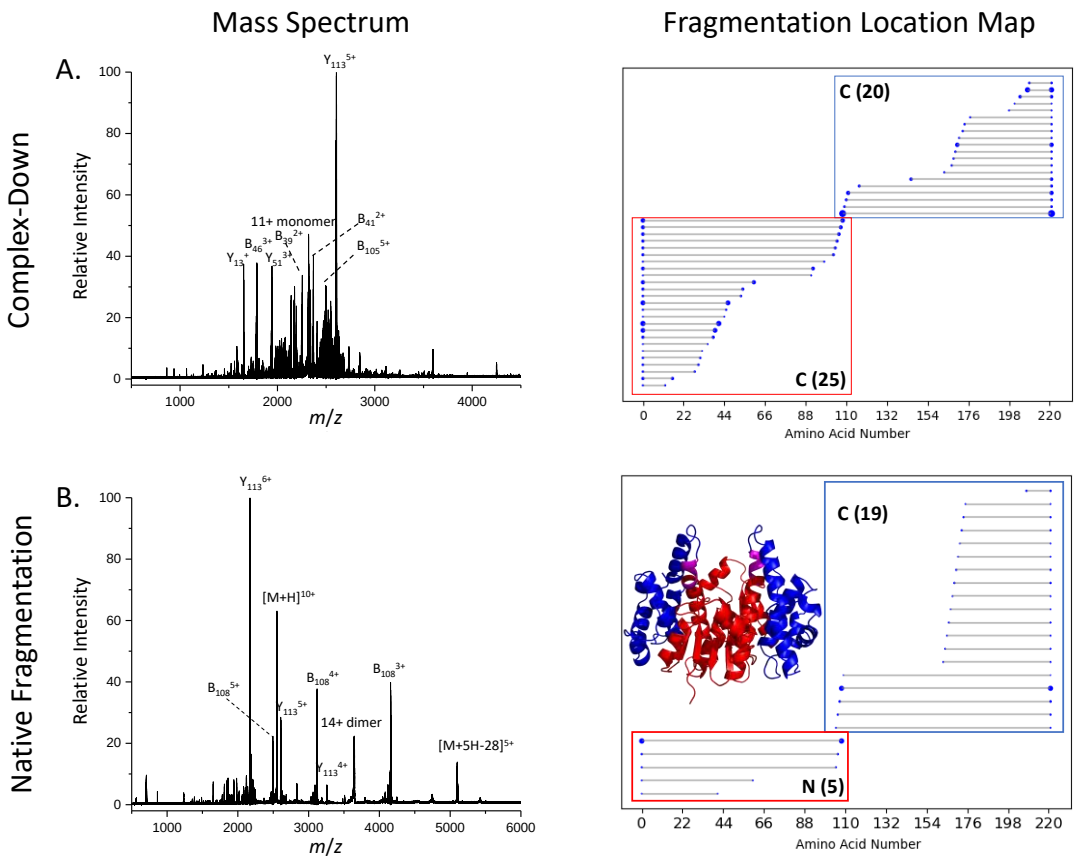

Figure S7. (A) A complex-down spectrum with the corresponding fragment location map and (B) a native top-down mass spectrum with the corresponding fragmentation location map for the human GST A1 dimer. The inset shows the structure of GST A1 with the region covered by N-terminal fragments labeled in red, the region covered by C-terminal fragments labeled in blue, and the region covered by N- and C-terminal fragments labeled in purple. Notice that most fragments contain the solvent exposed C-terminus and fewer fragments contain the interface forming N-terminus.

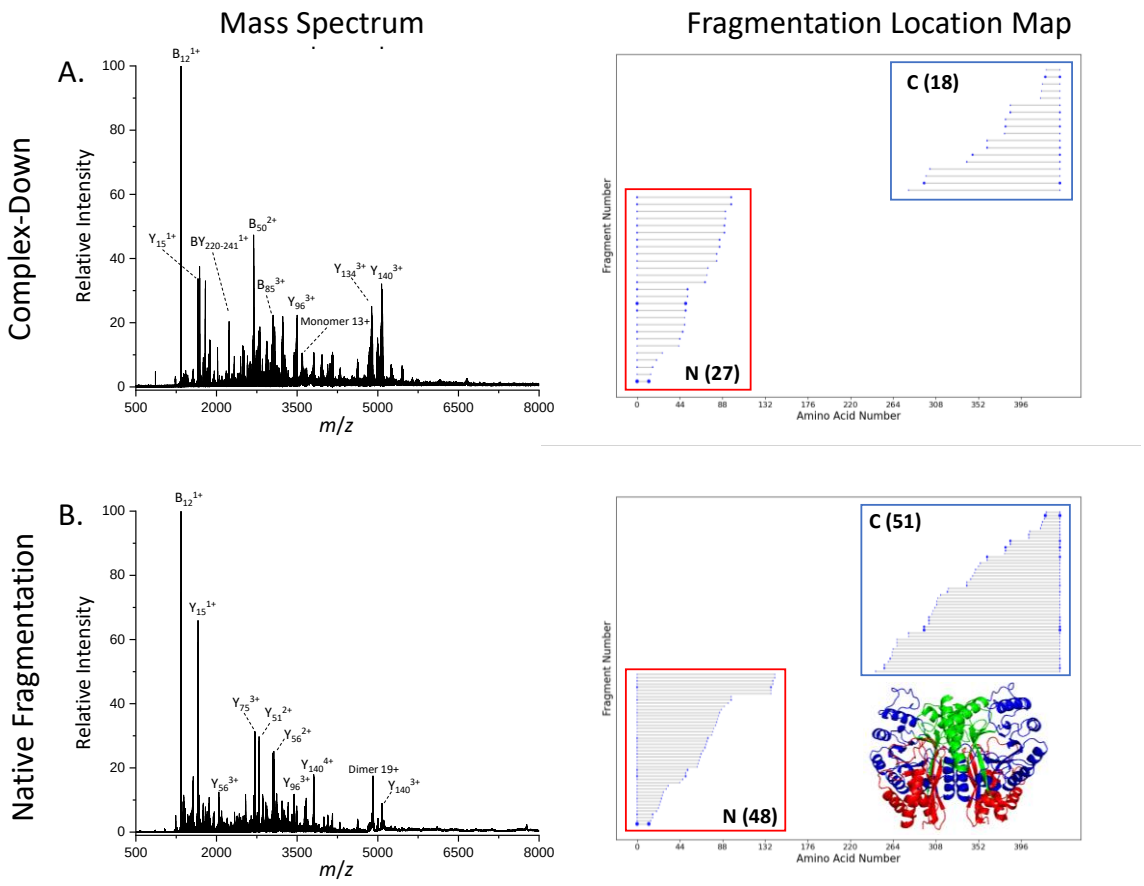

Figure S8. (A) A complex-down spectrum with the corresponding fragment location map and (B) a native top-down mass spectrum with the corresponding fragmentation location map for the enolase dimer. The inset shows the structure of enolase with the region covered by N-terminal fragments labeled in red and the region covered by C-terminal fragments labeled in blue. Extensive coverage of the N- and C-terminus are present because both termini are solvent exposed.

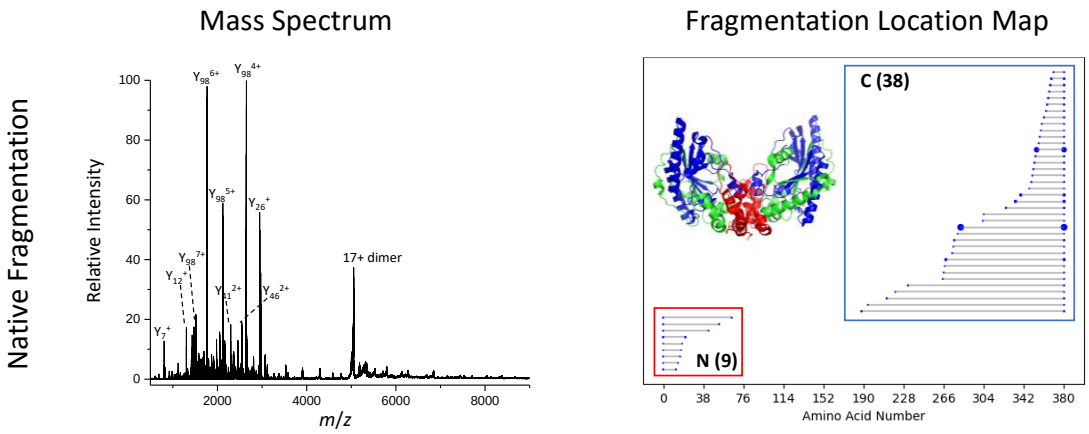

Figure S9. A native top-down mass spectrum with the corresponding fragmentation location map for creatine kinase. The inset shows the structure of creatine kinase with the region covered by N-terminal fragments labeled in red and the region covered by C-terminal fragments labeled in blue. Notice how more fragments contain the solvent exposed C-terminus and fewer fragments contain the interface forming N-terminus.

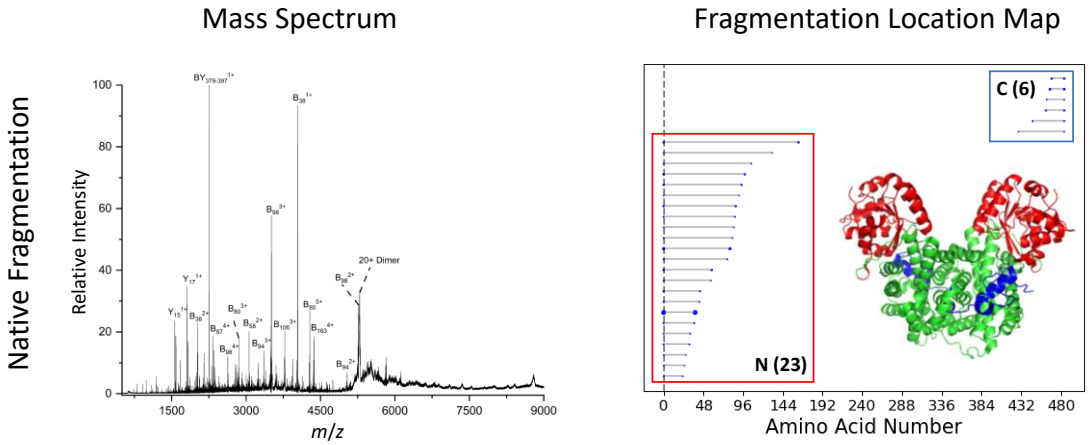

Figure S10. A native top-down mass spectrum with the corresponding fragmentation location map for the GND1 dimer with the vertical dotted line representing N-terminal acetylation. The inset shows the structure of GND1 with the region covered by N-terminal fragments labeled in red and the region covered by C-terminal fragments labeled in blue. Notice how more fragments contain the solvent exposed N-terminus and fewer fragments contain the interface forming C-terminus.

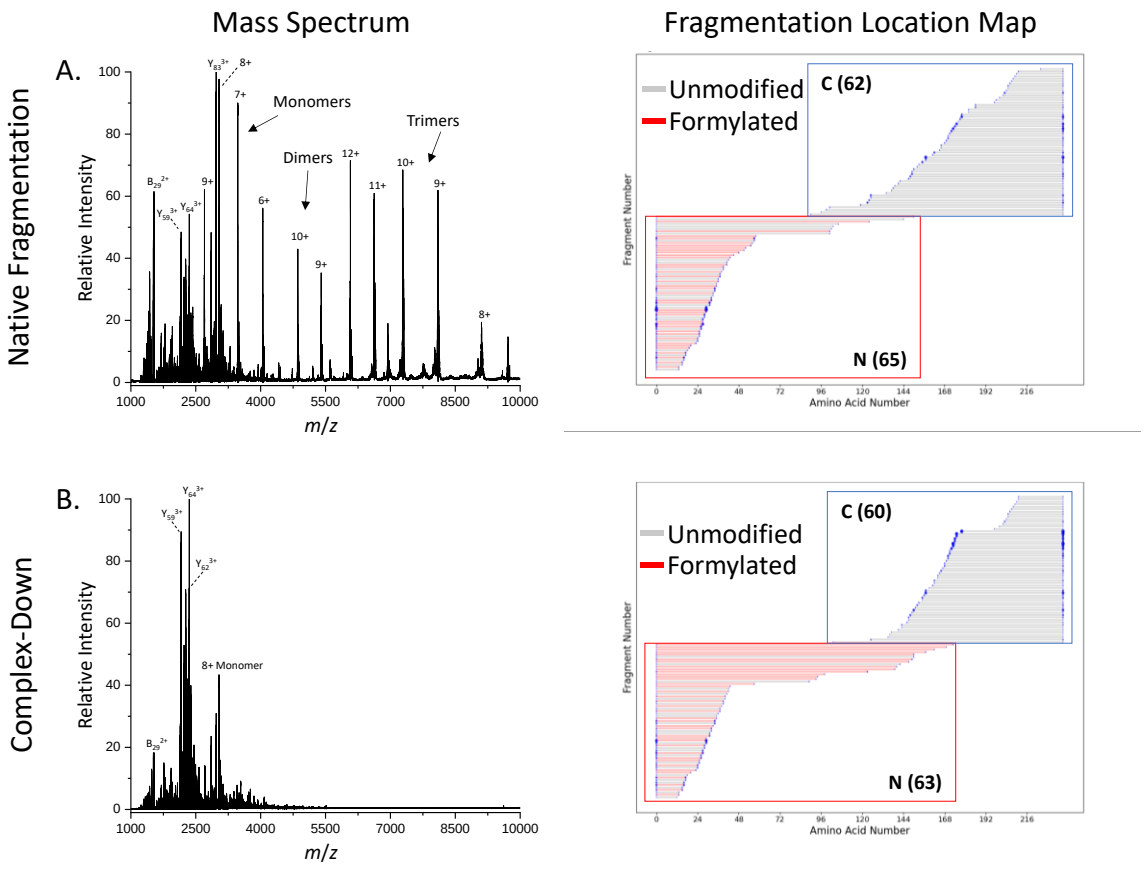

Figure S11. (A) A native top-down mass spectrum with the corresponding fragment location map and (B) a complex-down spectrum with the corresponding fragmentation location map for the AqpZ tetramer.

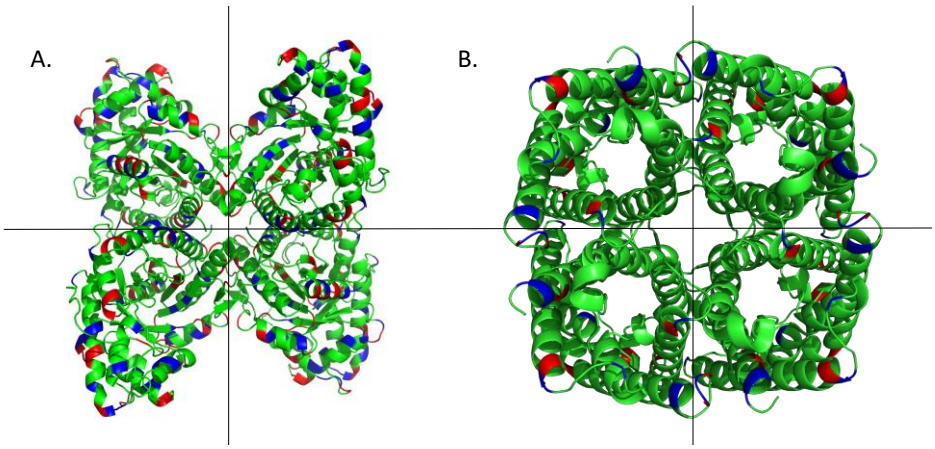

Figure S12. (A) The crystal structure of rabbit aldolase and (B) the crystal structure of aquaporin Z with positively charged amino acids (Lys and Arg) labeled in blue and negatively charged amino acids (Glu and Asp) labeled in red. The black lines indicate the complex interface. Aldolase contains many charged residues at the interface of the protein complex and aquaporin Z does not which may explain why aquaporin Z releases monomers and aldolase does not when HCD is applied to the intact complex.

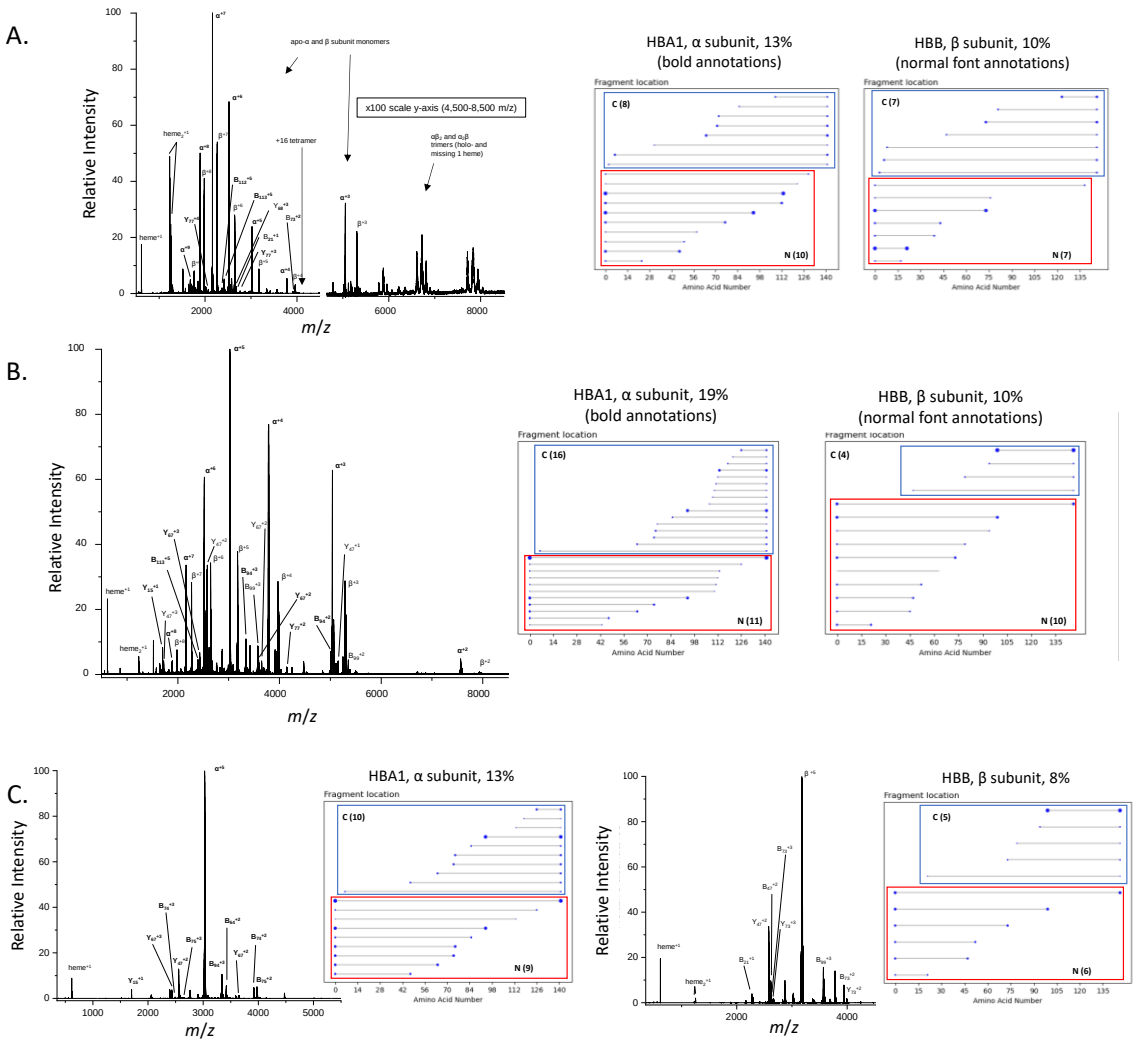

Figure S13. (A) A native top-down mass spectrum of the hemoglobin tetramer with the corresponding fragment location maps for the α-subunit and β-subunit, (B) a native top-down mass spectrum of the hemoglobin dimer with the corresponding fragmentation location maps for the α-subunit and β-subunit, and (C) complex-down fragmentation spectra and the corresponding fragment location maps for the α-subunit and β-subunit.

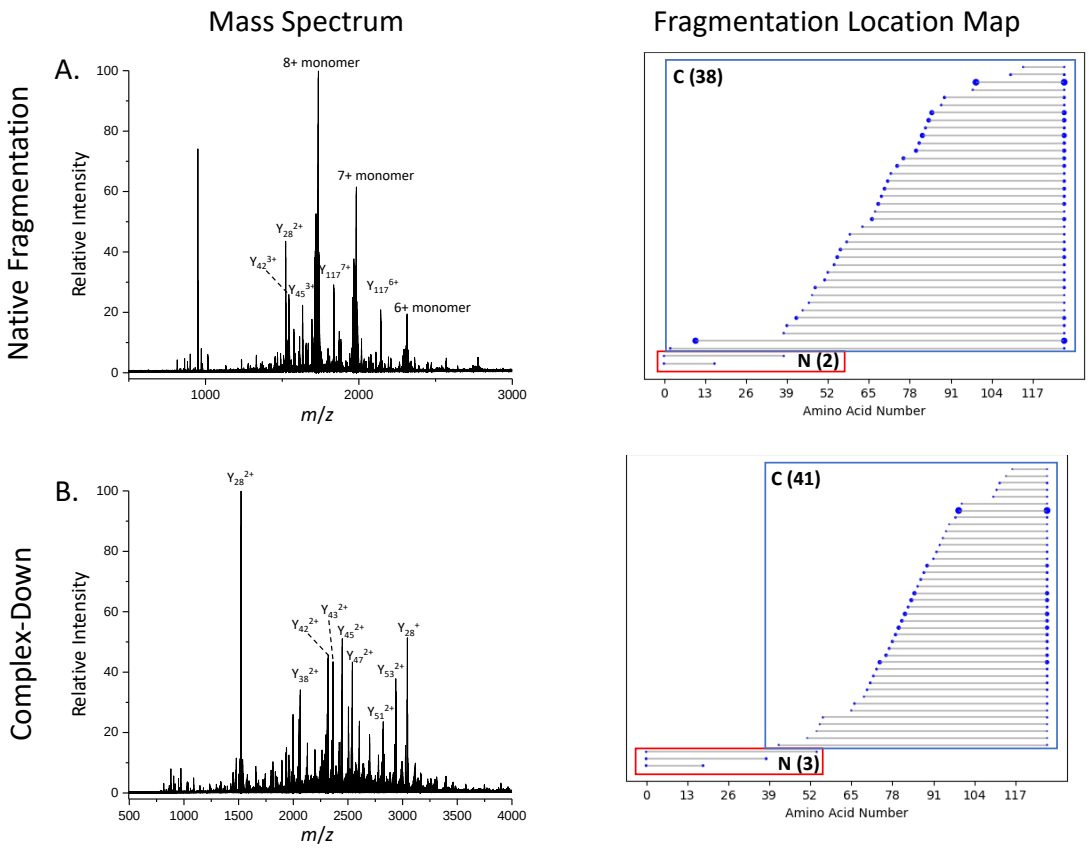

Figure S14. (A) A native top-down mass spectrum with the corresponding fragment location map and (B) a complex-down spectrum with the corresponding fragmentation location map for the TTR tetramer.

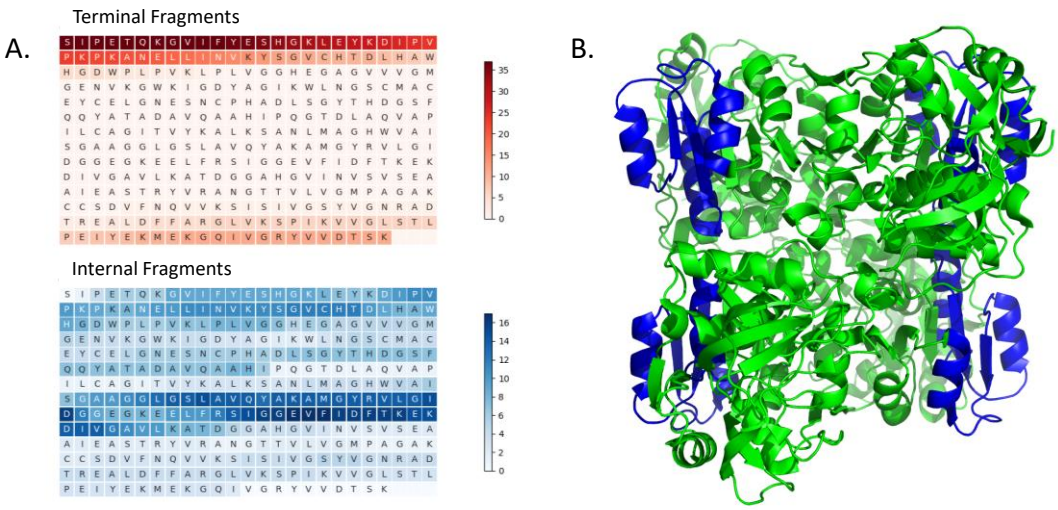

Figure S15. (A) A heatmap representing terminal and internal fragment analysis of ADH and (B) the structure of the ADH tetramer with an internal fragment hotspot (residues 178-236) highlighted in blue. Notice how this region of the ADH tetramer is solvent exposed.

Supplementary Tables

Table S1. Molecular weights of species present in a low HCD energy spectrum of aldolase. The high m/z ions in the spectrum correspond to the aldolase tetramer-y74.

Species	MW (Da)
Measured Molecular Weight of Aldolase	156,982
Measured Molecular Weight Higher m/z Peaks	149,088
Measured Molecular Difference	7,894
Theoretical Mass of Y74	7,896

Table S2. Information on the complexes analyzed in this study. (* CK refers to creatine kinase)

General Information				Native TDMS Fragmentation				Complex-Down Fragmentation			
Name of Complex	Type of Complex	MW Complex (Da)	MW Monomer (Da)	Monomer Release with HCD	#N-Term Frags	#C-Term Frags	Sequence Coverage	Monomer Release with CAD	#N-Term Frags	#C-Term Frags	Sequence Coverage
ADH	Tetramer	147,472	36,738	No	60	3	18%	Yes	24	18	12%
Aldolase	Tetramer	156,748	39,187	No	8	35	11%	Yes	19	16	8%
GSTA1	Dimer	51,000	25,500	No	5	19	11%	Yes	25	20	21%
Enolase	Dimer	93,312	46,656	No	48	51	18%	Yes	27	18	8%
CK*	Dimer	86,224	43,112	No	9	38	13%	No	N/A	N/A	N/A
GND1	Dimer	106,003	52,597	No	23	6	6%	No	N/A	N/A	N/A
AqpZ	Tetramer	24,269	97,076	Yes	65	62	38%	Yes	63	60	35%
Hemoglobin	Tetramer	61,986	α=15,126 β=15,867	Yes	α=10 β=7	α=8 β=7	α=13% β=10%	Yes	α=9 β=6	α=10 β=6	α=13% β=8%
	Dimer	30,993	α=15,126 β=15,867	Yes	α=11 β=10	α=16 β=4	α=19% β=10%	Yes	α=9 β=6	α=10 β=6	α=13% β=8%
Transthyretin	Tetramer	55,044	13,761	Yes	2	38	33%	Yes	3	41	36%

References

1. Lantz, C.; Zenaidee, M. A.; Wei, B.; Hemminger, Z.; Ogorzalek Loo, R. R.; Loo, J. A., ClipsMS: An Algorithm for Analyzing Internal Fragments Resulting from Top-Down Mass Spectrometry. *Journal of Proteome Research* **2021,** *20* (4), 1928-1935.

2. Vimer, S.; Ben-Nissan, G.; Morgenstern, D.; Kumar-Deshmukh, F.; Polkinghorn, C.; Quintyn, R. S.; Vasil'ev, Y. V.; Beckman, J. S.; Elad, N.; Wysocki, V. H.; Sharon, M., Comparative Structural Analysis of 20S Proteasome Ortholog Protein Complexes by Native Mass Spectrometry. *ACS Central Science* **2020,** *6* (4), 573-588.

3. Nshanian, M.; Lantz, C.; Wongkongkathep, P.; Schrader, T.; Klärner, F.-G.; Blümke, A.; Despres, C.; Ehrmann, M.; Smet-Nocca, C.; Bitan, G.; Loo, J. A., Native Top-Down Mass Spectrometry and Ion Mobility Spectrometry of the Interaction of Tau Protein with a Molecular Tweezer Assembly Modulator. *Journal of the American Society for Mass Spectrometry* **2019,** *30* (1), 16-23.

4. Xie, Y.; Zhang, J.; Yin, S.; Loo, J. A., Top-Down ESI-ECD-FT-ICR Mass Spectrometry Localizes Noncovalent Protein-Ligand Binding Sites. *Journal of the American Chemical Society* **2006,** *128* (45), 14432-14433.

5. O'Brien, J. P.; Li, W.; Zhang, Y.; Brodbelt, J. S., Characterization of Native Protein Complexes Using Ultraviolet Photodissociation Mass Spectrometry. *Journal of the American Chemical Society* **2014,** *136* (37), 12920-12928.

6. Zhou, M.; Lantz, C.; Brown, K. A.; Ge, Y.; Paša-Tolić, L.; Loo, J. A.; Lermyte, F., Higher-order structural characterisation of native proteins and complexes by top-down mass spectrometry. *Chemical Science* **2020,** *11* (48), 12918-12936.

7. Zhang, H.; Cui, W.; Wen, J.; Blankenship, R. E.; Gross, M. L., Native electrospray and electron-capture dissociation in FTICR mass spectrometry provide top-down sequencing of a protein component in an intact protein assembly. *Journal of the American Society for Mass Spectrometry* **2010,** *21* (12), 1966-1968.

8. Li, H.; Wongkongkathep, P.; Van Orden, S. L.; Ogorzalek Loo, R. R.; Loo, J. A., Revealing Ligand Binding Sites and Quantifying Subunit Variants of Noncovalent Protein Complexes in a Single Native Top-Down FTICR MS Experiment. *Journal of the American Society for Mass Spectrometry* **2014,** *25* (12), 2060-2068.

9. Li, H.; Nguyen, H. H.; Ogorzalek Loo, R. R.; Campuzano, I. D. G.; Loo, J. A., An integrated native mass spectrometry and top-down proteomics method that connects sequence to structure and function of macromolecular complexes. *Nature Chemistry* **2018,** *10* (2), 139-148.

10. Lermyte, F.; Sobott, F., Electron transfer dissociation provides higher-order structural information of native and partially unfolded protein complexes. *PROTEOMICS* **2015,** *15* (16), 2813-2822.

11. Williams, J. P.; Morrison, L. J.; Brown, J. M.; Beckman, J. S.; Voinov, V. G.; Lermyte, F., Top-Down Characterization of Denatured Proteins and Native Protein Complexes Using Electron Capture Dissociation Implemented within a Modified Ion Mobility-Mass Spectrometer. *Analytical Chemistry* **2020,** *92* (5), 3674-3681.

12. Zhou, M.; Liu, W.; Shaw, J. B., Charge Movement and Structural Changes in the Gas-Phase Unfolding of Multimeric Protein Complexes Captured by Native Top-Down Mass Spectrometry. *Analytical Chemistry* **2020,** *92* (2), 1788-1795.

13. Cammarata, M. B.; Thyer, R.; Rosenberg, J.; Ellington, A.; Brodbelt, J. S., Structural Characterization of Dihydrofolate Reductase Complexes by Top-Down Ultraviolet Photodissociation Mass Spectrometry. *Journal of the American Chemical Society* **2015,** *137* (28), 9128-9135.

14. Cammarata, M. B.; Brodbelt, J. S., Structural characterization of holo- and apo-myoglobin in the gas phase by ultraviolet photodissociation mass spectrometry. *Chemical Science* **2015,** *6* (2), 1324-1333.

15. Olsen, J. V.; Macek, B.; Lange, O.; Makarov, A.; Horning, S.; Mann, M., Higher-energy C-trap dissociation for peptide modification analysis. *Nature Methods* **2007,** *4* (9), 709-712.

16. Hale, O. J.; Cooper, H. J., Native Mass Spectrometry Imaging of Proteins and Protein Complexes by Nano-DESI. *Analytical Chemistry* **2021,** *93* (10), 4619-4627.

17. Lermyte, F.; Tsybin, Y. O.; O'Connor, P. B.; Loo, J. A., Top or Middle? Up or Down? Toward a Standard Lexicon for Protein Top-Down and Allied Mass Spectrometry Approaches. *Journal of the American Society for Mass Spectrometry* **2019,** *30* (7), 1149-1157.

18. Skinner, O. S.; Haverland, N. A.; Fornelli, L.; Melani, R. D.; Do Vale, L. H. F.; Seckler, H. S.; Doubleday, P. F.; Schachner, L. F.; Srzentić, K.; Kelleher, N. L.; Compton, P. D., Top-down characterization of endogenous protein complexes with native proteomics. *Nature Chemical Biology* **2018,** *14* (1), 36-41.

19. Li, H.; Wolff, J. J.; Van Orden, S. L.; Loo, J. A., Native Top-Down Electrospray Ionization-Mass Spectrometry of 158 kDa Protein Complex by High-Resolution Fourier

Transform Ion Cyclotron Resonance Mass Spectrometry. *Analytical Chemistry* **2014,** *86* (1), 317-320.

20. Campuzano, I. D. G.; Nshanian, M.; Spahr, C.; Lantz, C.; Netirojjanakul, C.; Li, H.; Wongkongkathep, P.; Wolff, J. J.; Loo, J. A., High Mass Analysis with a Fourier Transform Ion Cyclotron Resonance Mass Spectrometer: From Inorganic Salt Clusters to Antibody Conjugates and Beyond. *Journal of the American Society for Mass Spectrometry* **2020,** *31* (5), 1155-1162.

21. Laganowsky, A.; Reading, E.; Hopper, J. T. S.; Robinson, C. V., Mass spectrometry of intact membrane protein complexes. *Nature Protocols* **2013,** *8* (4), 639-651.

22. Lippens, J. L.; Nshanian, M.; Spahr, C.; Egea, P. F.; Loo, J. A.; Campuzano, I. D. G., Fourier Transform-Ion Cyclotron Resonance Mass Spectrometry as a Platform for Characterizing Multimeric Membrane Protein Complexes. *Journal of the American Society for Mass Spectrometry* **2018,** *29* (1), 183-193.

23. Loo, R. R. O.; Loo, J. A., Salt Bridge Rearrangement (SaBRe) Explains the Dissociation Behavior of Noncovalent Complexes. *Journal of the American Society for Mass Spectrometry* **2016,** *27* (6), 975-990.

24. Yin, S.; Loo, J. A., Elucidating the site of protein-ATP binding by top-down mass spectrometry. *Journal of the American Society for Mass Spectrometry* **2010,** *21* (6), 899-907.

25. Durbin, K. R.; Skinner, O. S.; Fellers, R. T.; Kelleher, N. L., Analyzing Internal Fragmentation of Electrosprayed Ubiquitin Ions During Beam-Type Collisional

Dissociation. *Journal of the American Society for Mass Spectrometry* **2015,** *26* (5), 782-787.

26. Schmitt, N. D.; Berger, J. M.; Conway, J. B.; Agar, J. N., Increasing Top-Down Mass Spectrometry Sequence Coverage by an Order of Magnitude through Optimized Internal Fragment Generation and Assignment. *Analytical Chemistry* **2021,** *93* (16), 6355-6362.

27. Wei, B.; Zenaidee, M. A.; Lantz, C.; Ogorzalek Loo, R. R.; Loo, J. A., Towards understanding the formation of internal fragments generated by collisionally activated dissociation for top-down mass spectrometry. *Analytica Chimica Acta* **2022,** *1194*, 339400.

28. Zenaidee, M. A.; Lantz, C.; Perkins, T.; Jung, W.; Loo, R. R. O.; Loo, J. A., Internal Fragments Generated by Electron Ionization Dissociation Enhance Protein Top-Down Mass Spectrometry. *Journal of the American Society for Mass Spectrometry* **2020,** *31* (9), 1896-1902.

29. Zenaidee, M. A.; Wei, B.; Lantz, C.; Wu, H. T.; Lambeth, T. R.; Diedrich, J. K.; Ogorzalek Loo, R. R.; Julian, R. R.; Loo, J. A., Internal Fragments Generated from Different Top-Down Mass Spectrometry Fragmentation Methods Extend Protein Sequence Coverage. *Journal of the American Society for Mass Spectrometry* **2021,** *32* (7), 1752-1758.

30. Harvey, S. R.; Porrini, M.; Konijnenberg, A.; Clarke, D. J.; Tyler, R. C.; Langridge-Smith, P. R. R.; MacPhee, C. E.; Volkman, B. F.; Barran, P. E., Dissecting the Dynamic Conformations of the Metamorphic Protein Lymphotactin. *The Journal of Physical Chemistry B* **2014,** *118* (43), 12348-12359.

31. Pagel, K.; Hyung, S.-J.; Ruotolo, B. T.; Robinson, C. V., Alternate Dissociation Pathways Identified in Charge-Reduced Protein Complex Ions. *Analytical Chemistry* **2010,** *82* (12), 5363-5372.

Appendix B: Native Top-Down Mass Spectrometry Reveals Structural and Relative Stability Information of Protein Complexes

Boyu Zhao[1], Rachel R. Ogorzalek Loo[1,2,3], Joseph A. Loo[1,2,3,4]

[1]Department of Chemistry and Biochemistry, University of California-Los Angeles, Los Angeles, CA, USA

[2]UCLA-DOE Institute, University of California-Los Angeles, Los Angeles, CA, USA

[3]Molecular Biology Institute, University of California-Los Angeles, Los Angeles, CA, USA

[4]Department of Biological Chemistry, University of California-Los Angeles, Los Angeles, CA, USA

Abstract

The gas phase stability of a protein analyte affects its fragmentation pattern measured by native top-down mass spectrometry (nTD-MS). A previous study by our laboratory suggested that Orbitrap-based high energy C-trap dissociation (HCD) fragments protein complexes directly, potentially revealing higher-order structure information for those assemblies. However, for the transthyretin tetramer (55 kDa), complex-down (tandem MS, or MS/MS of the dissociated subunit) and nTD-MS of the intact complex showed the same fragmentation pattern, consistent with relatively weak non-covalent interactions between monomer subunits. At low HCD energies, transthyretin tetramers decompose by ejecting a monomer subunit, while at higher HCD energies, they release a monomer and b-/y-fragment ions from the monomer. Here we report that by the addition of L-proline to the

transthyretin sample, we can stabilize the transthyretin complex and fragment protein complexes directly using HCD to reveal information on its higher-order structures.

Introduction

Identifying and characterizing the structures of protein complexes is important for understanding how they function in biology. Native top-down mass spectrometry (nTD-MS) enables us to analyze intact protein complexes and their individual protein components. We have found that Orbitrap-based high energy C-trap dissociation (HCD) fragments protein complexes *directly*, potentially revealing higher order structural information.[1] However, there are some exceptions, for example, for the streptavidin homotetramer (52 kDa) described in Chapter 3, complex-down (MS/MS of the dissociated subunit) and nTD-MS of the intact complex showed the same HCD fragmentation pattern, consistent with its weak noncovalent interactions between the monomer subunits. Therefore, the topology of the structure of the streptavidin complex cannot be revealed using nTD-MS. Another example in which nTD-MS fails to reveal higher-order structure information is the transthyretin homotetramer (55 kDa). For native HCD of protein complexes, products differ depending on the non-covalent interactions within the complex (*i.e.*, stability) and its 3D structure. Therefore, questions regarding the relatively stability of proteins in solution and how it relates to gas phase stability remain.

Previous research from the Venter group suggests that the addition of L-proline can stabilize intra-molecular noncovalent interactions by preventing thermal unfolding.[2] Similar questions are explored here by applying native MS, nTD-MS, and complex-down MS (in-source dissociation to eject a subunit of which a charge state is isolated for subsequent HCD) to the transthyretin tetramer with and without the addition of L-proline.

Experimental

Sample preparation. Transthyretin from human plasma (Sigma-Aldrich, St. Louis, MO, USA) with/without 10 mM L-proline (Sigma-Aldrich, St. Louis, MO, USA) dissolved in 200 mM ammonium acetate were buffer exchanged using 10 kDa Amicon filters (Sigma-Aldrich, St. Louis, MO, USA).

Native Top-Down and Complex-Down HCD MS. Protein solutions were sprayed from custom Pt-coated nanospray capillaries at voltages ranging from 1.2-1.5 kV. Fragmentation was performed in the HCD cell of a Q-Exactive UHMR orbitrap instrument (ThermoFisher Scientific) with voltages from 100-275 V. Native top-down MS experiments were performed by isolating the most abundant precursor ion charge state. Nitrogen was applied as the collision gas. 100 scans were averaged for each spectrum, and all spectra were externally calibrated with cesium iodide. No in-source CID voltages were applied. The complex-down experiments were performed on the UHMR with in-source CID voltages from 60 V.

Data Analysis. All MS/MS spectra were deconvoluted with BioPharma Finder 5.0 (ThermoFisher Scientific, Waltham, USA). Deconvolved peaks were assigned by ClipsMS 2.0.035 with an error tolerance of 3 ppm. Sequence assignment accommodated the major HCD (b, y) ion types without annotating neutral losses ions, except when explicitly mentioned. Terminal fragments were manually validated by confirming the isotopic distributions.

Results and Dissociation

Transthyretin is a 55 kDa homotetramer organized as a dimer of dimers in the native state.[3] However, the transthyretin gas-phase tetramer is not stable, and can dissociate into monomers and misassemble into amyloid fibrils.[4-6] In addition, previous studies have found that there are over 80 mutation sites including V30M and L55P.[7] It has been reported that these mutations affect transthyretin tetramer stabilities and increase the rate of transthyretin aggregation in the heart and kidneys.[8] Native MS analyses of the transthyretin homotetramer complex and the individual subunit provide a comprehensive overview of the composition and stoichiometry of the overall assembly. Two charge state distributions corresponding to transthyretin monomers (low *m/z* region) and transthyretin tetramers (high *m/z* region) were observed (Figure 1, top panel). Without the addition of L-proline, the monomer distribution is more abundant than the tetramer distribution. With the addition of 10 mM L-proline, two charge state distributions were still observed (Figure 1, bottom panel). However, the abundance of the monomer distribution has significantly reduced. This result may suggest that the addition of L-proline stabilized the noncovalent interactions between monomers, therefore, reducing the population of the monomers in the sample, *i.e.*, increasing the proportion of intact tetramers. Moreover, in both spectra, the peaks corresponding to the monomer and the tetramer are wider than expected. These wider peaks might be due to the high heterogeneity with the presence of all the mutations.

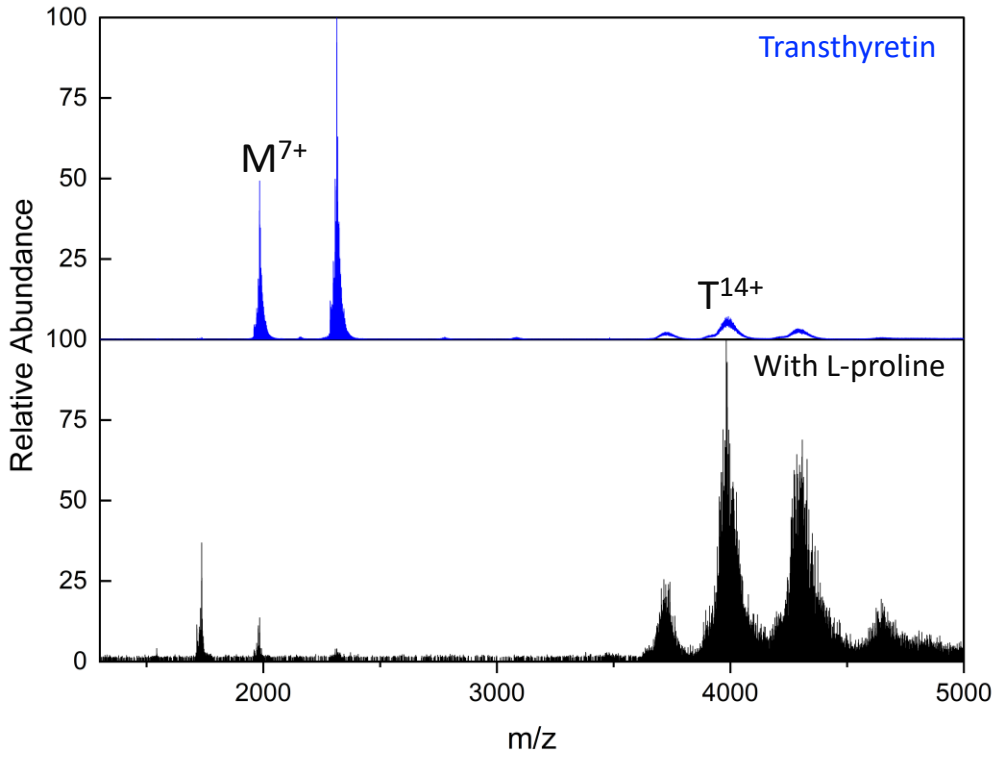

Figure 1. Native mass spectra of transthyretin (top) without the addition of L-proline and (bottom) with the addition of 10 mM L-proline.

We first performed nTD-MS HCD on the 15+ charge state of transthyretin tetramer. Dissociation of the homotetramer into its monomer components was observed at low HCD energy. This suggests that HCD ejects monomers from the complex at energies that are lower than those required to break covalent bonds. At a higher HCD energy, a few N-terminal *b*-fragments and mostly C-terminal *y*-fragments were generated (Figure 2A and B). We also observed the monomer charge state distribution. The data suggests that monomer subunits are ejected before generating sequence-bearing fragments, and the fragments are all generated from the monomer, not directly from the tetramer. To confirm this claim, complex-down HCD was performed, and compared to the native top-down HCD fragmentation pattern. Complex-down MS was performed by using in-source CID

(ISD) to eject a monomer from the tetramer and to subsequently subject the released 6+ transthyretin monomer for fragmentation[1]. The resultant complex-down HCD spectrum also revealed the similar fragmentation pattern (Figure 2C and D). The similarity between nTD and complex-down fragmentation patterns supports that the monomers were ejected from the tetramers prior to the backbone cleavages in the HCD cell. Therefore, native top-down HCD did not reveal higher-order structure information for transthyretin complex.

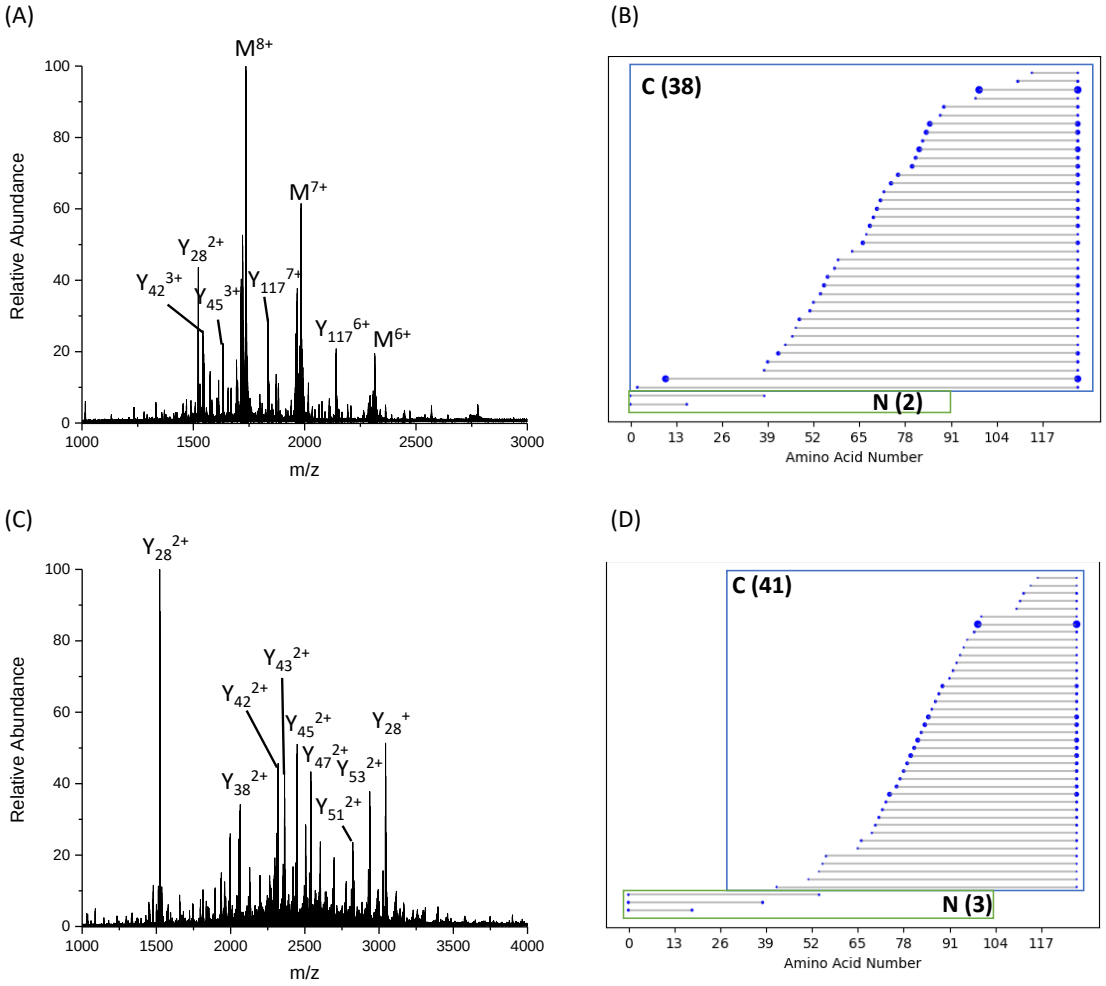

Figure 2. (A) Native top-down HCD MS of the 15+ charge state of transthyretin tetramer; (B) the corresponding fragmentation location map. (C) Complex-down HCD MS of the 6+ charge state of transthyretin monomer; (D) the corresponding fragmentation location map.

To examine the relationship between the stability of protein complexes and their HCD fragmentation patterns, native HCD fragmentation of transthyretin with/without L-proline, an additive that appears to stabilize protein ions[2], was performed. The MS/MS spectrum of stabilized transthyretin complexes revealed lower intensity and lower number of N-terminal fragments (Figure 3C and D). This differing fragmentation patterns in the two experiments indicates that HCD products are highly dependent on the gas-phase stability of the complexes.

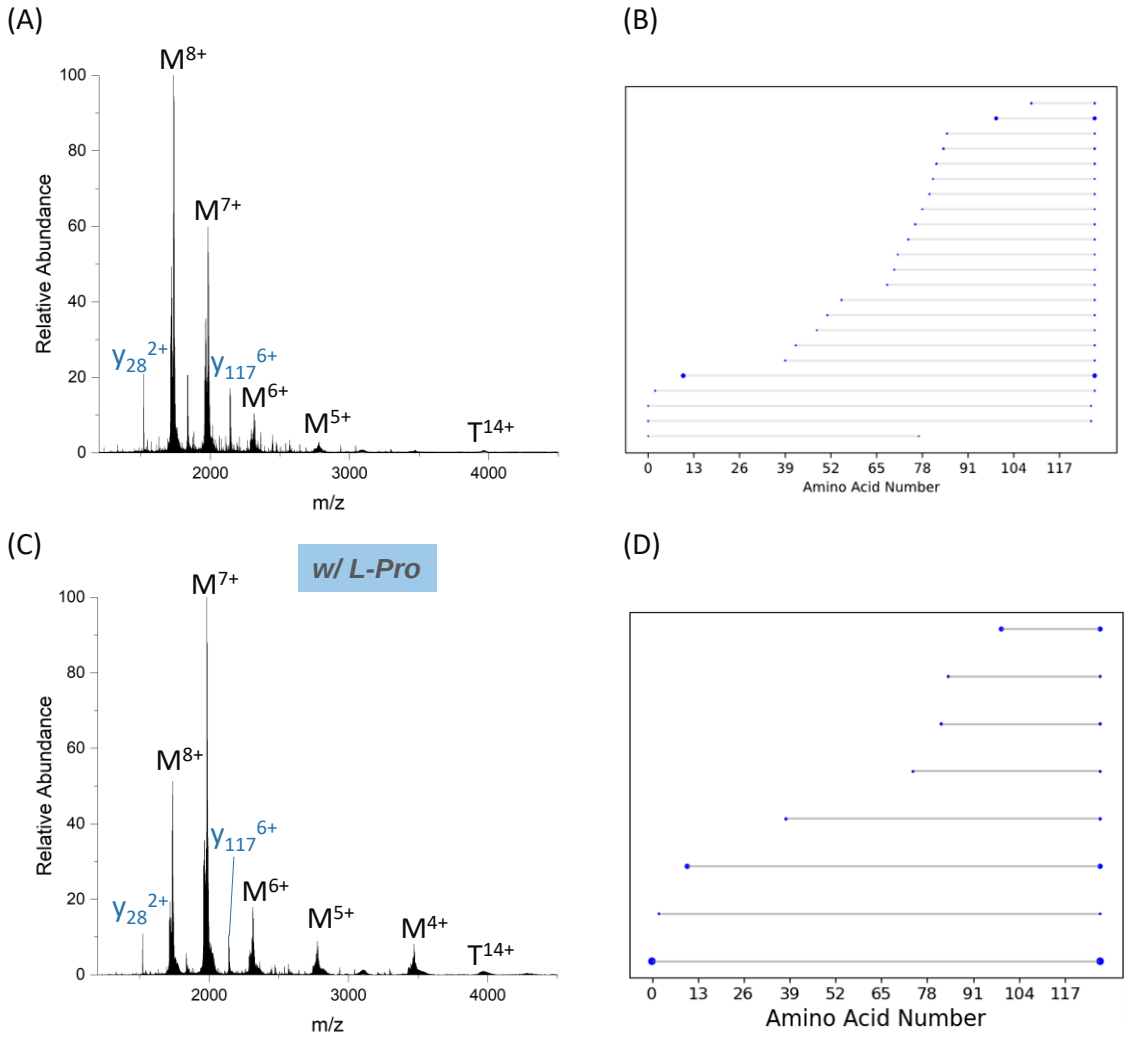

Figure 3. (A) Native top-down HCD MS of the 14+ charge state of transthyretin tetramer without the addition of L-proline; (B) the corresponding fragmentation location map. (C)

Native top-down HCD MS of the 14+ charge state of transthyretin tetramer with the addition of L-proline; (D) the corresponding fragmentation location map.

Conclusion

Here we show that transthyretin homotetramer decomposed by monomer ejection at low energies, but released fragments with excess collision energies. The addition of L-proline reduced the transthyretin monomer-to-tetramer ratio and reduced the number of terminal fragments observed for transthyretin, suggesting that the tetramer was stabilized in the presence of L-proline. At this point, it is not clear what is the mechanism of gas-phase stabilization imparted by the presence of L-proline. Binding of small molecule ligands are known to increase the melting temperature of proteins by stabilizing the protein. However, the native mass spectra do not show definitive binding of L-proline to transthyretin. This does not preclude a noncovalent interaction between the two molecules, as the interaction could be very weak or transient in the gas-phase. But clearly, the presence of L-proline changes the profile of the transthyretin mass spectra (Figure 1), suggesting a stabilizing effect. This should be a research topic for future consideration.

References

1. Lantz, C.; Wei, B.; Zhao, B.; Jung, W.; Goring, A. K.; Le, J.; Miller, J.; Loo, R. R. O.; Loo, J. A., Native Top-Down Mass Spectrometry with Collisionally Activated Dissociation Yields Higher-Order Structure Information for Protein Complexes. *Journal of the American Chemical Society* **2022,** *144* (48), 21826-21830.

2. Javanshad, R.; Panth, R.; Venter, A. R., Effects of Amino Acid Additives on Protein Stability during Electrothermal Supercharging in ESI-MS. *Journal of the American Society for Mass Spectrometry* **2024,** *35* (1), 151-157.

3. Blake, C. C. F.; Geisow, M. J.; Oatley, S. J.; Rérat, B.; Rérat, C., Structure of prealbumin: Secondary, tertiary and quaternary interactions determined by Fourier refinement at 1.8 Å. *Journal of Molecular Biology* **1978,** *121* (3), 339-356.

4. Colon, W.; Kelly, J. W., Partial denaturation of transthyretin is sufficient for amyloid fibril formation in vitro. *Biochemistry* **1992,** *31* (36), 8654-8660.

5. Lai, Z.; Colón, W.; Kelly, J. W., The Acid-Mediated Denaturation Pathway of Transthyretin Yields a Conformational Intermediate That Can Self-Assemble into Amyloid. *Biochemistry* **1996,** *35* (20), 6470-6482.

6. Quintas, A.; Vaz, D. C.; Cardoso, I.; Saraiva, M. J. M.; Brito, R. M. M., Tetramer Dissociation and Monomer Partial Unfolding Precedes Protofibril Formation in Amyloidogenic Transthyretin Variants*. *Journal of Biological Chemistry* **2001,** *276* (29), 27207-27213.

7. Jacobson, D. R.; Reveille, J. D.; Buxbaum, J. N., Frequency and genetic background of the position 122 (Val----Ile) variant transthyretin gene in the black population. *Am J Hum Genet* **1991,** *49* (1), 192-198.

8. Johnson, S. M.; Connelly, S.; Fearns, C.; Powers, E. T.; Kelly, J. W., The Transthyretin Amyloidoses: From Delineating the Molecular Mechanism of Aggregation Linked to Pathology to a Regulatory-Agency-Approved Drug. *Journal of Molecular Biology* **2012,** *421* (2), 185-203.

Appendix C: Solvent Leveling Explains Supercharging in Electrospray Ionization Mass Spectrometry

Boyu Zhao,[1] Reid O'Brien Johnson,[1] Carter Lantz,[1] Wonhyeuk Jung,[1] Muhammad Zenaidee,[1] Joseph A. Loo,[1-4] and Rachel R. Ogorzalek Loo[1,3,4]*

[1]Department of Chemistry and Biochemistry

[2]Department of Biological Chemistry, David Geffen School of Medicine

[3]UCLA-DOE Institute for Genomics and Proteomics

[4]Molecular Biology Institute

University of California-Los Angeles

***Corresponding Author**

Rachel R. Ogorzalek Loo

University of California-Los Angeles, Los Angeles, CA, United States

Email: rloo@mednet.ucla.edu

Abstract

Supplementing standard ESI solvents with certain low volatility organic compounds (*e.g.*, sulfolane or any positional isomer of nitrobenzyl alcohol), increases analyte charge in the phenomenon known as supercharging. The mechanism(s) responsible for increasing charge are considered and found to correlate highly to solvent leveling, as revealed by shifts in the average charge state of lysozyme electrosprayed from denaturing solutions unsupplemented or supplemented by 0.2% (w/v) of one of nine amides or of 9 nitriles of known basicity (pK_{BH+}). Consistently, amides or nitriles more basic than water reduced the average charge of lysozyme, while less basic amides increased the average charge, establishing the veracity of our supercharging model.

Introduction

"Supercharging" was introduced as a term in electrospray ionization-mass spectrometry (ESI-MS) to describe increases in the maximum and most abundant charge states observed when glycerol, ethylene glycol, *2*-methoxyethanol, and *m*-nitrobenzyl alcohol were added to acidified spray solutions.[1] Since then, the term has been bestowed to numerous, distinct approaches that increase charge on macromolecules, ranging from electrothermal supercharging from native-like solution compositions,[2-4] electrothermal supercharging with Hofmeister series ions or with small inner diameter capillaries,[5, 6] polarity reversal with salts,[7] spraying at super-atmospheric pressures,[8-10] protein denaturation, solvent supplementation with organic compounds (liquid or solid),[11-28] trivalent lanthanum addition,[29] trivalent chromium addition,[30, 31] and other phenomena.

The mechanisms proposed to elevate charge are contentious and confusing, becoming more so as an increasing number of distinct phenomena are labeled "supercharging." Here, we shall limit our consideration of supercharging to approaches that increase analyte charge by supplementing ESI solvents with *modest* amounts of certain low volatility organic compounds; *i.e.*, the phenomenon originally described. We also consider analogous approaches that *decrease* charge (subcharge) by supplementation with low volatility additives.

Iavarone and Williams[32, 33] promoted the hypothesis that increasing surface tension with *m*-nitrobenzyl alcohol (*m*-NBA) addition to evaporating water/methanol/acetic acid solvent elevated the maximum quantity of charge that mature ESI droplets accommodated before succumbing to Rayleigh decomposition. Hence, for any size (surface area) droplet,

comparatively more charge would be stored in a high surface tension liquid. Given the water, *m*-NBA, acetic acid, and methanol surface tensions, (γ), of 72, 50±5,[32] 27, and 22 mN/m,[34] respectively, the key assumption enabling those arguments was that evaporating acetic acid/water droplets concentrate acetic acid, such that *m*-NBA could feasibly be argued to increase the surface tension of droplets initiating with that composition. Low acetic acid volatility was similarly assumed to argue that, at the point of ion emission, surface tensions of evaporating droplets composed initially of 43% glycerol/3% acetic acid/54% H_2O would exceed those composed of 3% acetic acid/97% H_2O, despite glycerol's surface tension (γ = 63 mN/m) being lower than that of water.[32, 33] Later, the notion that equilibrium vapor pressures determine relative volatility[32] was shown to be incorrect; the key parameter for ranking volatility properly is a compound's evaporation rate.[35] *Thus, the published data,[32, 33] initially presumed as supporting, actually fail to show a significant role for surface tension in supercharging.* Furthermore, many results incompatible with the model have been reported.[11, 12, 17, 20, 35-38] Moreover, octyl glucoside, a surfactant reducing surface tension clearly increases protein charging,[38] most notably for membrane protein complexes, as compared to polyoxyethylene detergents [39, 40] and shifts in the average charge state induced by 14 supercharging agents showed no correlation to surface tension.[22]

It is also worth noting that the relationship between droplet surface tension and the maximum charge deposited on an analyte arises from Fernández de la Mora's formulation of the charge residue model (CRM).[41] *Should analyte ions be released prior to complete solvent evaporation and, e.g., from droplets sized considerably larger than the analyte, the extent of charging should be unrelated to surface tension.* Interestingly, the initial

supercharging observations[32] were made from denaturing solutions, a condition for which the CRM is expected *not to apply*,[41, 42] removing much of the perceived support for surface tension's role in supercharging.

Our laboratory proposed that low volatility, soluble, neutral compounds that are significantly weaker Brønsted bases than H_2O elevate positive ion charge, while involatile, soluble, neutral Brønsted acids that are weaker than H_2O, increase analyte deprotonation, elevating charge in negative ion mode.[23] We argued that, in electrospray ionization, analyte competes with solvent for charge. In positive ion mode charging is usually achieved by protonation; hence, the solvent/analyte charge competition will be modulated by respective Brønsted basicities. As supercharging additives concentrate in evaporating electrospray droplets, they alter the solvent composition and basicity. Ultra-weak base additives reduce solvent basicity, driving more charge (protons) to the analyte. Additives that are stronger bases than water, increase solvent basicity, steering more charge to solvent and reducing analyte charging. A second effect of adding very weak bases to the solvent is that they make neutral acids less likely to ionize (increase *pKa*), as the solvent's ability to accept protons decreases. For the same reason, *pKa* values of cationic acids (*e.g.*, protonated amines) increase. By the same logic, adding a very weak acid to water makes it harder to protonate neutral bases (reduces *pKa* of cationic acids) while enhancing ionization of neutral acid analytes (decrease *pKa*). Hence, adding an ultra-weak acid should increase analyte negative charging. Many neutral supercharging agents have *both* weak base and weak acid character, properties that reduce analyte ionization in the bulk solution. Fortunately, the ion emission event dumps charge, so the main consequence of very weak acid/very weak base

supercharging agents is to reduce opposite charge sites; *i.e.*, reduce the zwitterionic character of gas phase analyte ions, at least initially. [23, 43]

While the initial supercharging debate centered on the source of increased analyte charge from denaturing solutions, a secondary controversy revolved around charge increases observed with many of the same supercharging additives in native-like solutions. Because water has an extraordinarily high surface tension, the surface tension model predicts that adding nitrobenzyl alcohol or other supercharging agents to 100% aqueous solutions would reduce protein charge. That protein charge increases, instead,[11, 12] provides strong evidence countering that model. However, its proponents[44-47] argued that any charge increase observed from a native-like solution must reflect denaturation, instead, and so shouldn't be employed to discount a surface tension model.

Nevertheless, generous charge increases were observed in proteins sprayed from native-like solutions supplemented with *m*-NBA, sulfolane, and other supercharging agents[11, 12] and it is clear that modestly "supercharged" protein[39, 48-55] and oligonucleotide[56, 57] complexes remained associated.

That sulfolane destabilized myoglobin in aqueous guanidinium hydrochloride (GuHCl) solution by ~1.5 kcal/mol sulfolane/mole GuHCl was promoted as evidence that the mechanism for sulfolane's charge-elevating capacity was chemical denaturation. [44] However, an increased sensitivity to GuHCl unfolding is not equivalent to sulfolane driving denaturations from *any* solvent composition. Subsequent isothermal calorimetry, circular dichroism, and nuclear magnetic resonance spectroscopy measurements demonstrated that lysozyme's higher order structure and intermolecular interactions were not changed

significantly by sulfolane, leading to the conclusion that lysozyme supercharging with sulfolane was unrelated to protein unfolding during ESI. [53]

Some groups labeled dimethylsulfoxide (DMSO) a supercharging agent, [14, 19, 33, 46, 58-60]while others noted that, under conditions preserving higher order structure, it actually subcharged. [18, 23, 46, 61-66] The opposing labels led to confusion and an accidental 'straw man' argument that, because DMSO increased charging by disrupting higher order protein structure, the general mechanism of aqueous supercharging must be unfolding. [46]

Certainly, adding sufficient acid and/or organic solvent to most native protein or oligonucleotide solutions unfolds macromolecular conformations, shifting charge state distributions (CSDs) to lower *m/z*. [67, 68] We agree that altered conformations may have contributed in part to some observations initially called supercharging. [1, 32, 33] Numerous other supercharging observations, however, support a mechanism that increases charge independent of protein or oligonucleotide unfolding.

We contend that low volatility, soluble, neutral compounds that are significantly weaker Brønsted bases than H_2O ($pK_{BH+} << -1.7$) will elevate positive ion charge, while involatile, soluble, neutral Brønsted acids that are weaker than H_2O ($pK_a >> 15.7$), will increase analyte deprotonation, elevating charge in negative ion mode. [23] However, we noted previously that positive ion supercharging candidates fulfilling the $pK_{BH+} << -1.7$ criterion might still elevate charge weakly or not at all, should they also have sufficient acidity to dissociate in the employed solvent, thus generating anions to ion pair with analyte.

Here we test our proposed supercharging mechanism by supplementing protein solutions with related compounds of known basicity.

Experimental

Positive ion ESI mass spectra were acquired on a Synapt G2si hybrid quadrupole time-of-flight (QTOF) mass spectrometer with a Triwave ion mobility (IM) separator (Waters, Manchester, UK). Instrumental parameters were cone 40V, trap collision 20-50V, transfer collision 20-30V, and 4 mL/min trap gas flow. Nano-electrospray ionization of lysozyme (20 μM in 50% water/49.9% acetonitrile/0.1% formic acid) was performed with platinum-coated borosilicate capillaries (ThermoFisher Scientific, ES387) and sprayed at 1.0-1.2kV with a flow rate of 10-40 nL/min. The ion source was maintained at 100^{o}C. All measurements were performed in triplicate and the average chare states were calculated from the intensity-weighted average of all peaks with a signal-to-noise ratio greater than 5.

Compounds *3*-nitrobenzyl alcohol (*m*-NBA, CAS 619-25-0), sulfolane (CAS 126-33-0), formamide (CAS 75-12-7), *N,N*-dimethylformamide (DMF, CAS 68-12-2), *3*-nitrobenzonitrile (CAS 619-24-9), and chloroacetonitrile (CAS 107-14-2) were obtained from Sigma-Aldrich. *1,2*-butylene carbonate (CAS 4437-85-8), acetamide (60-35-5), chloroacetamide (CAS 79-07-2), *4*-methoxybenzamide (CAS 3424-93-9), *4*-nitrophenylacetonitrile (4NPACN, CAS 555-21-5), propionitrile (CAS 107-12-0), *4*-pyridinecarbonitrile (CAS 100-48-1), and *2*-pyridine carbonitrile (CAS 100-70-9) were purchased from TCI. Acros provided *N,N*-dimethylacetamide (DMA, CAS 127-19-5). Propionamide (CAS 79-05-0), *4*-Nitrobenzamide (CAS 619-80-7), and malononitrile (CAS 109-77-3) were sourced from Alfa Aesar. Benzamide (CAS 55-21-0), succinonitrile (CAS 110-61-2), and *3*-nitrophenylacetonitrile (3NPACN, CAS 621-50-1) were supplied by Ark Pharm, Combiblocks, and Matrix Scientific, respectively.

The candidate supercharging agents above were added to lysozyme solutions at a concentration of 0.2% (w/v).

Results and Discussion

Solution basicities of the neutral bases (B) employed in this study are described by equilibrium dissociations of their protonated forms (equation 1), while the protonation constant (K_{BH+}) and pK_{BH+} are defined by equations 2 and 3, respectively.

$$BH^+ + H_2O \rightleftharpoons B + H_3O^+ \quad (1)$$

$$K_{BH+} = [B][H_3O^+]/[BH^+] \quad (2)$$

$$pK_{BH+} = -\log_{10}(K_{BH+}) \quad (3)$$

We primarily relied on literature pK_{BH+} values that had been measured in various solvents and extrapolated values in water. When experimental values were not available, we used chemical intuition to rank basicities relative to the other compounds employed. In particular, electron withdrawing groups (*e.g.*, nitro- and chloro-) tend to reduce basicity, whereas electron donating groups (*e.g.*, methyl, methoxy) increase basicity. Table 1 displays pK_{BH+} values for the compounds examined, although values were not available for all compounds tested. The spread in the measured values reflects the challenges measuring and extrapolating basicities. It is important to note that basicities are not entirely independent of solvent and other parameters and that theoretical calculations of basicity and acidity have limited accuracy.[69-71] Consequently, comparisons *should not* rely on fine distinctions in basicity. limitations and they, too, should not be used to make fine distinctions in basicity. in accuracy.

Figure 1 compares data for the average charge state of lysozyme in denaturing solvent (50% H_2O/49.9% CH_3CN/0.1% HCOOH) with added amide or nitrile compounds (0.2% (w/v)) to data for unsupplemented solvent. For comparison, established supercharging agents *3*-nitrobenzyl alcohol (NBA), sulfolane, and 1,2-butylene carbonate were also added at 0.2% (w/v).

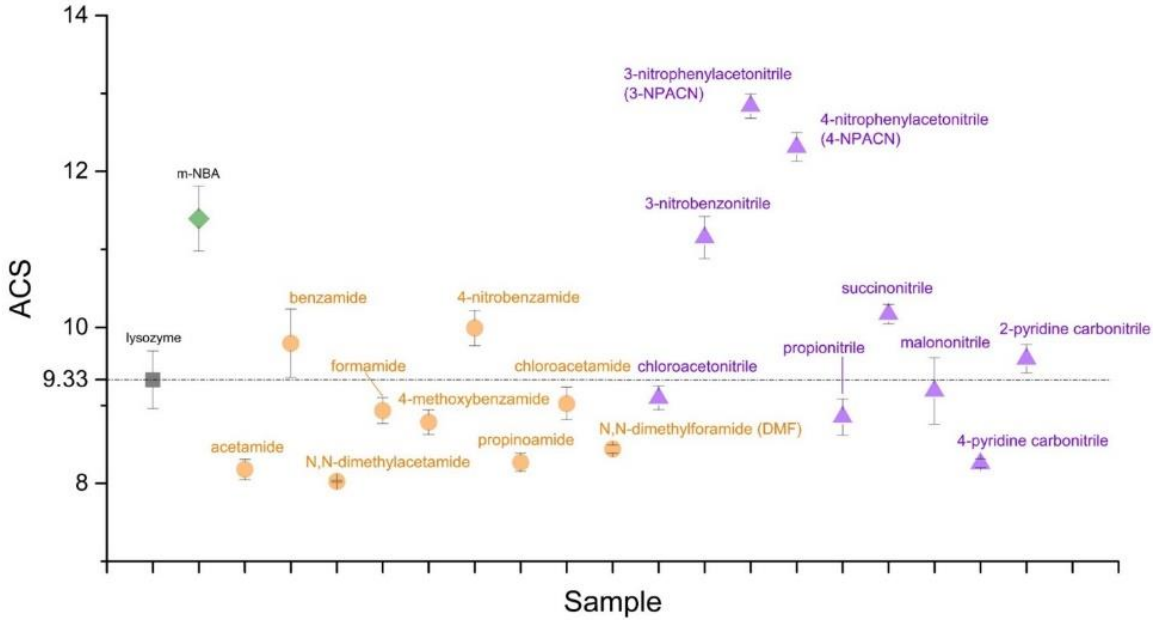

Figure 1. ACS of intact lysozyme in denaturing condition after treatment with conventional supercharging agents (black), amides (red), and nitriles (blue). Lysozyme was solubilized in 50% water, 49.9% acetonitrile, 0.1% formic acid. Every reagent was treated at 0.2% w/v. ACSs are the average charge state values from triplicate measurements and the error bar indicates standard deviation from the triplicate measurements. Along with the three conventional supercharging agents (m-NBA, 1,2-butylene carbonate, and sulfolane), 4-nitrobenzamide, succinonitrile, 3-NPACN, 4-NPACN, and 3-nitrobenzonitrile show supercharging behavior. Acetamide, DMA, DMF, propionamide, and 4-pyridinecarbonitrile show subcharging behavior. (m-NBA: 3-nitrobenzylalcohol, DMA: N, N-dimethylacetamide, DMF: N, N-dimethylformamide, 3-NPACN: 3-nitrophenylacetonitrile, 4-NPACN: 4-nitrophenylacetonitrile)

Considering the 9 amides first, it is apparent that only *4*-nitrobenzamide and benzamide show any propensity for increasing lysozyme protonation, behavior that is consistent with

measured basicities implying that both are weaker bases than water. Formamide, chloroacetamide, and 4-methoxybenzamide very slightly decrease lysozyme's average charge, while DMF, propionamide, acetamide, and DMA reduce it further. These observations, too, are consistent with the measured pK_{BH+} values. In general, we would expect acetamide to be more basic (charge-reducing) than chloroacetamide, due to the latter's electron withdrawing group. Similarly, electron donating groups in DMF, DMA, acetamide, and propionamide would lead us to expect them to lower lysozyme charge more than formamide. Clearly, supercharging and subcharging behaviors observed with nitriles support our supercharging model. Additives less basic than water increase charge; additives more basic than water decrease charge.

Considering the 9 nitriles is more challenging, given the dearth of experimental basicity measurements. However, given that acetonitrile is much less basic than water (and unsuitable as a supercharging agent only due to its volatility), we predict that *4*-NPACN, *3*-NPACN, and *3*-nitrobenzonitrile, as ultra-weak bases, will increase charge. We expect succinonitrile, and malononitrile to increase charge, as well, albeit less than the nitro compounds. pK_{BH+} measurements (Table 1) for chloroacetonitrile predict that it should increase charge strongly, whereas *2*-pyridinecarbonitrile may reduce charge, but *4*-pyridinecarbonitrile should reduce it more. We expect propionitrile to be more basic (charge reducing) than 6 of the other nitriles, but find it hard to predict its relationship to the pyridine carbonitriles.

Almost all the predictions above are borne out by Figure 1. The only surprises are the weakly charge-reducing behaviors of malononitrile, chloroacetonitrile, and propionitrile. Why dicyano compound malononitrile failed to increase charge is unclear at present. It has

sufficient water solubility and a low evaporation rate, implying that it should have been present throughout the ESI droplet lifetime. In principle, it's acidity (pKa = 11.2)[72] may have reduced charge by ion pairing to protonated sites. In retrospect, that propionitrile failed to increase charge is attributed to its volatility; its evaporation rate is 1.91 (butyl acetate=1), more than 6 times higher than water.[73] Chloroacetonitrile likely failed to increase charge due to insolubility in water.[74]

Table 1. Selected compounds and corresponding experimental pK_{BH+}.

Compound	pK_{BH}	Reference	pK_{BH}	Reference	pK_{BH}	Reference
N,N-Dimethylacetamide	-0.29	[75]	2.44	[76]	0.62	[77]
Acetamide	-0.57	[75]	-0.66	[76]	-0.25	[77]
Propionamide	N/A		N/A		-0.9	[78]
N,N-Dimethylformamide	-1.15	[75]	-1.2	[79]	0.18	[77]
Formamide	-1.15	[75]	-1.2	[79]	0.18	[77]
Chloroacetamide	N/A		N/A		-0.26	[77]
4-Methoxybenzamide	N/A		N/A		-1.8	[80]
Benzamide	N/A		N/A		-2.16	[80]
4-Nitrobenzamide	N/A		N/A		-3.23	[80]
4-Pyridinecarbonitrile	1.9	[81]				
2-Pyridinecarbonitrile	-0.26	[82]				
Chloroacetonitrile	-12.8	[76]				
Malononitrile	N/A					
Succinonitrile	N/A					
Propionitrile	N/A					
3-Nitrobenzonitrile	N/A					
4-NPACN	N/A					
3-NPACN	N/A					

Conclusion

Consistently, amides or nitriles more basic than water reduced the average charge of lysozyme, while less basic amides increased the average charge, establishing the veracity of our supercharging model. Low volatility, soluble, neutral compounds that are significantly weaker Brønsted bases than H_2O ($pK_{BH+} << -1.7$) will elevate positive ion charge, while involatile, soluble, neutral Brønsted acids that are weaker than H_2O ($pK_a >> 15.7$), will increase analyte deprotonation, elevating charge in negative ion mode.[23]

References

1. Iavarone, A. T.; Jurchen, J. C.; Williams, E. R., Supercharged Protein and Peptide Ions Formed by Electrospray Ionization. *Anal. Chem.* **2001,** *73*, 1455-1460.

2. Sterling, H. J.; Cassou, C. A.; Susa, A. C.; Williams, E. R., Electrothermal Supercharging of Proteins in Native Electrospray Ionization. *Anal. Chem.* **2012,** *84*, 3795-3801.

3. Hedges, J. B.; Vahidi, S.; Yue, X.; Konermann, L., Effects of Ammonium Bicarbonate on the Electrospray Mass Spectra of Proteins: Evidence for Bubble-Induced Unfolding. *Anal. Chem.* **2013,** *85*, 6469-6476.

4. Lin, H.; Kitova, E. N.; Johnson, M. A.; Eugenio, L.; Ng, K. K. S.; Klassen, J. S., Electrospray Ionization-Induced Protein Unfolding. *J. Am. Soc. Mass Spectrom.* **2012,** *23*, 2122-2131.

5. Cassou; Williams, E. R., Anions in Electrothermal Supercharging of Proteins with Electrospray Ionization Follow a Reverse Hofmeister Series. *Anal. Chem.* **2014,** *86*, 1640-1647.

6. Mortensen, D. N.; Williams, E. R., Electrothermal Supercharging of Proteins in Native MS: Effects of Protein Isoelectric Point, Buffer, and NanoESI-Emitter Tip Size. *Analyst* **2016,** *141*, 5598-5606.

7. Gong, X.; Li, C.; Zhai, R.; Xie, J.; Jiang, Y.; Fang, X., Supercharging of Proteins by Salts During Polarity Reversed Nano-Electrospray Ionization. *Anal. Chem.* **2019,** *91*, 1826-1837.

8. Rahman, M. M.; Chen, L. C., Analytical Characteristics of Nano-Electrospray Operated under Super-Atmospheric Pressure. *Anal Chim Acta* **2018,** *1021*, 78-84.

9. Wang, Y.; Olesik, S. V., Enhanced-Fluidity Liquid Chromatography−Mass Spectrometry for Intact Protein Separation and Characterization. *Anal. Chem.* **2019,** *91*, 935-942.

10. Yin, Z.; Huang, J.; Miao, H.; Hu, O.; Li, H., High-Pressure Electrospray Ionization Yields Supercharged Protein Complexes from Native solutions while Preserving Noncovalent Interactions. *Anal. Chem.* **2020,** *92*, 12312-12321.

11. Lomeli, S. H.; Yin, S.; Ogorzalek Loo, R. R.; Loo, J. A., Increasing Charge While Preserving Noncovalent Protein Complexes for ESI-MS. *J. Am. Soc. Mass Spectrom.* **2009,** *20*, 593-596.

12. Lomeli, S. H.; Peng, I. X.; Yin, S.; Ogorzalek Loo, R. R.; Loo, J. A., New Reagents for Increasing ESI Multiple Charging of Proteins and Protein Complexes. *J. Am. Soc. Mass Spectrom.* **2010,** *21*, 127-131.

13. Hogan, C. J., Jr.; Ogorzalek Loo, R. R.; Loo, J. A.; Fernández de la Mora, J., Ion Mobility–Mass Spectrometry of Phosphorylase *B* Ions Generated with Supercharging Reagents but in Charge-Reducing Buffer. *Phys. Chemistry Chem. Phys.* **2010,** *12*, 13476-13483.

14. Valeja, S. G.; Tipton, J. D.; Emmett, M. R.; Marshall, A. G., New Reagents for Enhanced Liquid Chromatographic Separation and Charging of Intact Protein Ions for Electrospray Ionization Mass Spectrometry. *Anal. Chem.* **2010,** *82*, 7515-7519.

15. Huang, Y.; Shi, X.; Yu, X.; Leymarie, N.; Staples, G. O.; Yin, H.; Killeen, K.; Zaia, J., Improved Liquid Chromatography-MS/MS of Heparan Sulfate Oligosaccharides via Chip-Based Pulsed Makeup Flow. *Anal. Chem.* **2011,** *83*, 8222-8229.

16. Ogorzalek-Loo, R. R.; Lakshmanan, R.; Zhang, J.; Loo, J. A., Supercharging and Subcharging Proteins and Protein Complexes to Explore Electrospray Ionization. In *60th ASMS Conference on Mass Spectrometry and Allied Topics*, Vancouver, British Columbia, Canada, 2012.

17. Douglass, K. A.; Venter, A. R., Investigating the Role of Adducts in Protein Supercharging with Sulfolane. *J. Am. Soc. Mass Spectrom.* **2012,** *23*, 489-497.

18. Meyer, J. G.; Komives, E. A., Charge State Consolidation During Electrospray Ionization Improves Peptide Identification by Tandem Mass Spectrometry. *J. Am. Soc. Mass Spectrom.* **2012,** *23*, 1390-1399.

19. Miladinovic, S. M.; Fornelli, L.; Lu, Y.; Piech, K. M.; Girault, H. H.; Tsybin, Y. O., In-Spray Supercharging of Peptides and Proteins in Electrospray Ionization Mass Spectrometry. *Anal. Chem.* **2012,** *84*, 4647-4651.

20. Brahim, B.; Alves, S.; Cole, R. B.; Tabet, J.-C., Charge Enhancement of Single-Stranded DNA in Negative Electrospray Ionization Using the Supercharging Reagent *meta*-Nitrobenzyl Alcohol. *J. Am. Soc. Mass Spectrom.* **2013,** *24*, 1988-1996.

21. Chingin, K.; Xu, N.; Chen, H., Soft Supercharging of Biomolecular Ions in Electrospray Ionization Mass Spectrometry. *J. Am. Soc. Mass Spectrom.* **2014,** *25*, 928-934.

22. Teo, A. C.; Donald, W. A., Solution Additives for Supercharging Proteins beyond the Theoretical Maximum Proton-Transfer Limit in Electrospray Ionization Mass Spectrometry. *Anal. Chem.* **2014,** *85*, 4455-4462.

23. Ogorzalek Loo, R. R.; Lakshmanan, R.; Loo, J. A., What Protein Charging (and Supercharging) Reveal about the Mechanism of Electrospray Ionization. *J. Am. Soc. Mass Spectrom.* **2014,** *25*, 1675-1693.

24. Douglass, K. A.; Venter, A. R., On the Role of a Direct Interaction Between Protein Ions and Solvent Additives During Protein Supercharging by Electrospray Ionization Mass Spectrometry. *Eur. J. Mass Spectrom.* **2015,** *21* (3), 641-647.

25. Zhang, J.; Ogorzalek Loo, R. R.; Loo, J. A., Increasing Fragmentation of Disulfide-Bonded Proteins for Top-Down Mass Spectrometry by Supercharging. *Int. J. Mass spectrom.* **2015,** *377*, 546-556.

26. Steinkoenig, J.; Cecchini, M. M.; S, R.; Goldmann, A. S.; Barner-Kowollik, C., Supercharging Synthetic Polymers: Mass Spectrometric Access to Nonpolar Synthetic Polymers. *Macromolecules* **2017,** *50*, 8033-8041.

27. Zenaidee, M. A.; Leeming, M. G.; Zhang, F.; Funston, T. T.; Donald, W. A., Highly Charged Protein Ions: The Strongest Organic Acids to Date. *Angew. Chem. Int. Ed.* **2017,** *56*, 8522-8526.

28. Nshanian, M.; Lakshmanan, R.; Chen, H.; Ogorzalek Loo, R. R.; Loo, J. A., Enhancing Sensitivity of Liquid Chromatography–Mass Spectrometry of Peptides and Proteins using Supercharging Agents. *Int. J. Mass Spectrom.* **2018,** *427*, 157-164.

29. Flick, T. G.; Williams, E. R., Supercharging with Trivalent Metal Ions in Native Mass Spectrometry. *J Am Soc Mass Spectrom.* **2012,** *23,* 1885-1895.

30. Feng, C.; Commodore, J. J.; Cassady, C. J., The Use of Chromium (III) to Supercharge *J. Am. Soc. Mass Spectrom.* **2015,** *26*, 347-358.

31. Jing, X.; Edwards, K. C.; Vincent, J. B.; Cassady, C. J., The Use of Chromium (III) Complexes to Enhance Peptide Protonation by Electrospray Ionization Mass Spectrometry. *J. Mass Spectrom.* **2018,** *53*, 1198-1206.

32. Iavarone, A. T.; Williams, E. R., Supercharging in Electrospray Ionization: Effects on Signal and Charge. *Int. J. Mass Spectrom.* **2002,** *219,* 63-72.

33. Iavarone, A. T.; Williams, E. R., Mechanism of Charging and Supercharging Molecules in Electrospray Ionization. *J. Am. Chem. Soc.* **2003,** *125*, 2319-2327.

34. Diversified_Enterprises_AccuDyne Viscosity, Surface Tension, Specific Density and Molecular Weight of Selected Liquids. (accessed July 7).

35. Šamalikova, M.; Grandori, R., Testing the Role of Solvent Surface Tension in Protein Ionization by Electrospray. *J. Mass Spectrom.* **2005,** *40* (4), 503-510.

36. Šamalikova, M.; Grandori, R., Protein Charge-State Distributions in Electrospray-Ionization Mass Spectrometry Do Not Appear to be Limited by the Surface Tension of the Solvent. *J. Am. Chem. Soc.* **2003,** *125*, 13352-13353.

37. Šamalikova, M.; Matecko, I.; Müller, N.; Grandori, R., Interpreting Conformational Effects in Protein Nano-ESI-MS Spectra. *Anal. Bioanal. Chem.* **2004,** *378*, 1112-1123.

38. Ogorzalek Loo, R. R.; Dales, N.; Andrews, P. C., The Effect of Detergents on Proteins Analyzed by Electrospray Ionization. In *Protein and Peptide Analysis by Mass Spectrometry*, Chapman, J. R., Ed. Humana Press: Totowa, NJ, 1996; Vol. 61, pp 141-160.

39. Yen, H.-Y.; Abramsson, M. L.; Agasid, M. T.; Lama, D.; Gault, J.; Liko, I.; Kaldmäe, M.; Saluri, M.; Qureshi, R. A.; Suades, A.; Drew, D.; Degiacomi, M. T.; Marklund, E. G.; Allison, T. M.; Robinson, C. V.; Landreh, M., Electrospray Ionization of Native Membrane Proteins Proceeds via a Charge Equilibration Step. *RSC Adv.* **2022,** *12*, 9671-9680.

40. Keener, J. E.; Zhang, G.; Marty, M. T., Native Mass Spectrometry of Membrane Proteins. **2021,** *93*, 583-597.

41. Fernández de la Mora, J., Electrospray Ionization of Large Multiply Charged Species Proceeds via Dole's Charged Residue Mechanism. *Anal. Chim. Acta* **2000,** *406*, 93-104.

42. Konermann, L.; Ahadi, E.; Rodriguez, A. D.; Vahidi, S., Unraveling the Mechanism of Electrospray Ionization. *Anal. Chem.* **2013,** *85*, 2-9.

43. Ogorzalek Loo, R. R.; Loo, J. A., Salt Bridge Rearrangement (SaBRe) Explains the Dissociation Behavior of Noncovalent Complexes. *J. Am. Soc. Mass Spectrom.* **2016,** *27*, 975-990.

44. Sterling, H. J.; Daly, M. P.; Feld, G. K.; Thoren, K. L.; Kintzer, A. F.; Krantz, B. A.; Williams, E. R., Effects of Supercharging Reagents on Noncovalent Complex Structure in Electrospray Ionization from Aqueous Solutions. *J. Am. Soc. Mass Spectrom.*

2010, *21*, 1762-1774.

45. Sterling, H. J.; Kintzer, A. F.; Feld, G. K.; Cassou, C. A.; Krantz, B. K.; Williams, E. R., Supercharging Protein Complexes from Aqueous Solution Disrupts their Native Conformations. *J. Am. Soc. Mass Spectrom.* **2011,** *23*, 191-200.

46. Sterling, H. J.; Prell, J. S.; Cassou, C. A.; Williams, E. R., Protein Conformation and Supercharging with DMSO from Aqueous Solution. *J. Am. Soc. Mass Spectrom.* **2011,** *22*, 1178-1186.

47. Sterling, H. J.; Williams, E. R., Origin of Supercharging in Electrospray Ionization of Non-Covalent Complexes from Aqueous Solution. *J. Am. Soc. Mass Spectrom.* **2009,** *20*, 1933-1943.

48. Yin, S.; Loo, J. A., Top-Down Mass Spectrometry of Supercharged Native Protein–Ligand Complexes. *Int. J. Mass Spectrom.* **2011,** *300*, 118-122.

49. Hall, Z.; Politis, A.; Bush, M. F.; Smith, L. J.; Robinson, C. V., Charge-State Dependent Compaction and Dissociation of Protein Complexes: Insights from Ion Mobility and Molecular Dynamics. *J. Am. Chem. Soc.* **2012,** *34*, 3429-3438.

50. Hall, Z.; Robinson, C. V., Do Charge State Signatures Guarantee Protein Conformations? *J. Am. Soc. Mass Spectrom.* **2012,** *23*, 1161-1168.

51. Zhou, M.; Dagan, S.; Wysocki, V. H., Impact of Charge State on Gas-Phase Behaviors of Noncovalent Protein Complexes in Collision Induced Dissociation and Surface Induced Dissociation. *Analyst* **2013,** *138*, 1353-1362.

52. Mikhailov, V. A.; Liko, I.; Mize, T. H.; Bush, M. F.; Benesch, J. L. P.; Robinson,

C. V., Infrared Laser Activation of Soluble and Membrane Protein Assemblies in the Gas Phase. *Anal. Chem.* **2016,** *in press*.

53. Yao, Y.; Richards, M. R.; Kitova, E. N.; Klassen, J. S., Influence of Sulfolane on ESI-MS Measurements of Protein-Ligand Affinities. *J. Am. Soc. Mass Spectrom.* **2016,** *27*, 498-506.

54. Sipe, S. N.; Brodbelt, J. S., Impact of Charge State on 193 nm Ultraviolet Photodissociation of Protein Complexes. *Phys. Chem. Chem. Phys.* **2019,** *21*, 9265-9276.

55. Yang, Y.; Niu, C.; Bobst, C.; Kaltashov, I., Ionic Charge Manipulation Using Solution and Gas-Phase Chemistry to Facilitate Analysis of Highly Heterogeneous Protein Complexes in Native Mass Spectrometry. *Anal. Chem.* **2021,** *93*, 3337-3342.

56. Xu, N.; Chingin, K.; Chen, H., Ionic Strength of Electrospray Droplets Affects Charging of DNA Oligonucleotides. *J. Mass Spectrom.* **2014,** *49*, 103-107.

57. Porrini, M.; Rosu, F.; Rabin, C.; Darré, L.; Gómez, H.; Orozco, M.; Gabelica, V., Compaction of Duplex Nucleic Acids upon Native Electrospray Mass Spectrometry. *ACS Cent. Sci.* **2017,** *3*, 454-461.

58. Khanal, D. D.; Baghdady, Y. Z.; Figard, B. J.; Schug, K. A., Supercharging and Multiple Reaction Monitoring of High Molecular Weight Intact Proteins using Triple Quadrupole Mass Spectrometry. *Rapid Commun. Mass Spectrom.* **2019,** *33*, 821-830.

59. Källsten, M.; Visanu, D.; Pijnappel, M.; Lehmann, F.; Bergquist, J.; Lind, S. B.; Kovac, L., The Potential use of Supercharging Agents for Improved Mass Spectrometric Analysis of Monoclonal Antibodies and Antibody-Drug Conjugates. *J. Am. Soc. Mass*

Spectrom. **2022**.

60. Eremin, D. B.; Fokin, V. V., Dual Electrospray Ionization Enhancement of Proteins Enabled by DMSO Supercharging Reagent. *J. Am. Soc. Mass Spectrom.* **2022,** *33*, 203-206.

61. Tjernberg, A.; Carno, S.; Oliv, F.; Benkestock, K.; Edlund, P.-O.; Griffiths, W. J.; Hallen, D., Determination of Dissociation Constants for Protein-Ligand Complexes by Electrospray Ionization Mass Spectrometry. *Anal. Chem.* **2004,** *76*, 4325-4331.

62. Tjernberg, A.; Markova, N.; Griffiths, W. J.; Hallen, D., DMSO-Related Effects in Protein Characterization. *J. Biomol. Screening* **2006,** *11* (2), 131-137.

63. Landreh, M.; Alvelius, G.; Johansson, J.; Jörnvall, H., Protective Effects of Dimethyl Sulfoxide on Labile Protein Interactions during Electrospray Ionization. *Anal. Chem.* **2014,** *85*, 4135-4139.

64. Chan, D. S.-H.; Matak-Vinković, D.; Coyne, A. G.; Abell, C., Insight into Protein Conformation and Subcharging by DMSO from Native Ion Mobility Mass Spectrometry. *Chem. Select* **2016,** *1* (18), 5686-5690.

65. Chan, D. S.-H.; Kavanagh, M. E.; McLean, K. J.; Munro, A. W.; Matak-Vinković, D.; Coyne, A. G.; Abell, C., Effect of DMSO on Protein Structure and Interactions Assessed by Collision-Induced Dissociation and Unfolding. *Anal. Chem.* **2017,** *89*, 9976-9983.

66. Van Wanseele, Y.; Segers, K.; Viaene, J.; De Bundel, D.; Vander Heyden, Y.; Smolders, I.; Van Eeckhaut, A., Assessing Mixtures of Supercharging Agents to Increase

the Abundance of a Specific Charge State of Neuromedin U. *Talanta* **2019,** *198*, 206-214.

67. Chowdhury, S. K.; Katta, V.; Chait, B. T., Probing Conformational Changes in Proteins by Mass Spectrometry. *J. Am. Chem. Soc.* **1990,** *112*, 9012-9013.

68. Loo, J. A.; Ogorzalek Loo, R. R.; Udseth, H. R.; Edmonds, C. G.; Smith, R. D., Solvent-induced Conformational Changes of Polypeptides Probed by Electrospray Ionization-Mass Spectrometry. *Rapid Commun. Mass Spectrom.* **1991,** *5* (3), 101-105.

69. Mujika, J. I.; Mercero, J. M.; Lopez, X., A Theoretical Evaluation of the pKa for Twisted Amides Using Density Functional Theory and Dielectric Continuum Methods. *J. Phys. Chem. A* **2003,** *107*, 6099-6107.

70. Murłowska, K.; Sadlej-Sosnowska, N., Absolute Calculations of Acidity of C-Substituted Tetrazoles in Solution. *J. Phys. Chem. A* **2005,** *109*, 5590-5595.

71. Fukaya, H.; Ono, T.; Sonoda, T.; Mishima, M., Prediction of Gas-Phase Acidities of Strong Brønsted Acids by ONIOM Method. *Chemistry-Methods* **2022**, e202100079.

72. Tsunoda, T.; Kaku, H.; Itô, S., New Mitsunobu Reagents. *TCI Mail* **2005,** *123*.

73. Airgas Safety Data Sheet for Propiontrile. https://www.airgas.com/sds-search (accessed 7/19/2024).

74. del Valle, J. C.; Blanco, F.; Catalán, J., Empirical Parameters for Solvent Acidity, Basicity, Dipolarity, and Polarizability of the Ionic Liquids [BMIM][BF4] and [BMIM][PF6]. *J. Phys. Chem. B* **2015,** *119*, 4683-4692.

75. Stojković, G.; Dimitrieska-Stojković, E.; Popovski, E., Determination of Protonation Constants and Structural Correlations for some Tertiary Formamides and

Acetamides in Sulfuric Acid with UV Spectroscopy. *Maced. J. Chem. Eng.* **2015,** *34*, 255-265.

76. Laurence, C.; Brameld, K. A.; Graton, J.; Le Questel, J.-Y.; Renault, E., The pK_{BHX} Database: Toward a Better Understanding of Hydrogen-Bond Basicity for Medicinal Chemists. *J. Med. Chem.* **2009,** *52*, 4073-4086.

77. Wada, G.; Takenaka, T., Basicities of Formamide, Acetamide, and their Alkyl Derivatives in Aqueous Solution. *Bull. Chem. Soc. Japan* **1971,** *44*, 2877.

78. Edward, J. T.; Wang, I. C., Ionization of Organic Compounds III. Basicities of Propionic Acid and Propionamide. *Can. J. Chem.* **1962,** *40*, 966-975.

79. Karaman, R.; Bruice, T. C., Unusual Behavior of 5,10,15,20-Tetraphenylporphine Diacid toward Oxygen Bronsted Bases. *Inorg. Chem.* **1992,** *31*, 2455-2459.

80. Edward, J. T.; Chang, H. S.; Yates, K.; Stewart, R., Protonation of the Amide Group. I. The Basicities of Substituted Benzamides. *Can. J. Chem.* **1960,** *38*, 1518-1525.

81. Hamza, M. S. A.; Pratt, J. M., The Chemistry of Vitamin B_{12}, Part 30. Co-ordination of Amines, Pyridines and Diazines by Aquacyanocobinamide; Nitrogen-containing Bases as Probes for Basicity and Other Effects in Metal-Ligand Bonding *J. Chem. Soc. Dalton Trans.* **1994**, 1377-1382.

82. Perrin, D. D., *Dissociation Constants of Organic Bases in Aqueous Solution*. Butterworths: London, 1965.